Theory of intrinsic and extrinsic tunnelling in cuprates

Theory of Intrinsic and Extrinsic Tunnelling in Cuprates

by
Joanne Beanland

A Doctoral Thesis
Submitted in partial fulfilment of the requirements
for the award of
the degree of Doctor of Philosophy

Physics Department, Loughborough University, Loughborough, UK

Supervisor: Professor A. S. Alexandrov

October 25, 2010

DECLARATION

I, Joanne Beanland, declare that this thesis titled, 'Theory of Intrinsic and Extrinsic Tunnelling in Cuprate Superconductors' and the work presented in it are my own. I confirm that:

- This work was done wholly or mainly while in candidature for a research degree at this University.
- Where any part of this thesis has previously been submitted for a degree or any other qualification at this University or any other institution, this has been clearly stated.
- Where I have consulted the published work of others, this is always clearly attributed.
- Where I have quoted from the work of others, the source is always given. With the exception of such quotations, this thesis is entirely my own work.
- I have acknowledged all main sources of help.
- Where the thesis is based on work done by myself jointly with others, I have made clear exactly what was done by others and what I have contributed myself.

Signed: _____

Date: _____

PUBLICATIONS

- A. S. Alexandrov and J. Beanland, "*Superconducting Gap, Normal State Pseudogap, and Tunneling Spectra of Bosonic and Cuprate Superconductors*", Physical Review Letters **104** 026401 (2010).
- J. Beanland and A. S. Alexandrov, "*Theory of Intrinsic and Extrinsic Tunnelling in Cuprates*", Journal of Physics: Condensed Matter **22** 403202 (2010).

SEMINARS AND ORAL PRESENTATIONS AT CONFERENCES

- "*Superconducting Gap, Normal State Pseudogap, and Tunneling Spectra of Bosonic and Cuprate Superconductors*", IOP Condensed Matter and Materials Physics conference, Warwick, UK, December 2009.
- Invited seminar at Jozef Stefan Institute, Ljubljana, Slovenia, May 2010.
- "*Theory of Intrinsic and Extrinsic Tunnelling in Cuprates*", IOP Superconductivity Group Summer Science Meeting, London, UK, July 2010.

ACKNOWLEDGEMENTS

First and foremost I would like to thank my supervisor, Prof. A. S. Alexandrov, without his guidance and support this thesis would not have been possible.

I would like to thank participants at the conferences for their questions and comments. I would like to thank the Jozef Stefan Institute who were very welcoming, offering discussions and constructive criticism with regards to this work.

On a more personal level, I would like to thank the people closest to me, in particular my parents, Adele and Jack - thank you for your unwavering belief and support, I really do appreciate everything you do for me.

Thanks also to my friends in the physics department.

ABSTRACT

This thesis addresses the tunnelling of charge carriers in different materials. First looking at the simplest case of electron tunnelling in metals at zero, then finite temperature, the current is obtained using the Fermi-Dirac golden rule and then the conductance is obtained. This is extended to take into account the spatial dependence of one of the metals being a tip since experimentally this is done by scanning tunnelling microscopy where a tip traces over the surface of a sample. The next step is to look at tunnelling between a metal and a semiconductor, again the current is found. Semiconductors can be doped and the effect this has on tunnelling is examined. Next superconductors are introduced. The purpose of my research has been to look at the tunnelling spectra of high-temperature superconducting cuprates for both extrinsic (metal-superconductor) and intrinsic (superconductor-superconductor) tunnelling. The main features seen experimentally with cuprate tunnelling are identified and then a theory capable of explaining these features is discussed. The theory is compared to experimental results and we find good agreement.

CONTENTS

LIST OF FIGURES

1. INTRODUCTION

The purpose of this thesis is to discuss a theory of intrinsic and extrinsic tunnelling in cuprates. Before I can do this I have developed the skills to allow me to do so by looking at simpler cases. First looking at the tunnelling of electrons between two metallic planes allows the derivation of the well known Ohm's Law. This is done in the limit of zero temperature and also for finite temperature. Then moving onto the use of quantum statistics and eventually examining the use of a metallic tip tracing over a plane metallic sample.

Metal-semiconductor tunnelling is then examined. Here the Bloch theorem is discussed along with the idea of energy bands and gaps. This is then extended as I look at the affect of doping a semiconductor has on the tunnelling current. This means some electrons become localised and are bound in a hydrogen-like state thus requiring the use of Wannier site representation.

Then I move onto superconductors with a brief introduction of what they are and their history. I then discuss the features seen in experiments: two gaps and asymmetry, and the types of experiments that exhibit these characteristics. From there I go on to discuss a key pairing interaction in cuprates which is the real-space pairing of two electrons mediated by the electron-phonon interaction, this is an extension of the well-known BCS theory (which it is agreed describes elemental (or type I) superconductors) in the strong coupling regime.

From here I describe the Hamiltonian which is the energy operator of the system and explain the energy band structure of cuprates. I base the idea on an "LDA+GTB" model which describes the band structure as a Mott-Hubbard insulator with impurity

bandtails. Before continuing with calculations, the density of states is discussed and a model is produced that can be used analytically rather than having to make numerical calculations. Only here am I then able to go on to look at the actual tunnelling of charge carriers in cuprates.

First looking at extrinsic tunnelling (the tunnelling of charge carriers between a metal and superconducting sample) the tunnelling current is obtained using the Fermi-Dirac golden rule initially for zero temperature, then for finite temperature, including the normal-state.

Second, examining intrinsic tunnelling (the tunnelling of charge carrier between two superconductors), the tunnelling current is obtained and the conductance in the normal-state is found. Comparing this to experiment gives a nice but not perfect fit as there is some residual conductance at zero bias in the experiments. Considering temperature effects shows that this non-zero conductance at zero bias can be recreated analytically within the framework of the theory. From this it drops out that theoretically there is also a temperature dependence of the pseudogap (one of the two characteristic gaps seen in cuprates), which, when tested, follows the same dependence as indicated by experiments.

All in all, this thesis presents an analytical collection of work that can describe experimental results. Beginning with tunnelling with metals only, then including semiconductors that are undoped then doped and finally I present a theory of intrinsic and extrinsic tunnelling in cuprates which has a good agreement with experimental results.

2. METALS

Metals have a large number of free electrons enabling them to have a high electrical conductivity. The electrons available to propagate are called conduction electrons and many physical properties of metals can be understood in terms of the free electron model where ions are immersed in a "sea" of conduction electrons. In classical mechanics particles have individuality, however in quantum mechanics there exists the Heisenberg uncertainty principle which means the concept of an electron path ceases to have any meaning. There is also the principle of indistinguishability of two or more identical particles which gives the result that the wavefunction can only be symmetric or antisymmetric, see Appendix A. The particles described by symmetrical wavefunctions have integer spin, they obey Bose-Einstein statistics and are known as bosons. On the other hand, particles described by antisymmetrical wavefunctions can be shown to have half-odd integer spin, they obey Fermi-Dirac statistics and are called fermions. In a stationary state, in a system of identical fermions it can be shown that no two (or more) particles can be in identical quantum states. This stipulation is known as the Pauli exclusion principle, see Appendix A. Two electrons could still share the same energy but, for example have different spins, this would make them "degenerate". The ground state of a fermionic system involves the filling of quantum states from the bottom ($n = 1$) energy level upwards obeying the Pauli exclusion principle. The energy of the highest filled level is defined as the Fermi Energy, E_F. Temperature has an effect on the ground state. As the temperature is increased, the kinetic energy of the electron gas increases, some levels that would be occupied at zero temperature are no longer occupied and instead higher levels are filled. The Fermi-Dirac distribution gives the

probability that a system is occupied by fermion at energy E in thermal equilibrium:

$$f(E) = \frac{1}{e^{\frac{E-\mu}{k_B T}} + 1}, \tag{2.1}$$

μ is the chemical potential which is a function of temperature, it is chosen to keep the number of particles in the system equal to N. At all temperatures the Fermi-Dirac distribution is equal to one half when $E = \mu$, so for zero temperature the Fermi energy is the same as the chemical potential. k_B is the Boltzmann constant $1.3806503 \times 10^{-23} \mathrm{m^2 kgs^{-2} K^{-1}}$.

The ground state of a bosonic system is the condensation of bosons into a coherent macromolecule where all bosons share the same quantum state. In thermal equilibrium, the probability that a boson occupies the energy state E is described by the Bose-Einstein distribution, which takes into account temperature effects:

$$f(E) = \frac{1}{e^{\frac{E-\mu}{k_B T}} - 1}. \tag{2.2}$$

The density of states (DOS) describes the number of quantum states per unit energy. It is given by

$$\rho(E) = \sum_{\nu} \delta(E - E_\nu). \tag{2.3}$$

In three dimensions the DOS of a metal is proportional to the square-root of the energy. Here we discuss the tunnelling of electrons. Only electrons very close to the Fermi energy need to be considered at low enough voltages since only these will contribute to the current as they require the least amount of energy before they can tunnel. This means that $\sqrt{E} = \sqrt{E_F} \pm$ small correction. Therefore the DOS of the metal can be treated as a constant.

Sommerfeld and Bethe [1] were the first to make a theoretical study of the quantum phenomena of tunnelling between two metals separated by a thin insulating layer. They looked at what happened for very low and high voltages. Later, Holm [2] extended this to include the intermediate voltages. For further reading into tunnelling between two metals, see for example Reference [3].

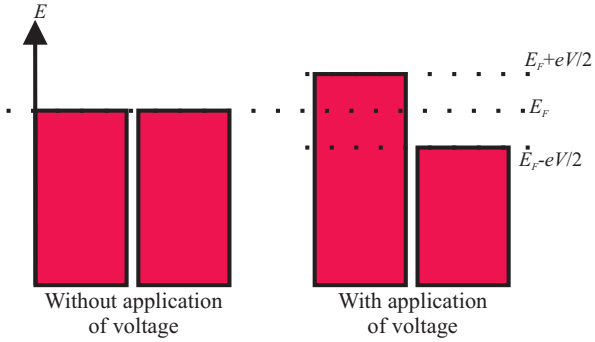

Fig. 2.1: Energy diagram of two metals separated by a thin vacuum. The left is without an applied voltage, the right shows how a bias alters the energy of the metals.

2.1 Tunnelling Between Two Metals at Zero Temperature

Initially the tunnelling of a single-particle from one metal to another through a small vacuum is considered at zero temperature. Without an applied voltage the two metals are in equilibrium and their Fermi energies are equal. The left and right electrodes are regarded as two non-interacting systems and so their wavefunctions are multiplied together to give the wavefunction of the whole system. The proximity of the electrodes provides a perturbation and so the perturbation theory can be used. All states up to E_F are filled at zero temperature. With the application of a bias the left electrode has an increase in energy of $eV/2$, (half the electron charge e, multiplied by the voltage V), the right electrode experiences the same magnitude decrease in energy. See Fig. 2.1. Considering the tunnelling of electrons with a certain spin, say spin up only, means the spin quantum number can be omitted and the Hamiltonian describing the system is given by:

$$H = \sum_{\boldsymbol{k}} \xi_{\boldsymbol{k}} a^\dagger_{\boldsymbol{k}} a_{\boldsymbol{k}} + \sum_{\boldsymbol{p}} \xi_{\boldsymbol{p}} b^\dagger_{\boldsymbol{p}} b_{\boldsymbol{p}} + \sum_{\boldsymbol{kp}} t_{\boldsymbol{kp}} \left(a^\dagger_{\boldsymbol{k}} b_{\boldsymbol{p}} + b^\dagger_{\boldsymbol{p}} a_{\boldsymbol{k}} \right). \tag{2.4}$$

The first term gives the energy of the first metallic electrode, on the left. The second is the energy of the metallic electrode on the right. The third part describes the tunnelling of electrons between electrodes and is called H_{tun}. $\boldsymbol{k}$ and $\boldsymbol{p}$ are the wavevectors of an electron in the left and right electrodes respectively, $a_{\boldsymbol{k}}$, $a^\dagger_{\boldsymbol{k}}$, $b_{\boldsymbol{p}}$ and $b^\dagger_{\boldsymbol{p}}$ are the

annihilation and creation operators of a particle in state $\boldsymbol{k}$ or $\boldsymbol{p}$ in the left and right metals respectively. $t_{\boldsymbol{kp}}$ is the hopping integral.

To find the tunnelling current, the standard perturbation theory is used in the form of the Fermi-Dirac golden rule (FDGR) which is given by:

$$W_{if} = \frac{2\pi}{\hbar} \left| \left\langle f \middle| H_{\text{tun}} \middle| i \right\rangle \right|^2 \delta \left(E_f - E_i \right), \tag{2.5}$$

which gives the probability of tunnelling from the initial state, i, to the final state f. When the charge carriers tunnel they stay in the same energy level, only the quantum state is altered, the term $\delta(E_f - E_i)$ in the FDGR ensures this. First consider the matrix element of the tunnelling Hamiltonian, $\langle f \left| H_{\text{tun}} \right| i \rangle$:

$$\left\langle f \middle| H_{\text{tun}} \middle| i \right\rangle \propto \underbrace{\left\langle f \middle| b^\dagger_{\boldsymbol{p}} a_{\boldsymbol{k}} \middle| i \right\rangle}_{(i)} + \underbrace{\left\langle f \middle| a^\dagger_{\boldsymbol{k}} b_{\boldsymbol{p}} \middle| i \right\rangle}_{(ii)}. \tag{2.6}$$

In the following it is assumed that there are no specific selection rules for the momenta, i.e. the hopping integral is a constant, $t_{\boldsymbol{kp}} = t$.

To respect the Pauli exclusion principle, in (i) the conditions are $\boldsymbol{p} > \boldsymbol{k}_F$ and $\boldsymbol{k} \leq \boldsymbol{k}_F$. This reduces (i) to unity providing the tunnelling conditions of the annihilation of an electron on the left and creation of one on the right, otherwise it gives zero. Similarly, if we have $\boldsymbol{p} \leq \boldsymbol{k}_F$ and $\boldsymbol{k} > \boldsymbol{k}_F$, then the conjugate gives either one or zero. Upon substitution of this into Equation (2.5) we have

$$W_{if} = \frac{2\pi}{\hbar} \sum_{\boldsymbol{p}>\boldsymbol{k}_F, \boldsymbol{k}\leq\boldsymbol{k}_F} t^2 \delta(E_f - E_i). \tag{2.7}$$

The summation over the wavevectors $\boldsymbol{k}$ and $\boldsymbol{p}$:

$$\sum_{\boldsymbol{k}} = \frac{V}{(2\pi)^3} \int d^3\boldsymbol{k} = \frac{V}{(2\pi)^3} \cdot 4\pi \int k^2 dk, \tag{2.8}$$

here V is the normalisation volume. $E_{\boldsymbol{k}} = \frac{\hbar^2 \boldsymbol{k}^2}{2m}$, taking the energy relative to the chemical potential, we have $\xi_{\boldsymbol{k}} = E_{\boldsymbol{k}} - \mu$ and so

$$\sum_{\boldsymbol{k}} \to 2\pi V \left(\frac{2m}{\hbar} \right)^{\frac{3}{2}} \int \sqrt{\xi + \mu}\, d\xi = \int \rho(\xi) d\xi. \tag{2.9}$$

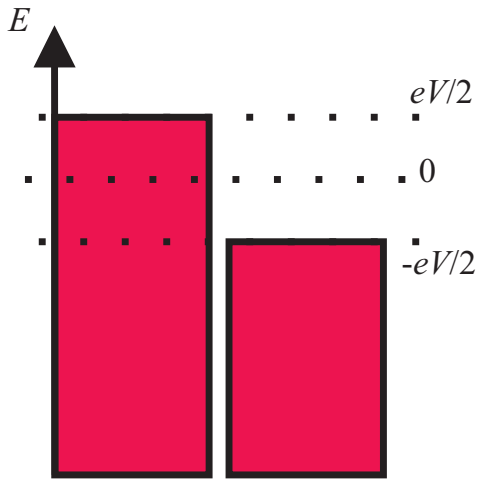

Fig. 2.2: Energy is taken relative to the chemical potential, when the voltage is applied the left electrode has energy $eV/2$ and the right electrode has energy $-eV/2$.

Similarly, for the wavevector $\boldsymbol{p}$,

$$\sum_{\boldsymbol{p}} \to 2\pi V \left(\frac{2m}{\hbar}\right)^{\frac{3}{2}} \int \sqrt{\xi' + \mu} d\xi' = \int \rho(\xi') d\xi', \tag{2.10}$$

$\rho(\xi)$ and $\rho(\xi')$ are the DOS of the left and right electrodes respectively, as aforementioned these can be approximated to be a constant. Supposing that each metal is made of the same material gives $\rho(0) \equiv g$.

Tunnelling can only occur in the energy region where the left electrode has occupied states that correspond with unoccupied states at the same energy level in the right electrode, this is in the energy range:

$$\begin{aligned} -\infty < \xi < \frac{eV}{2}; \\ -\frac{eV}{2} < \xi' < \infty. \end{aligned} \tag{2.11}$$

See Fig. 2.2.

Substituting this back into Equation (2.7)

$$W_{if} = \frac{2\pi}{\hbar} t^2 g^2 \int_{-\infty}^{eV/2} d\xi \int_{-eV/2}^{\infty} d\xi' \delta(E_f - E_i). \tag{2.12}$$

The energy of the final state is equal to the energy of the initial state with the addition of a hole on the left electrode and an electron on the right:

$$\begin{aligned} E_f &= E_i - \left(\frac{\hbar^2 \boldsymbol{k}^2}{2m} - E_F\right) + \left(\frac{\hbar^2 \boldsymbol{p}^2}{2m} - E_F\right) \\ &= E_i - \xi_{\boldsymbol{k}} + \xi_{\boldsymbol{p}} \\ E_f - E_i &= \xi_{\boldsymbol{p}} - \xi_{\boldsymbol{k}}. \end{aligned} \tag{2.13}$$

and so

$$W_{if} = \frac{2\pi}{\hbar} t^2 g^2 \int_{-\infty}^{eV/2} d\xi \int_{-eV/2}^{\infty} d\xi' \delta\left(\xi - \xi'\right). \tag{2.14}$$

Using a fundamental property of the delta function

$$\int_{-\infty}^{\infty} f(x)\delta(x-a)dx = f(a), \tag{2.15}$$

we have:

$$W_{if} = \frac{2\pi}{\hbar} t^2 g^2 \int_{-eV/2}^{eV/2} d\xi = \frac{2\pi t^2 g^2}{\hbar} eV. \tag{2.16}$$

It is clear to see that there will be no tunnelling of electrons opposing this motion, since it would violate the Pauli exclusion principle. Therefore

$$W_{fi} = 0. \tag{2.17}$$

The current is given by

$$I = e(W_{if} - W_{fi}). \tag{2.18}$$

Therefore

$$I = \frac{2\pi t^2 g^2}{\hbar} e^2 V, \tag{2.19}$$

and the conductance is

$$\sigma = \frac{dI}{dV}, \tag{2.20}$$

so

$$\sigma = \frac{2\pi t^2 g^2}{\hbar} e^2. \tag{2.21}$$

2.2 Tunnelling Between Two Metals at Finite Temperature

The results found in Equations (2.19) and (2.21) can be verified by considering temperature effects. At finite temperature there is a probability that states above the Fermi energy may be occupied without an applied voltage, this probability is given by the Fermi-Dirac distribution (Equation (2.1)) but with the added term of an applied voltage.

$$\begin{aligned} f(\xi - eV/2) &= \frac{1}{e^{\frac{\xi - eV/2}{k_B T}} + 1}; \\ f(\xi' + eV/2) &= \frac{1}{e^{\frac{\xi' + eV/2}{k_B T}} + 1}. \end{aligned} \tag{2.22}$$

Since there is an increase in energy of "$eV/2$" on the left and a decrease on the right by the same magnitude, see Fig. 2.2,

$$\begin{aligned} E_l &= \frac{\hbar^2 \boldsymbol{k}^2}{2m} - \left(E_F + \frac{eV}{2} \right) = \xi - \frac{eV}{2}; \\ E_r &= \frac{\hbar^2 \boldsymbol{p}^2}{2m} - \left(E_F - \frac{eV}{2} \right) = \xi' + \frac{eV}{2}. \end{aligned} \tag{2.23}$$

Therefore, for tunnelling from the left to the right, the left electrode has to have a charge carrier in state $\xi - eV/2$, the probability of which is given by $f(\xi - eV/2)$. As well as this we need a hole in the right in state $\xi' + eV/2$, the probability of having this is $[1 - f(\xi' + eV/2)]$ (which is the same as the probability of not having an electron in state $\xi' + eV/2$). Therefore Equation (2.12) can be written

$$W_{if} = \frac{2\pi}{\hbar} t^2 g^2 \int_{-\mu}^{\infty} d\xi \int_{-\mu}^{\infty} d\xi' f(\xi - eV/2) \left[1 - f(\xi' + eV/2) \right] \delta(\xi - \xi'), \tag{2.24}$$

where the lower limit is $-\mu$ since the energy ξ, ξ' is taken relative to the chemical potential. For tunnelling from the right to the left electrode we modify the above equation to read

$$W_{fi} = \frac{2\pi}{\hbar} t^2 g^2 \int_{-\mu}^{\infty} d\xi \int_{-\mu}^{\infty} d\xi' f(\xi' + eV/2) \left[1 - f(\xi - eV/2) \right] \delta(\xi - \xi'). \tag{2.25}$$

Using Equation (2.18) we have the current:

$$I = \frac{2\pi t^2 g^2}{\hbar} e \int_{-\mu}^{\infty} d\xi \int_{-\mu}^{\infty} d\xi' \left[f(\xi - eV/2) - f(\xi' + eV/2) \right] \delta(\xi - \xi'). \tag{2.26}$$

$$I = \frac{2\pi t^2 g^2}{\hbar} e \int_{-\mu}^{\infty} d\xi \frac{1}{e^{\frac{\xi - eV/2}{k_B T}} + 1} - \frac{2\pi t^2 g^2}{\hbar} e \int_{-\mu}^{\infty} d\xi \frac{1}{e^{\frac{\xi + eV/2}{k_B T}} + 1}. \tag{2.27}$$

These integrals are evaluated by making a change of variables, letting $h = e^{\frac{\xi + eV/2}{k_B T}}$, then $\ln h = (\xi + eV/2)/k_B T$, implies for the first term $\xi = k_B T \ln h - eV \Rightarrow\ d\xi = k_B T dh/h$. Also letting $l = e^{\frac{\xi - eV/2}{k_B T}}$ then similarly for the second term we find $\xi = k_B T \ln l + eV$ and we have

$$\begin{aligned}
I &= \frac{2\pi t^2 g^2 k_B T}{\hbar} e \left[\int_{e^{\frac{eV/2-\mu}{k_B T}}}^{\infty} \frac{1}{h+1}\frac{1}{h} dh - \int_{e^{-\frac{eV/2+\mu}{k_B T}}}^{\infty} \frac{1}{l+1}\frac{1}{l} dl \right] \\
&= \frac{2\pi t^2 g^2 k_B T}{\hbar} e \left[\int_{e^{\frac{eV/2-\mu}{k_B T}}}^{\infty} \left(\frac{1}{h} - \frac{1}{h+1} \right) dh - \int_{e^{-\frac{eV/2+\mu}{k_B T}}}^{\infty} \left(\frac{1}{l} - \frac{1}{l+1} \right) dl \right] \\
&= \frac{2\pi t^2 g^2 k_B T}{\hbar} e \left\{ [\ln h - \ln(h+1)]_{e^{\frac{eV/2-\mu}{k_B T}}}^{\infty} - [\ln l - \ln(l+1)]_{e^{-\frac{eV/2+\mu}{k_B T}}}^{\infty} \right\} \\
&= \frac{2\pi t^2 g^2 k_B T}{\hbar} e \left\{ \left[\frac{1}{k_B T}(\mu - eV/2) + \ln\left(e^{\frac{eV/2-\mu}{k_B T}} + 1 \right) \right] \right. \\
&\qquad \left. - \left[\frac{1}{k_B T}(\mu + eV/2) + \ln\left(1 + e^{\frac{\mu+eV/2}{k_B T}} \right) \right] \right\} \\
&= \frac{2\pi t^2 g^2}{\hbar} e \left[eV - k_B T \ln\left(\frac{1 + e^{\frac{eV-\mu}{k_B T}}}{1 + e^{-\frac{eV+\mu}{k_B T}}} \right) \right].
\end{aligned} \tag{2.28}$$

But the chemical potential is of the order of $10eV$ and so $\mu >> eV, k_B T$, which leaves the current as

$$I = \frac{2\pi t^2 g^2}{\hbar} e^2 V. \tag{2.29}$$

Therefore

$$\sigma = \frac{2\pi t^2 g^2}{\hbar} e^2. \tag{2.30}$$

So the conductance has no temperature dependence and we have Ohm's Law, see Figs. 2.3 and 2.4.

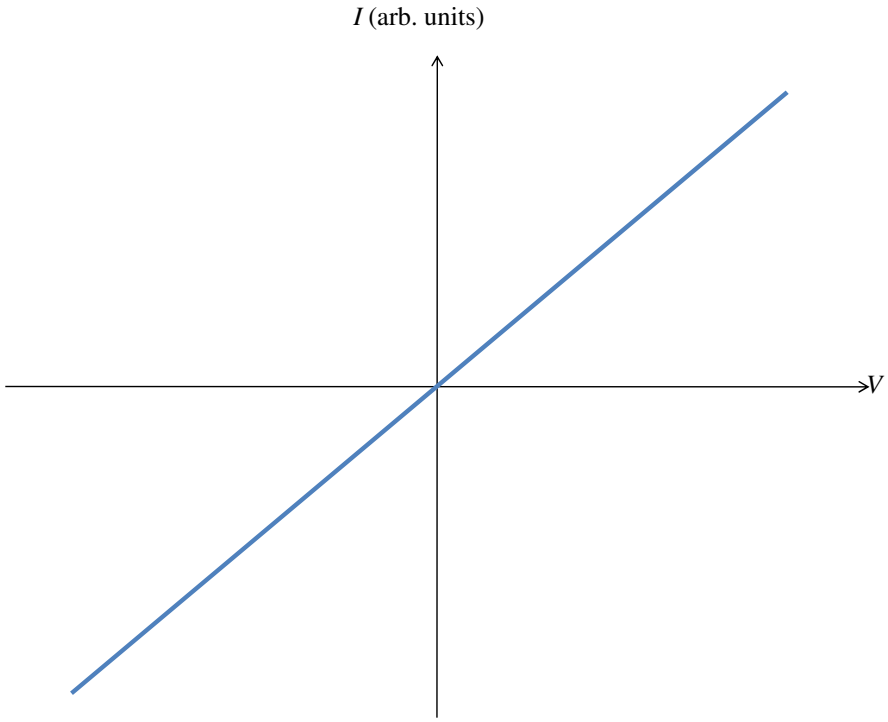

Fig. 2.3: IV curve for metal-metal tunnelling. This figure depicts both Equations (2.19) and (2.29) at zero and finite temperature respectively.

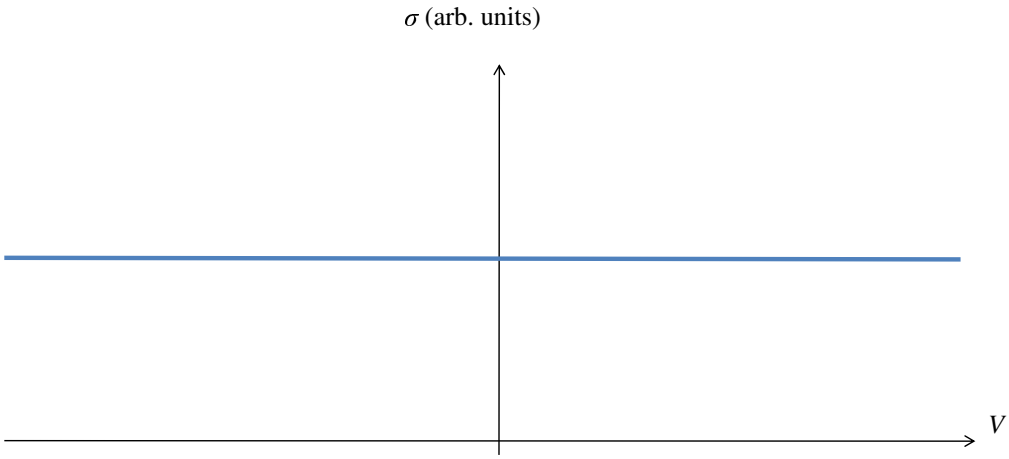

Fig. 2.4: Tunnelling spectra (or conductance vs. voltage) for metal-metal tunnelling, the same for both Equations (2.21) and (2.30) at zero and finite temperature respectively.

2.3 Tunnelling using Quantum Statistics

Let us justify the simple considerations in Sections 2.1 and 2.2 by applying quantum statistics and averaging with the density matrix. Equation (2.5) can be written as

$$W_{if} = \frac{2\pi}{\hbar}\Big\langle f\Big|H_{\text{tun}}\Big|i\Big\rangle\Big\langle i\Big|H_{\text{tun}}^{\dagger}\Big|f\Big\rangle\delta\left(E_f - E_i\right). \tag{2.31}$$

To take into consideration the different tunnelling states, we write

$$W_{m_1\to m_2} = \frac{2\pi}{\hbar}\sum_i\sum_f P(E_i)W_{if}, \tag{2.32}$$

where $P(E_i) = Z^{-1}e^{-\beta(E_i-\mu N_i)}$ is the density matrix which gives the "weighting" of W_{if}, Z is the grand partition function, N_i is the number of particles in the initial state and $\beta = (k_BT)^{-1}$. Upon substitution:

$$\begin{aligned} W_{m_1\to m_2} &= \frac{2\pi}{\hbar}\sum_i\sum_f\Big\langle f\Big|H_{\text{tun}}\Big|i\Big\rangle P(E_i)\Big\langle i\Big|H_{\text{tun}}^{\dagger}\Big|f\Big\rangle\delta\left(E_f - E_i\right) \\ &= \frac{2\pi}{\hbar}t^2\sum_i\sum_f\Big\langle f\Big|\sum_{\boldsymbol{kp}}a_{\boldsymbol{k}}^{\dagger}b_{\boldsymbol{p}}\Big|i\Big\rangle P(E_i)\Big\langle i\Big|\sum_{\boldsymbol{kp}}b_{\boldsymbol{p}}^{\dagger}a_{\boldsymbol{k}}\Big|f\Big\rangle \\ &\qquad\qquad \times\delta\left(\xi_{\boldsymbol{p}} - \xi_{\boldsymbol{k}} + eV\right). \end{aligned} \tag{2.33}$$

However, the energy of the initial state can be separated into two parts since the hopping constant, t, is not included in the summation as it does not depend on $\boldsymbol{k}$ or $\boldsymbol{p}$. This means that the energy of the system in the initial state - without perturbation - can be described explicitly as $E_i = E_i^A + E_i^B$ where superscripts A and B describe the left and right electrodes respectively. The same can be applied to the particle number and so the density matrix can be written:

$$P(E_i) = Z^{-1}e^{-\beta\left[(E_i^A+E_i^B)-\mu(N_i^A+N_i^B)\right]} = P(E_i^A)P(E_i^B). \tag{2.34}$$

So now we have

$$\begin{aligned} W_{m_1\to m_2} &= \frac{2\pi}{\hbar}t^2\sum_i\sum_f\sum_{\boldsymbol{kp}}P(E_i^A)\Big\langle i_L\Big|a_{\boldsymbol{k}}^{\dagger}\Big|f_L\Big\rangle\Big\langle f_L\Big|a_{\boldsymbol{k}}\Big|i_L\Big\rangle P(E_i^B)\Big\langle i_R\Big|b_{\boldsymbol{p}}\Big|f_R\Big\rangle\Big\langle f_R\Big|b_{\boldsymbol{p}}^{\dagger}\Big|i_R\Big\rangle \\ &\qquad\qquad \times\delta\left(\xi_{\boldsymbol{p}} - \xi_{\boldsymbol{k}} + eV\right), \end{aligned} \tag{2.35}$$

where the subscripts L and R denote left and right respectively. We can use the identities

$$\begin{aligned}\Big\langle i\Big|a_{\boldsymbol{k}}^{\dagger}a_{\boldsymbol{k}}\Big|i\Big\rangle &= \sum_{f}\Big\langle i\Big|a_{\boldsymbol{k}}^{\dagger}\Big|f\Big\rangle\Big\langle f\Big|a_{\boldsymbol{k}}\Big|i\Big\rangle,\\ \sum_{f}\Big|f\Big\rangle\Big\langle f\Big| &= 1,\end{aligned} \tag{2.36}$$

to get

$$\begin{aligned}W_{m_1\to m_2} = \frac{2\pi}{\hbar}t^2\sum_{i}\sum_{\boldsymbol{k}}P(E_i^A)\Big\langle i_L\Big|a_{\boldsymbol{k}}^{\dagger}a_{\boldsymbol{k}}\Big|i_L\Big\rangle\sum_{\boldsymbol{p}}P(E_i^B)\Big\langle i_R\Big|b_{\boldsymbol{p}}b_{\boldsymbol{p}}^{\dagger}\Big|i_R\Big\rangle\\ \times\delta\left(\xi_{\boldsymbol{p}}-\xi_{\boldsymbol{k}}+eV\right).\end{aligned} \tag{2.37}$$

Using the definition of the trace gives:

$$W_{m_1\to m_2} = \frac{2\pi}{\hbar}t^2\sum_{\boldsymbol{kp}}\mathrm{Tr}\Big(P(E_i^A)a_{\boldsymbol{k}}^{\dagger}a_{\boldsymbol{k}}\Big)\mathrm{Tr}\Big(P(E_i^B)b_{\boldsymbol{p}}b_{\boldsymbol{p}}^{\dagger}\Big)\delta\left(\xi_{\boldsymbol{p}}-\xi_{\boldsymbol{k}}+eV\right). \tag{2.38}$$

The definition of the Fermi-Dirac distribution in statistical form is:

$$n_{\boldsymbol{k}} = \sum_{i}P(E_i)\Big\langle i\,\Big|a_{\boldsymbol{k}}^{\dagger}a_{\boldsymbol{k}}\Big|\,i\Big\rangle = \mathrm{Tr}\Big(P(E_i)a_{\boldsymbol{k}}^{\dagger}a_{\boldsymbol{k}}\Big). \tag{2.39}$$

Using anti-commutation relations for fermions, where $b_{\boldsymbol{p}}b_{\boldsymbol{p}}^{\dagger} = 1 - b_{\boldsymbol{p}}^{\dagger}b_{\boldsymbol{p}}$ we have

$$W_{m_1\to m_2} = \frac{2\pi}{\hbar}t^2\sum_{\boldsymbol{kp}}n_{\boldsymbol{k}}\left(1-n_{\boldsymbol{p}}\right)\delta\left(\xi_{\boldsymbol{p}}-\xi_{\boldsymbol{k}}+eV\right), \tag{2.40}$$

where $n_{\boldsymbol{k}},\ n_{\boldsymbol{p}}$ is the occupation number of electrons in state $\boldsymbol{k}$ and $\boldsymbol{p}$ respectively.

Now we can look at tunnelling in the opposite direction. As before, the electrons tunnel from the sample to the tip. Here we expect the energy to be different, with the loss of an electron on the sample, $(-\xi_{\boldsymbol{p}})$, and the gain of an electron on the tip, $(+\xi_{\boldsymbol{k}})$. Now, we have the term "-eV" since the direction of the electrons is opposing the push from the power supply. Following the same procedure we have

$$W_{m_2\to m_1} = \frac{2\pi}{\hbar}t^2\sum_{\boldsymbol{kp}}n_{\boldsymbol{p}}\left(1-n_{\boldsymbol{k}}\right)\delta\left(\xi_{\boldsymbol{k}}-\xi_{\boldsymbol{p}}-eV\right). \tag{2.41}$$

From Equation (2.18), the current is given by

$$I = e\left(W_{m_1 \to m_2} - W_{m_2 \to m_1}\right), \tag{2.42}$$

so substitution of $W_{m_1 \to m_2}$ and $W_{m_2 \to m_1}$ gives the current as

$$I = \frac{2\pi}{\hbar} t^2 e \sum_{\boldsymbol{kp}} \left(n_{\boldsymbol{k}} - n_{\boldsymbol{p}}\right) \delta\left(\xi_{\boldsymbol{p}} - \xi_{\boldsymbol{k}} + eV\right). \tag{2.43}$$

2.4 Tunnelling Between a Metallic Tip and a Metallic Sample

The previous method describes tunnelling between two planar surfaces. Depicting tunnelling between a tiny tip and a sample like STM spectroscopy with atomic resolution requires a new Hamiltonian that takes into account the spatial position of the tip. Equation (2.4) takes the summation over momentum-space, so the Hamiltonian is described in momentum-space and is not spatially dependent. When a tip is traced along the surface of a sample the translational symmetry is lost and so we need to have real-space coordinates rather than discussing the momentum-space. To do this we need to use field operators, defined as:

$$\begin{aligned} \Psi_\alpha(\boldsymbol{r}) &= \sum_{\boldsymbol{k}} \psi_{\boldsymbol{k}}(\boldsymbol{r}) a_{\boldsymbol{k}} \qquad (2.44) \\ \Psi_\beta(\boldsymbol{r'}) &= \sum_{\boldsymbol{p}} \psi_{\boldsymbol{p}}(\boldsymbol{r'}) b_{\boldsymbol{p}} \\ \Psi^\dagger_\alpha(\boldsymbol{r}) &= \sum_{\boldsymbol{k}} \psi^*_{\boldsymbol{k}}(\boldsymbol{r}) a^\dagger_{\boldsymbol{k}} \\ \Psi^\dagger_\beta(\boldsymbol{r'}) &= \sum_{\boldsymbol{p}} \psi^*_{\boldsymbol{p}}(\boldsymbol{r'}) b^\dagger_{\boldsymbol{p}}, \qquad (2.45) \end{aligned}$$

where

$$\begin{aligned} \psi_{\boldsymbol{k}}(\boldsymbol{r}) &= u_{\boldsymbol{k}}(\boldsymbol{r}) e^{\mathrm{i}\boldsymbol{k}\cdot\boldsymbol{r}} \\ \psi_{\boldsymbol{p}}(\boldsymbol{r'}) &= u_{\boldsymbol{p}}(\boldsymbol{r'}) e^{\mathrm{i}\boldsymbol{p}\cdot\boldsymbol{r'}}, \qquad (2.46) \end{aligned}$$

are Bloch waves (see Equation (3.2)) with $u_{\boldsymbol{k}}(\boldsymbol{r})$, $u_{\boldsymbol{p}}(\boldsymbol{r'})$ periodic in the lattice constant $\boldsymbol{l}$: $u_{\boldsymbol{k}}(\boldsymbol{r}+\boldsymbol{l}) = u_{\boldsymbol{k}}(\boldsymbol{r})$ and $u_{\boldsymbol{p}}(\boldsymbol{r'}+\boldsymbol{l}) = u_{\boldsymbol{p}}(\boldsymbol{r'})$. α and β subscripts denote the tip and sample respectively. See Appendix B for information on Bloch and Wannier functions.

This means the Hamiltonian can now be expressed as

$$\begin{aligned} H = \int \underbrace{d\boldsymbol{r}}_{dxdydz} \Psi^\dagger_\alpha(\boldsymbol{r}) \left[-\frac{\hbar^2\nabla^2}{2m} + V(\boldsymbol{r}) \right] \Psi_\alpha(\boldsymbol{r}) \\ + \int d\boldsymbol{r'} \Psi^\dagger_\beta(\boldsymbol{r'}) \left[-\frac{\hbar^2\nabla^2}{2m} + V(\boldsymbol{r'}) \right] \Psi_\beta(\boldsymbol{r'}) \\ + \int d\boldsymbol{r} \int d\boldsymbol{r'} t(\boldsymbol{r},\boldsymbol{r'}) \left[\Psi^\dagger_\alpha(\boldsymbol{r}) \Psi_\beta(\boldsymbol{r'}) + \Psi^\dagger_\beta(\boldsymbol{r'}) \Psi_\alpha(\boldsymbol{r}) \right]. \qquad (2.47) \end{aligned}$$

where $V(\boldsymbol{r})$ is the periodic potential energy. The hopping depends on the position of the tip on the metallic sample, $\boldsymbol{r}$ and $\boldsymbol{r}'$ respectively. Hopping can only occur when the tip is at the same place as the sample, so $\boldsymbol{r} = \boldsymbol{r}'$, this is the only place tunnelling can occur, so we need to include a function that is zero everywhere else, a delta function. This means we can make the assumption:

$$t(\boldsymbol{r}, \boldsymbol{r}') = t(\boldsymbol{r})\delta(\boldsymbol{r} - \boldsymbol{r}'). \tag{2.48}$$

We now have:

$$H = H_0 + \int d\boldsymbol{r}\ t(\boldsymbol{r}) \left[\Psi^\dagger_\alpha(\boldsymbol{r})\Psi_\beta(\boldsymbol{r}) + \Psi^\dagger_\beta(\boldsymbol{r})\Psi_\alpha(\boldsymbol{r})\right]. \tag{2.49}$$

However, the position of the tip is fixed by the experimentalist at $\boldsymbol{r}_0$, so another approximation can be made for the hopping constant

$$t(\boldsymbol{r}) = t\ \delta(\boldsymbol{r} - \boldsymbol{r}_0). \tag{2.50}$$

So an approximation of two delta functions has been made and we have

$$H = H_0 + t \left[\Psi^\dagger_\alpha(\boldsymbol{r}_0)\Psi_\beta(\boldsymbol{r}_0) + \Psi^\dagger_\beta(\boldsymbol{r}_0)\Psi_\alpha(\boldsymbol{r}_0)\right]. \tag{2.51}$$

We can use this Hamiltonian and follow the same procedure as before to find the spatially dependent tip-metal tunnelling current.

We can substitute this new tunnelling Hamiltonian, Equation (2.51) into the FDGR, Equation (2.5), and using Equation (2.32) we have

$$\begin{aligned} W_{t\to s} &= \frac{2\pi}{\hbar} t^2 \sum_i \sum_f \sum_{\boldsymbol{kp}} \left\langle f \middle| e^{\mathrm{i}\boldsymbol{r}_0(\boldsymbol{k}-\boldsymbol{p})} u_{\boldsymbol{k}}(\boldsymbol{r}_0) u^*_{\boldsymbol{p}}(\boldsymbol{r}_0) b^\dagger_{\boldsymbol{p}} a_{\boldsymbol{k}} \middle| i \right\rangle P(E_i) \\ &\quad \left\langle i \middle| e^{\mathrm{i}\boldsymbol{r}_0(\boldsymbol{p}-\boldsymbol{k})} u^*_{\boldsymbol{k}}(\boldsymbol{r}_0) u_{\boldsymbol{p}}(\boldsymbol{r}_0) a^\dagger_{\boldsymbol{k}} b_{\boldsymbol{p}} \middle| f \right\rangle \delta\left(\xi_{\boldsymbol{p}} - \xi_{\boldsymbol{k}} + eV\right). \end{aligned} \tag{2.52}$$

The subscript t denotes the metallic tip and s the sample, $\delta(E_f - E_i) = \delta(\xi_{\boldsymbol{p}} - \xi_{\boldsymbol{k}} + eV)$ since there is a gain of an electron from the metal sample with energy $\xi_{\boldsymbol{p}}$ and the loss of an electron in the tip with energy $\xi_{\boldsymbol{k}}$, the "eV" term is included due to the push from the power supply. The density matrix is used as before in Equation (2.34). Following the same procedure as before:

$$W_{t\to s} = \frac{2\pi}{\hbar} t^2 \sum_i \sum_f \sum_{\boldsymbol{k}} P(E^A_i) \left\langle i \middle| e^{\mathrm{i}\boldsymbol{r}_0\boldsymbol{k}} u_{\boldsymbol{k}}(\boldsymbol{r}_0) a^\dagger_{\boldsymbol{k}} \middle| f \right\rangle \left\langle f \middle| e^{-\mathrm{i}\boldsymbol{r}_0\boldsymbol{k}} u^*_{\boldsymbol{k}}(\boldsymbol{r}_0) a_{\boldsymbol{k}} \middle| i \right\rangle$$

$$
\begin{aligned}
& \sum_{\boldsymbol{p}} P(E_i^B)\Big\langle i\Big|e^{-\mathrm{i}\boldsymbol{r}_0\boldsymbol{p}}u_{\boldsymbol{p}}^*(\boldsymbol{r}_0)b_{\boldsymbol{p}}\Big|f\Big\rangle\Big\langle f\Big|e^{\mathrm{i}\boldsymbol{r}_0\boldsymbol{p}}u_{\boldsymbol{p}}(\boldsymbol{r}_0)b_{\boldsymbol{p}}^\dagger\Big|i\Big\rangle\delta\left(\xi_{\boldsymbol{p}}-\xi_{\boldsymbol{k}}+eV\right) \\
= \; & \frac{2\pi}{\hbar}t^2\sum_i\sum_{\boldsymbol{k}} P(E_i^A)\Big\langle i\Big|e^{\mathrm{i}\boldsymbol{r}_0\boldsymbol{k}}e^{-\mathrm{i}\boldsymbol{r}_0\boldsymbol{k}}u_{\boldsymbol{k}}(\boldsymbol{r}_0)u_{\boldsymbol{k}}^*(\boldsymbol{r}_0)a_{\boldsymbol{k}}^\dagger a_{\boldsymbol{k}}\Big|i\Big\rangle \\
& \sum_{\boldsymbol{p}} P(E_i^B)\Big\langle i\Big|e^{-\mathrm{i}\boldsymbol{r}_0\boldsymbol{p}}e^{\mathrm{i}\boldsymbol{r}_0\boldsymbol{p}}u_{\boldsymbol{p}}^*(\boldsymbol{r}_0)u_{\boldsymbol{p}}(\boldsymbol{r}_0)b_{\boldsymbol{p}}b_{\boldsymbol{p}}^\dagger\Big|i\Big\rangle\delta\left(\xi_{\boldsymbol{p}}-\xi_{\boldsymbol{k}}+eV\right) \\
= \; & \frac{2\pi}{\hbar}t^2\sum_{\boldsymbol{kp}}\mathrm{Tr}\Big(P(E_i^A)\left|u_{\boldsymbol{k}}(\boldsymbol{r}_0)\right|^2 a_{\boldsymbol{k}}^\dagger a_{\boldsymbol{k}}\Big)\mathrm{Tr}\Big(P(E_i^B)\left|u_{\boldsymbol{p}}(\boldsymbol{r}_0)\right|^2 b_{\boldsymbol{p}}b_{\boldsymbol{p}}^\dagger\Big)\delta\left(\xi_{\boldsymbol{p}}-\xi_{\boldsymbol{k}}+eV\right) \\
= \; & \frac{2\pi}{\hbar}t^2\sum_{\boldsymbol{kp}}\left|u_{\boldsymbol{k}}(\boldsymbol{r}_0)\right|^2\left|u_{\boldsymbol{p}}(\boldsymbol{r}_0)\right|^2 n_{\boldsymbol{k}}\left(1-n_{\boldsymbol{p}}\right)\delta\left(\xi_{\boldsymbol{p}}-\xi_{\boldsymbol{k}}+eV\right). \qquad (2.53)
\end{aligned}
$$

Similarly, for the electron tunnelling in the opposite direction (from the metallic sample to the tip),

$$
W_{s\to t}=\frac{2\pi}{\hbar}t^2\sum_{\boldsymbol{kp}}\left|u_{\boldsymbol{k}}(\boldsymbol{r}_0)\right|^2\left|u_{\boldsymbol{p}}(\boldsymbol{r}_0)\right|^2\left(1-n_{\boldsymbol{k}}\right)n_{\boldsymbol{p}}\delta\left(\xi_{\boldsymbol{p}}-\xi_{\boldsymbol{k}}+eV\right). \qquad (2.54)
$$

Therefore, using Equation (2.18) the current is given by

$$
I=\frac{2\pi}{\hbar}t^2e\sum_{\boldsymbol{kp}}\left|u_{\boldsymbol{k}}(\boldsymbol{r}_0)\right|^2\left|u_{\boldsymbol{p}}(\boldsymbol{r}_0)\right|^2\delta\left(\xi_{\boldsymbol{p}}-\xi_{\boldsymbol{k}}+eV\right)\left(n_{\boldsymbol{k}}-n_{\boldsymbol{p}}\right). \qquad (2.55)
$$

3. METAL-SEMICONDUCTOR TUNNELLING

To continue with tunnelling, materials other than metals can be investigated. Here, the tunnelling of an electron between a semiconductor and metal is examined. The energy structure of a semiconductor cannot be described using the free electron model, instead we need to consider the periodic potential felt by the electron from the ions. This means Bloch's Theorem must be incorporated.

Electron waves can propagate freely through a periodic lattice, however ionic cores vibrate about their equilibrium positions and so the electron wavefunctions in a periodic potential are Bloch waves, which obey the Schrödinger equation

$$\left[-\frac{\hbar^2}{2m}\nabla^2 + V(\boldsymbol{r})\right]\psi(\boldsymbol{r}) = E\psi(\boldsymbol{r}), \tag{3.1}$$

where $V(\boldsymbol{r})$ is the periodic potential such that $V(\boldsymbol{r}+\boldsymbol{l}) = V(\boldsymbol{r})$, $\boldsymbol{l}$ is any lattice vector connecting two atoms and $V(\boldsymbol{r})$ is symmetric, $V(\boldsymbol{r}) = V(-\boldsymbol{r})$. Here, any interactions of carriers with impurities and phonons are neglected, and the mean-field approximation is adopted for the Coulomb repulsion between carriers. The eigenstates of this equation are Bloch waves:

$$\psi_{n\boldsymbol{k}}(\boldsymbol{r}) = u_{n\boldsymbol{k}}(\boldsymbol{r})e^{\mathrm{i}\boldsymbol{k}\cdot\boldsymbol{r}}, \tag{3.2}$$

where n is the band index and by Bloch's theorem $u_{n\boldsymbol{k}}(\boldsymbol{r})$ is a function with the same periodicity as the potential and the wavevector $\boldsymbol{k}$ is real. This theorem leads to energy being quantized into bands. Semiconductors have a conduction and a valence band separated by an energy gap, in which there are no energy levels that a carrier can occupy, see Fig. 3.1.

See Appendix B for more information on the Bloch theorem.

Tunnelling of electrons through a metal-semiconductor barrier has been calculated in previous literature, for example see Reference [4] and for further reading see, for example, Reference [5].

At absolute zero temperature in a homogenous semiconductor without any perturbations, the chemical potential (or Fermi energy) lies in the middle of the energy gap, leaving the valence band states occupied and conduction band states unoccupied. This is a state of equilibrium, no tunnelling can occur due to the Pauli exclusion principle if the voltage drop is less than the energy gap, see Fig. 3.2.

When a larger voltage is applied, tunnelling can take place. There must be an occupied state for a charge carrier to tunnel from and an unoccupied state for it to be able to tunnel to. The application of a potential difference to the system can supply the perturbation for this to happen.

To apply this potential difference we need to make a complete circuit, this is done by attaching a metallic electrode to either side of the semiconductor. This causes an internal electric field, $E = eV/d$, where the two electrodes act as a capacitor separated by distance d, see Fig. 3.3. Since the probability of tunnelling is exponentially dependent on the distance the electron must travel, only the conduction band near the surface needs to be considered.

For positive voltage, the electrons in the metal on the left have an increase of energy of $eV/2$, the semiconductor experiences the same magnitude decrease. In a metal, the energy is given by

$$\xi_{\boldsymbol{k}} = \frac{\hbar^2 k^2}{2m} - \mu. \tag{3.3}$$

This sets the chemical potential as the zero point. The energy of the conduction band is given by

$$\xi_{\boldsymbol{p}} = \frac{\hbar^2 p^2}{2m} + \frac{E_g}{2}. \tag{3.4}$$

The electron distribution in the metal is governed by the Fermi-Dirac distribution, Equation (2.1). In equilibrium, the chemical potential of the semiconductor lies halfway between the conduction and valence band, as the semiconductor experiences a decrease

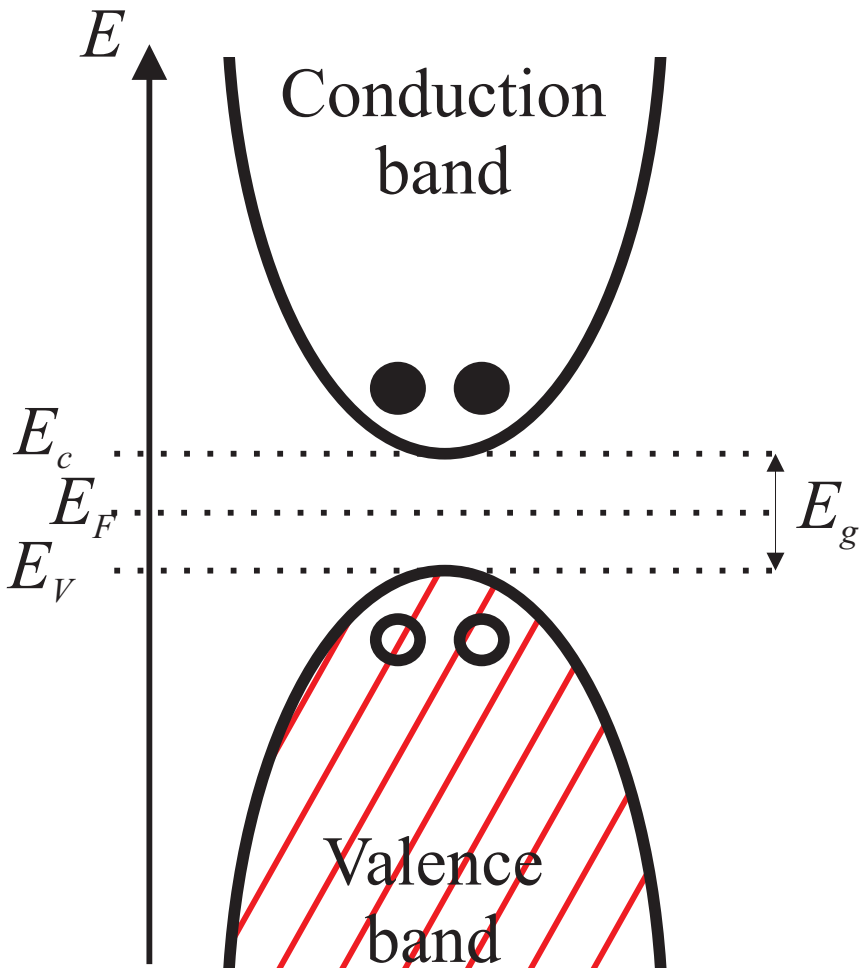

Fig. 3.1: This is the energy diagram of a semiconductor, note the conduction and valence bands separated by the energy gap, E_g, in which there are no energy states. There are holes in the valence band and conduction electrons in the conduction band at finite temperature. A hole is a vacant orbital which acts as though it has a positive charge in applied electric and magnetic fields.

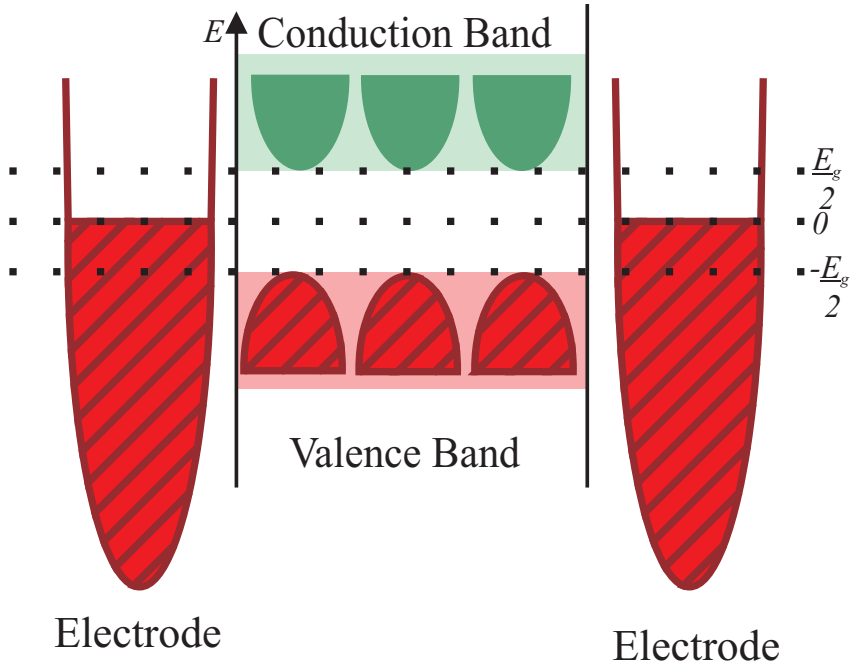

Fig. 3.2: The arrangement of the semiconductor with an electrode on either side, without application of a bias. Tunnelling cannot occur at zero temperature due to the Pauli exclusion principle. The energy here is taken relative to the chemical potential.

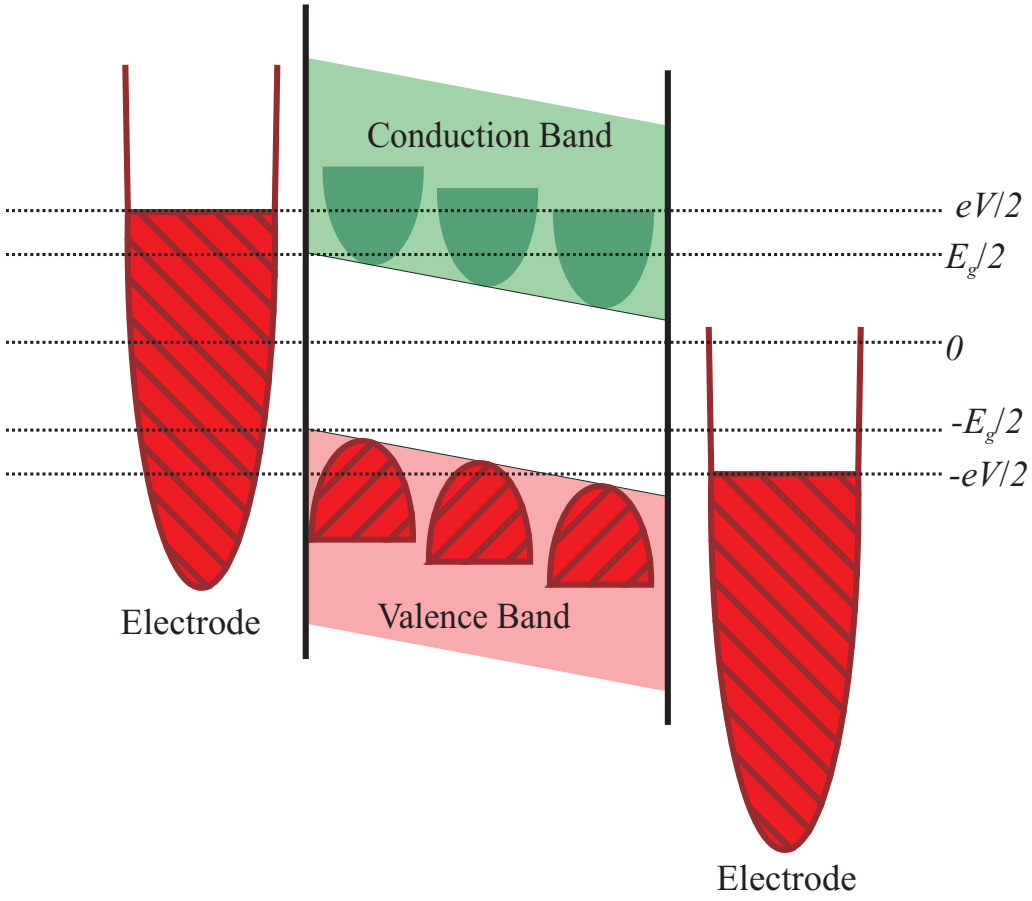

Fig. 3.3: The semiconductor energy structure is altered with the application of voltage. The two electrodes act as a capacitor causing an internal electric field.

in energy when the voltage is applied in this direction the probability of finding an electron in the conduction band (with energy $\xi_{\boldsymbol{p}}$), is zero,

$$f(\xi_{\boldsymbol{p}}) = 0. \tag{3.5}$$

The FDGR, Equation (2.5), is again used to find the probability of tunnelling. In this instance, it can be written as being proportional to the probability of finding an electron in the metal multiplied by the probability of not finding an electron in the conduction band, a delta function is included to ensure the tunnelling process costs no energy. Using Equations (2.9) and (2.10) we have

$$\begin{aligned} W_{m1\to c} &\propto \sum_{\boldsymbol{kp}} f(\xi_{\boldsymbol{k}})[1 - f(\xi_{\boldsymbol{p}})]\delta(\xi_{\boldsymbol{p}} - \xi_{\boldsymbol{k}} + eV/2) \\ &\approx \int_{-\infty}^{\infty} d\xi \int_{-\infty}^{\infty} d\xi' N_{m1}(\xi - \frac{eV}{2}) N_c(\xi') f(\xi - \frac{eV}{2}) \delta(\xi - \xi'). \end{aligned} \tag{3.6}$$

Where the substitution $\xi_{\boldsymbol{k}} + eV/2 = \xi$ has been made. Note that $f(\xi - eV/2) = 1/\left[\exp\left(\frac{\xi - eV/2}{k_B T}\right) + 1\right]$. The subscripts $m1$ and c denote the left metal and the conduction band respectively, $N_{m1}(\xi)$ and $N_c(\xi')$ denote the DOS of the metal and conduction band respectively. $N_{m1}(\xi)$ is taken to be a constant as previously explained. The DOS of the semiconductor conduction band is a step function, since it only has a value in the conduction band and there are no states in the energy gap, so the DOS in the energy gap is zero. Assuming a constant DOS for a semiconductor (which is strictly speaking valid only for 2D only), means $N_c(\xi')$ can be written as

$$N_c(\xi') = \Theta\left(\frac{eV}{2} - \xi'\right) = \begin{cases} N_c, & \xi' > \frac{E_g}{2}, \\ 0, & \xi' < \frac{E_g}{2}. \end{cases} \tag{3.7}$$

This is implemented by applying it to the integration limits

$$W_{m1\to c} = N_{m1} N_c \int_{-\infty}^{\infty} d\xi \int_{\frac{E_g}{2}}^{\infty} d\xi' f\left(\xi - \frac{eV}{2}\right) \delta(\xi - \xi'). \tag{3.8}$$

The region in which tunnelling can occur is determined by the voltage applied. The maximum energy of an electron in the metal is $eV/2$ and the minimum in the conduction band is $E_g/2$ at zero temperature. This means the tunnelling of an electron (from the

metal to the semiconductor) has to occur within these energy restrictions. These constraints are included in the integration limits

$$W_{m1\to c} = N_{m1}N_c \int_{-\infty}^{\frac{eV}{2}} d\xi \int_{\frac{E_g}{2}}^{\frac{eV}{2}} d\xi' f\left(\xi - \frac{eV}{2}\right)\delta(\xi - \xi'). \tag{3.9}$$

The probability of finding an electron within these limits for the metal is equal to one at zero temperature, so $f(\xi - \frac{eV}{2}) = 1$

$$W_{m1\to c} = N_{m1}N_c \int_{-\infty}^{\frac{eV}{2}} d\xi \int_{\frac{E_g}{2}}^{\frac{eV}{2}} d\xi' \delta(\xi - \xi'). \tag{3.10}$$

Within the region $E_g/2 < \xi' < eV/2$ the integration $\int_{-\infty}^{eV/2} d\xi\delta(\xi - \xi')$ is equal to one. Now we have

$$W_{m1\to c} = N_{m1}N_c \int_{\frac{E_g}{2}}^{\frac{eV}{2}} d\xi' = N_{m1}N_c\left(\frac{eV}{2} - \frac{E_g}{2}\right). \tag{3.11}$$

From the conditions specified, this is valid in the region $eV/2 > E_g/2$ and otherwise is zero. Therefore, we have:

$$I_{m1\to c} \propto eN_{m1}N_c\left(\frac{eV}{2} - \frac{E_g}{2}\right)\Theta\left(\frac{eV}{2} - \frac{E_g}{2}\right). \tag{3.12}$$

Tunnelling in the opposite direction can be found:

$$W_{c\to m_2} \propto \sum_{\boldsymbol{kp}} f(\xi_{\boldsymbol{p}})\left[1 - f(\xi_{\boldsymbol{k}})\right]\delta\left(\xi_{\boldsymbol{k}} - \xi_{\boldsymbol{p}} - \frac{eV}{2}\right). \tag{3.13}$$

But from earlier $f(\xi_{\boldsymbol{p}}) = 0$, so this term gives no contribution to the current. This is due to the Pauli exclusion principle (there are no occupied states for electrons to tunnel from and no unoccupied states with the same energy for them to tunnel to).

The same procedure can be followed for the application of voltage in the opposite direction, where we now have the involvement of the semiconductor conduction band and the electrode on the right. This gives the result

$$I_{c\to m2} \propto eN_{m2}N_c\left(-\frac{eV}{2} - \frac{E_g}{2}\right)\Theta\left(-\frac{eV}{2} - \frac{E_g}{2}\right). \tag{3.14}$$

Note that here it is assumed that the semiconductor DOS is a constant which is the case for a two dimensional electron spectrum only.

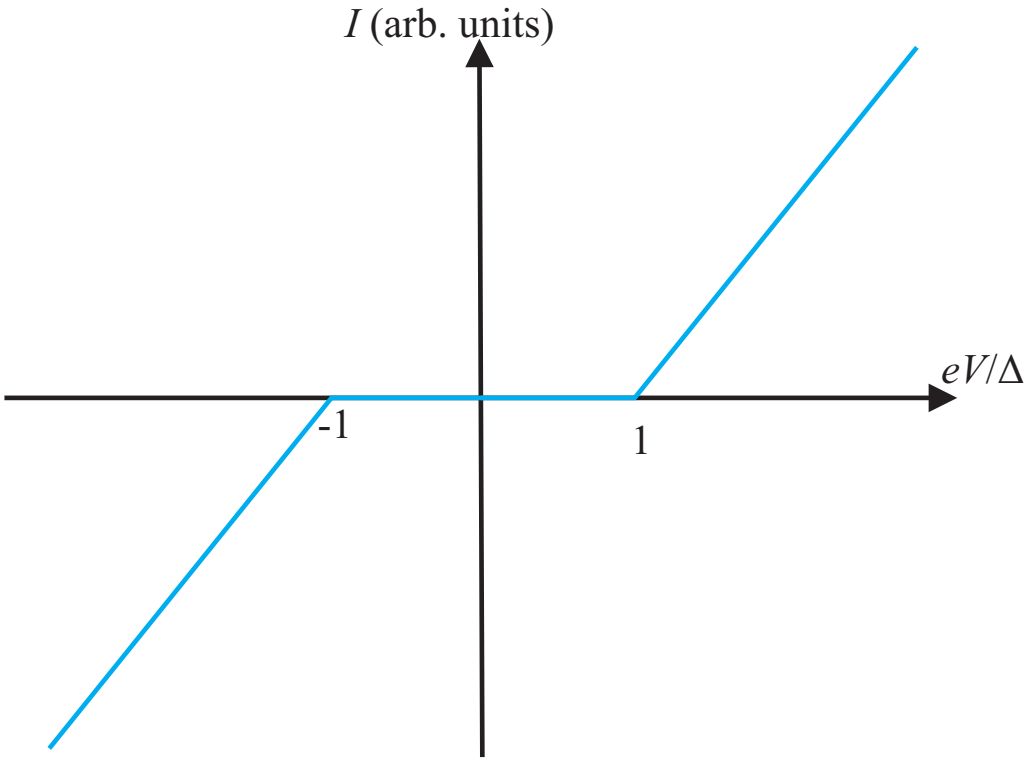

Fig. 3.4: IV curve for metal-semiconductor tunnelling. There is no current in the region $-\Delta < eV < \Delta$ (where $\Delta = E_g/2$) as this is the energy gap in which there are no states that charge carriers can occupy.

.

We can assume the electrodes are each the same metal so they have the same DOS, $N_{m1} = N_{m2} = N_m$. The total current can be written

$$\begin{aligned} I &= I_{m1\to c} - I_{c\to m2} \\ &= eN_mN_c\left(\frac{eV}{2} - \frac{E_g}{2}\right)\Theta\left(\frac{eV}{2} - \frac{E_g}{2}\right) \\ &\quad + eN_mN_c\left(-\frac{eV}{2} - \frac{E_g}{2}\right)\Theta\left(\frac{eV}{2} + \frac{E_g}{2}\right), \end{aligned} \tag{3.15}$$

which is illustrated in Fig. 3.4. The conductance is found by applying Equation (2.20) and is shown in Fig. 3.5.

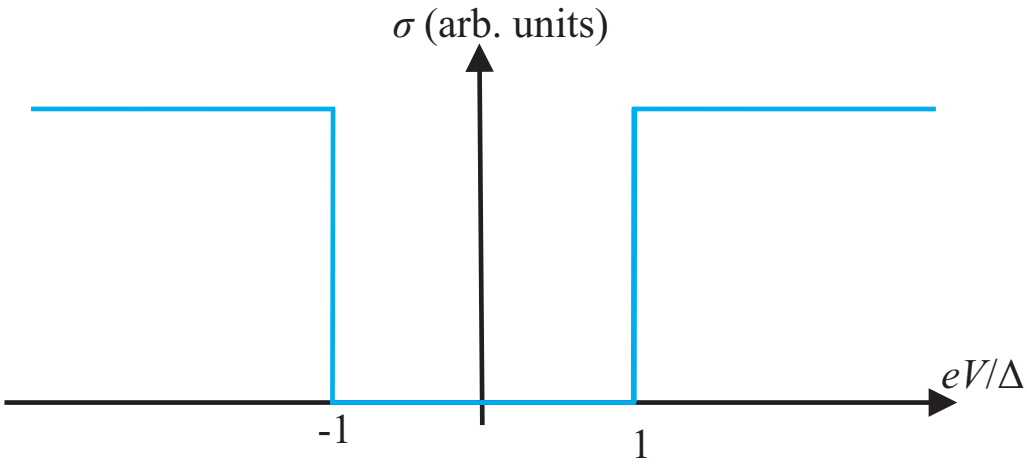

Fig. 3.5: There is no conductance in the region $-\Delta < eV < \Delta$ (where $\Delta = E_g/2$) as there is no current (the conductance is the differential of the current with respect to voltage).

.

3.1 Doping a Semiconductor

The action of doping a semiconductor introduces impurities, each impurity introduces an additional field that acts on the electrons in the semiconductor. It is supposed that the Coulomb potential changes slowly so the effective mass approximation can be utilised.

Certain impurities and imperfections can have a drastic effect on the electrical properties of a semiconductor. When doping is performed it is done to add either donor or acceptor states to the system. Reference [6] considers the effect of doping silicon or germanium, these atoms crystallise in the diamond structure, each atom forms four covalent bonds, one with each of its nearest neighbours corresponding to the chemical valence four. If an impurity atom of valence five, such as phosphorous, arsenic or antimony is substituted into the lattice in place of an atom, there will be one valence electron from the impurity atom left over after the four covalent bonds are established with the nearest neighbours, that is, after the impurity atom has been accommodated

in the structure with as little disturbance as possible. Impurity atoms that give up an electron are called donors. The impurity atoms take the position of normal atoms rather than in interstitial positions. The crystal as a whole remains neutral as the extra electron remains within the crystal. The electron moves in the Coulomb potential of the impurity ion. The semiconductor can conduct in the impurity band by electron hopping from donor to donor.

Alternatively, a hole may be bound to a trivalent impurity in germanium or silicon, just as an electron is bound to a pentavalent impurity. Trivalent impurities such as boron, aluminium, gallium and indium are called acceptors because they accept electrons from the valence band in order to complete covalent bonds with neighbour atoms, leaving holes in the band [6].

If a neutral foreign atom is implanted into semiconductor that has an extra valence electron with weaker bonds with the lattice site, it can move in the lattice field. The extra electron can exist in a bound state on an energy level just below the conduction band, or if it has enough energy, as a free electron in the conduction band. The implanted atom is a donor impurity. The loss of the extra electron means we are left with a positive impurity ion.

If the foreign atom has one fewer electron then it can borrow an electron from the valence band, leaving behind a hole in the valence band. This sort of impurity is an acceptor. The binding of the extra electron with the impurity atom, means we are left with a negative impurity ion.

This means that we have the splitting off of an energy level from the bottom of the valence band or the top of the conduction band, creating bound electron states of the acceptor or donor type respectively, see Fig. 3.6 and Fig. 3.7. Our previous tunnelling Hamiltonian for the tunnelling of charge carriers through a semiconductor and metal had translational symmetry and was thus described in terms of the wavevector quantum number. However, if we think of one of the electrodes as now being a tip, the translational symmetry is broken and rather than using the wavevector, we now need to have our Hamiltonian in terms of spatial coordinates. A further complication

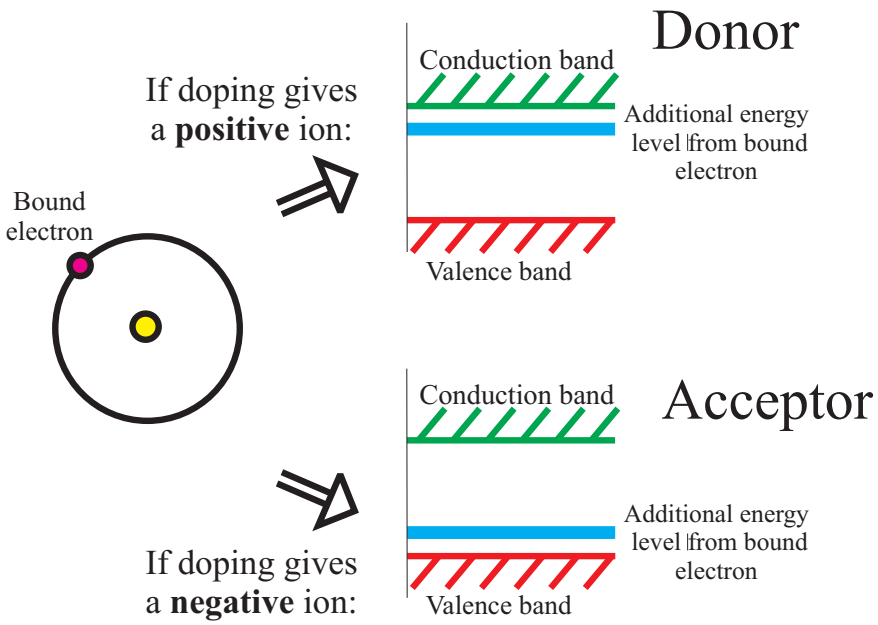

Fig. 3.6: When a semiconductor is doped, the impurity brings with it an energy level which sits in the energy gap. For a donor impurity the energy level splits from the conduction band, with an acceptor impurity the energy level splits from the valence band.

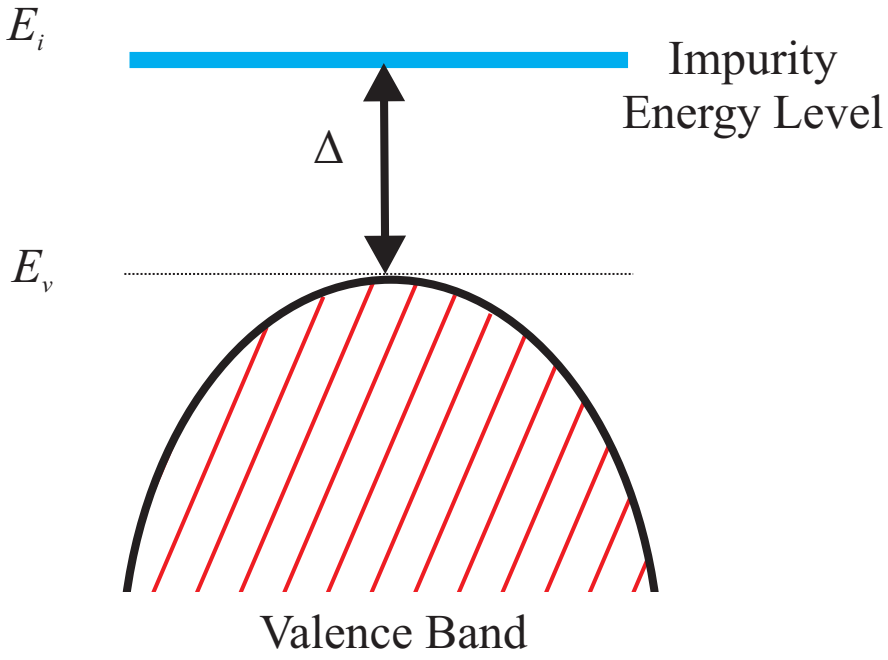

Fig. 3.7: The impurity level sits above the valence band when a acceptor atom is added to the system, it has energy Δ more than the top most energy of the valence band.

is that our semiconductor sample is no longer homogeneous, instead we now have a random doping of impurities.

This means using field operators for the metal (given earlier by Equations (2.44), (2.45) and (2.46)), for the semiconductor we have:

$$\begin{aligned} \Phi(\boldsymbol{r}') &= \sum_j F_j(\boldsymbol{r}')b_j \\ \Phi^\dagger(\boldsymbol{r}') &= \sum_j F_j^*(\boldsymbol{r}')b_j^\dagger, \end{aligned} \tag{3.16}$$

where j describes quantum numbers $(\boldsymbol{l}, n)$. If we assume the impurity sits in the ground state ($n = 1$) of a hydrogen-like atom, we have

$$F_{\boldsymbol{l}}(\boldsymbol{r}') = u(\boldsymbol{r}')\frac{1}{(\pi a_B^3)^{\frac{1}{2}}}e^{-\frac{|\boldsymbol{r}'-\boldsymbol{a_l}|}{a_B}}. \tag{3.17}$$

$\boldsymbol{a_l}$ is the impurity position vector in the host lattice, a_B is the Bohr radius, $\hbar^2/m^*e^{*2}$, $u(\boldsymbol{r}')$ is the periodic multiplier of the Bloch function at the top of the band (i.e. with $\boldsymbol{k} = 0$) (for more information on Wannier representation, see Appendix B). The Hamiltonian can be expressed as

$$H = H_0 + \int_{-\infty}^{\infty} d\boldsymbol{r} \int_{-\infty}^{\infty} d\boldsymbol{r}'\ t(\boldsymbol{r}, \boldsymbol{r}')\Big[\Psi^\dagger(\boldsymbol{r})\Phi(\boldsymbol{r}') + \Phi^\dagger(\boldsymbol{r}')\Psi(\boldsymbol{r})\Big], \tag{3.18}$$

where H_0 describes the energy of the metallic tip and semiconductor sample (with impurities) without a perturbation. Following the same procedure as for the metal-metal tunnelling case, Section 2.4,

$$t(\boldsymbol{r}, \boldsymbol{r}') = t(\boldsymbol{r})\delta(\boldsymbol{r} - \boldsymbol{r}'), \tag{3.19}$$

so

$$H = H_0 + \int_{-\infty}^{\infty} d\boldsymbol{r}\ t(\boldsymbol{r})\left[\Psi^\dagger(\boldsymbol{r})\Phi(\boldsymbol{r}) + \Phi^\dagger(\boldsymbol{r})\Psi(\boldsymbol{r})\right]. \tag{3.20}$$

The position of the tip is controlled by the experimentalist at $\boldsymbol{r}_0$, so we can rewrite

$$t(\boldsymbol{r}) = t\delta(\boldsymbol{r} - \boldsymbol{r}_0). \tag{3.21}$$

So the tunnelling Hamiltonian is given by:

$$H_{\text{tun}} = t\left[\Psi^\dagger(\boldsymbol{r}_0)\Phi(\boldsymbol{r}_0) + \Phi^\dagger(\boldsymbol{r}_0)\Psi(\boldsymbol{r}_0)\right]$$

$$= t\sum_{\boldsymbol{kl}}\left[\psi^*_{\boldsymbol{k}}(\boldsymbol{r}_0)F_{\boldsymbol{l}}(\boldsymbol{r}_0)a^\dagger_{\boldsymbol{k}}b_{\boldsymbol{l}} + F_{\boldsymbol{l}}(\boldsymbol{r}_0)\psi_{\boldsymbol{k}}(\boldsymbol{r}_0)b^\dagger_{\boldsymbol{l}}a_{\boldsymbol{k}}\right]. \tag{3.22}$$

Using the FDGR, Equation (2.5) we have

$$\begin{aligned} W &= \frac{2\pi t^2}{\hbar}\left\langle f\left|\sum_{\boldsymbol{kl}}F_{\boldsymbol{l}}(\boldsymbol{r}_0)\psi_{\boldsymbol{k}}(\boldsymbol{r}_0)b^\dagger_{\boldsymbol{l}}a_{\boldsymbol{k}}\right|i\right\rangle\left\langle i\left|\sum_{\boldsymbol{kl}}F_{\boldsymbol{l}}(\boldsymbol{r}_0)\psi^*_{\boldsymbol{k}}(\boldsymbol{r}_0)a^\dagger_{\boldsymbol{k}}b_{\boldsymbol{l}}\right|f\right\rangle \\ &\qquad \times\delta(E_f - E_i). \end{aligned} \tag{3.23}$$

To find tunnelling from all possible initial to all possible final states, we need to use the density matrix, $P(E_i) = Z^{-1}e^{-\beta(E_i-\mu N_i)}$, where Z is the grand partition function. We have

$$\begin{aligned} W_{t\to s} &= \frac{2\pi}{\hbar}\sum_i\sum_f P(E_i)W \\ &= \frac{2\pi t^2}{\hbar}\sum_i\sum_f\left\langle f\left|\sum_{\boldsymbol{kl}}F_{\boldsymbol{l}}(\boldsymbol{r}_0)\psi_{\boldsymbol{k}}(\boldsymbol{r}_0)b^\dagger_{\boldsymbol{l}}a_{\boldsymbol{k}}\right|i\right\rangle P(E_i) \\ &\qquad \left\langle i\left|\sum_{\boldsymbol{kl}}F_{\boldsymbol{l}}(\boldsymbol{r}_0)\psi^*_{\boldsymbol{k}}(\boldsymbol{r}_0)a^\dagger_{\boldsymbol{k}}b_{\boldsymbol{l}}\right|f\right\rangle\delta(E_f - E_i). \end{aligned} \tag{3.24}$$

The energy of the system in its initial state can be described as a summation of the energy of the tip and the energy of the sample, as can the number of particles, so as before we have Equation (2.34) and we can write

$$\begin{aligned} W_{t\to s} &= \frac{2\pi t^2}{\hbar}\sum_i\sum_f\sum_{\boldsymbol{k}}P(E_i^{\text{tip}})\left\langle i\middle|\psi^*_{\boldsymbol{k}}(\boldsymbol{r}_0)a^\dagger_{\boldsymbol{k}}\middle|f\right\rangle\left\langle f\middle|\psi_{\boldsymbol{k}}(\boldsymbol{r}_0)a_{\boldsymbol{k}}\middle|i\right\rangle \\ &\quad \sum_{\boldsymbol{l}}P(E_i^{\text{sample}})\left\langle i\left|F_{\boldsymbol{l}}(\boldsymbol{r}_0)b_{\boldsymbol{l}}\right|f\right\rangle\left\langle f\middle|F_{\boldsymbol{l}}(\boldsymbol{r}_0)b^\dagger_{\boldsymbol{l}}\middle|i\right\rangle\delta(E_f - E_i) \\ &= \frac{2\pi t^2}{\hbar}\sum_i\sum_{\boldsymbol{k}}P(E_i^{\text{tip}})\left\langle i\left|\psi^*_{\boldsymbol{k}}(\boldsymbol{r}_0)\psi_{\boldsymbol{k}}(\boldsymbol{r}_0)a^\dagger_{\boldsymbol{k}}a_{\boldsymbol{k}}\right|i\right\rangle \\ &\quad \sum_{\boldsymbol{l}}P(E_i^{\text{sample}})\left\langle i\left|F^2_{\boldsymbol{l}}(\boldsymbol{r}_0)b_{\boldsymbol{l}}b^\dagger_{\boldsymbol{l}}\right|i\right\rangle\delta(E_f - E_i) \\ &= \frac{2\pi t^2}{\hbar}\sum_i\sum_{\boldsymbol{kl}}\text{Tr}(P(E_i^{\text{tip}})a^\dagger_{\boldsymbol{k}}a_{\boldsymbol{k}})\text{Tr}(P(E_i^{\text{sample}})F^2_{\boldsymbol{l}}(\boldsymbol{r}_0)b_{\boldsymbol{l}}b^\dagger_{\boldsymbol{l}})\delta(E_f - E_i) \\ &= \frac{2\pi t^2}{\hbar}\sum_{\boldsymbol{kl}}F^2_{\boldsymbol{l}}(\boldsymbol{r}_0)n_{\boldsymbol{k}}(1-n_{\boldsymbol{l}})\delta(E_f - E_i). \end{aligned} \tag{3.25}$$

Similarly,

$$W_{s\to t} = \frac{2\pi t^2}{\hbar} \sum_{\boldsymbol{kl}} F_{\boldsymbol{l}}^2(\boldsymbol{r}_0)(1 - n_{\boldsymbol{k}})n_{\boldsymbol{l}}\delta(E_f - E_i). \tag{3.26}$$

Using Equation (2.18) the current is given by

$$\begin{aligned} I &= e\,(W_{t\to s} - W_{s\to t}) \\ &= \frac{2\pi t^2 e}{\hbar} \sum_{\boldsymbol{kl}} F_{\boldsymbol{l}}^2(\boldsymbol{r}_0)(n_{\boldsymbol{k}} - n_{\boldsymbol{l}}). \end{aligned} \tag{3.27}$$

where $n_{\boldsymbol{k}}$ and $n_{\boldsymbol{l}}$ are the occupation numbers of the tip (in state $\boldsymbol{k}$) and impurity state (in state $\boldsymbol{l}$).

4. SUPERCONDUCTORS

4.1 Introduction to Superconductors

Before the discovery of superconductivity in 1911 no one knew what happened to the resistance of materials at low temperatures, it was speculated that particles would become static and so the resistance would be infinite, or perhaps it would become a constant at some temperature and then remain at this value as temperature decreased, perhaps the resistance would decrease linearly with temperature. The idea that the resistance would completely vanish at a temperature called the transition temperature was a complete shock when it was discovered by Heike Kamerlingh Onnes (or rather one of his assistants) in 1911. Eventually this behaviour was explained in 1957 by J. Bardeen, J. Cooper and R. Schrieffer in the form of their BCS theory [7]. This theory is based on a Fermi-liquid normal-state with an interaction with a bosonic field (phonons). It is argued that electrons form Cooper pairs [8], where electrons with equal and opposite momenta experience an attraction to one another near the Fermi level through their interaction with phonons. Pair formation corresponds to the onset of superconductivity and the transition temperature, this is in contrast to the mechanism of superfluidity in He^4, where bosons exist above the superfluid temperature and superfluidity relates to the Bose-Einstein condensation (BEC).

This works for elemental superconductors with a weak electron-phonon interaction (EPI). This theory was extended in 1960 to give a strong coupling theory [9] which explains the properties of superconductors with intermediate EPI strength and is applicable when the electron correlation length is large compared to the distance between them. It was Fröhlich in 1950 [10] who first realised that electrons could be coupled

to each other through their phonon interactions, he suggested that superconductivity was instigated by EPI.

Reference [11] discusses evidence supporting this suggestion in the form of the isotope effect. The origin of the electron-electron interaction can be tested by isotope substitution, when an ion mass M is varied without any change of electronic configuration of the ion. There are two parameters in the BCS expression for the transition temperature, $T_c = 2e^{0.577}\omega_D/\pi \exp\left[-\frac{1}{\lambda}\right]$, where ω_D is the characteristic phonon frequency and λ is the coupling constant which depends on the mechanism of the interaction. ω_D is proportional to $1/\sqrt{M}$ as a frequency of any harmonic oscillator. However, λ is independent of the ion mass. Hence the isotope exponent is found as

$$\alpha = -\frac{d\ln T_c}{d\ln M} = 0.5. \tag{4.1}$$

In fact, α could be less than 0.5 for a BCS superconductor because of the Coulomb repulsion and the anharmonicity of phonons. The finite value of α measured experimentally proves that phonons are involved in the pairing mechanism [11].

Research with superconductors then began to dwindle as it was believed that the mechanism behind superconductivity was fully explained and it had few applications due to its low transition temperature. This was compromised in 1986 with the discovery of high-T_c superconductivity [12]. A lanthanum barium copper oxide was the first compound displaying a transition temperature beyond the threshold predicted by the BCS theory, implying a different mechanism behind the superconductivity. Now, we know there are many compounds containing copper and oxygen that exhibit high-temperature superconductivity, these form the cuprate family. Cuprates are distinguishable from conventional superconductors by originating from the doping of the parent insulator lattice. The superconducting parts are weakly coupled two dimensional doped layers, held together by the parent lattice.

More recently doped fullerenes, MgB_2 and in particular iron based high-temperature superconductors called “pnictides” have been discovered. These pnictides present their own challenge in the pursuit towards a theory of high-temperature superconductivity. They appear to be different from cuprates in terms of their electronic structure, mag-

netic order, correlation effects, superconducting symmetry, and their parent state is metallic rather than insulating. Currently the most popular suggestion for the pairing mechanism is the interaction between a mediating boson and spin fluctuations with wavevectors close to $Q = (\pi, \pi)$. However, the interplay between spin fluctuations and EPI remains a complex problem, taking into account the peculiarities of pnictides (for example controversial isotope effects, structural instabilities and low carrier densities).

4.2 Two Gaps in Cuprates

Cuprates have unique properties, as well as their high transition temperature they also possess two energy scales, or gaps: The BCS-like "superconducting" gap (SG) present in cuprates and other related compounds, develops at the superconducting critical temperature. There also exists another energy gap, the "pseudogap" (PG) which is a large anomalous gap that exists well above the transition temperature.

The SG is a coherent gap present only in the superconducting state. It can be seen by different experimental techniques including angle resolved photoemission spectroscopy (ARPES), scanning tunnelling spectroscopy and microscopy (STS/M), break junction experiments, femtosecond spectroscopy, etc. The tunnelling experiments indicate that the SG is independent of position and it does not appear to change when the doping concentration is altered. Because the PG persists above the transition temperature it can be seen in both the normal and superconducting states of cuprates. It was first observed in spin responses [13] and STS [14] in underdoped YBCO. Many experiments have since exhibited this gap. There have been quite a few different theories offered towards the explanation of the PG. These can be roughly divided into two groups. The first group argues that the PG originates from some order, static or fluctuating; the second group understands the PG is the precursor of the SG and reflects pair fluctuations above the transition temperature, as explained in Reference [15].

Some of the theories from the first group see the superconducting state as being a result of a doped Mott insulator (for example Reference [16], see Reference [17] for a review). In his resonating valence bond (RVB) theory, Anderson focuses on the ground state and low lying excitations, the origin of the PG is seen as the spin gap associated with the breaking of RVB singlets [18]. It has been suggested that adding impurities to (or doping) cuprates could weaken the order parameter (for example this order parameter could be antiferromagnetic spin fluctuations [19]) and thus be the cause of the PG. It has been argued that the PG is a consequence of a spin density wave (SDW) or charge density wave (CDW) state [20], or an interplay between the two [21]. Another idea is that the PG could be the result of inhomogeneous charge distribution containing

hole-rich and hole-poor domains [22, 23], or the cause of the SG and PG could be the inter-band pairing of an itinerant band and defect states [24].

The second group bases the understanding of the PG and high-T_c superconductivity on pairing interactions. The first explanation of the PG was offered in the form of real-space preformed hole pairs [25] called small bipolarons, bound together by a strong electron-phonon interaction (EPI). Another idea was the momentum-space pairing of preformed Cooper pairs [26]. It has however been implied that the short coherence length of cuprate superconductors suggests they lie somewhere between the BCS limit of very large momentum-space pairs and the opposite case of small real-space pairs undergoing a Bose-Einstein condensation (BEC) [27]. The BCS-BEC crossover has been studied in detail, for example in Reference [28] a superfluid state is approached in a system of localised bosons (tightly bound electron pairs) in contact with a reservoir of itinerant fermions (electrons), it is assumed the spontaneous decay and recombination between the two species causes superconductivity and the PG is a consequence of this, opening up in the fermionic density of states (DOS). Another idea into the BCS-BEC crossover came from the nearest-neighbour attractive Hubbard model, where the cause of the PG was the existence of two different bosonic modes leading to an angle-dependent boson distribution function where two-particle states "eat" the single-particle spectral weight in certain areas of momentum [29]. Reference [15] elucidates that attractive Hubbard models have been considered as the origin of superconductivity and the PG (for example see References [30, 31]). Another idea with incoherent d-wave quasiparticles suggests that when the phase-coherence length exceeds the Cooper pair size, a PG appears [32], the phase fluctuations of a $d_{x^2-y^2}$ pairing gap in a two dimensional BCS-like Hamiltonian approach is thought to be the origin of the PG [33]. A phenomenological theory was produced that allowed the modelling of the effect of local superconducting correlations and long-range phase fluctuations on the spectral properties of high-temperature superconductors by reasoning that the PG is connected to the character of the excitations that are responsible for destroying superconductivity [34].

Despite all these ideas, we are currently without general consensus as to the origin of

high-temperature superconductivity, the PG and the gapped tunnelling conductance in cuprates.

Femtosecond spectroscopy is a useful tool for studying the temperature dependence of gaps, for example Reference [35, 36] explores the temperature independence of the PG and dependence of the SG in $Y_{1-x}CaBa_2Cu_3O_{7-\delta}$ and $HgBa_2Ca_2Cu_3O_{8+\delta}$. Raman spectroscopies have found two energy scales [37]. ARPES has provided constructive information about cuprates, ARPES performed on Bi2212 [38, 39, 40, 41], Bi2201 [42], LSCO [43], LBCO [44] and CaNaCuOCl [45] has demonstrated the existence of two energy scales in cuprates.

Scanning tunnelling microscopy (STM) offers a powerful technique for looking at the doping, temperature and spatial dependence of the DOS with high resolution. It is sensitive to the DOS near the Fermi energy and to a gap in the quasiparticle excitation spectrum [46]. Extrinsic tunnelling experiments have left us with many questions regarding the properties of cuprates. STM tunnelling spectra exhibit an SG and PG [47, 48, 49] whose origins remains unaccounted for, despite many ideas already partially discussed. STM results on single crystals of Bi2212 (for example [50, 51, 52]) and LSCO [53, 54] have verified the temperature, doping and spatial dependence of the SG and PG. In particular, in NS tunnelling, Kato et al [54] found that the PG is not uniform in real-space and its spatial average increases with decreasing hole concentration in spite of suppression of critical temperature. On the other hand a smaller gap (presumable SG) is uniform across the sample and is less doping dependent. See Figs. 4.1 and 4.2 for recent examples of STM with cuprates.

Intrinsic (superconductor-superconductor, SS) tunnelling experiments on small Bi2212 [55, 56, 57, 58] and LSCO [59] mesas have found sharp quasiparticle peaks at the SG and broad humps that represent the PG [55]. The advantages of intrinsic tunnelling are that it is a direct spectroscopic technique that avoids problems like surface deterioration [57], it probes the bulk electronic properties of samples, it provides a high resolution whilst being mechanically stable so it is perfectly suited for temperature dependent studies of high-T_c superconductors [58]. Break junction experiments also exhibit the

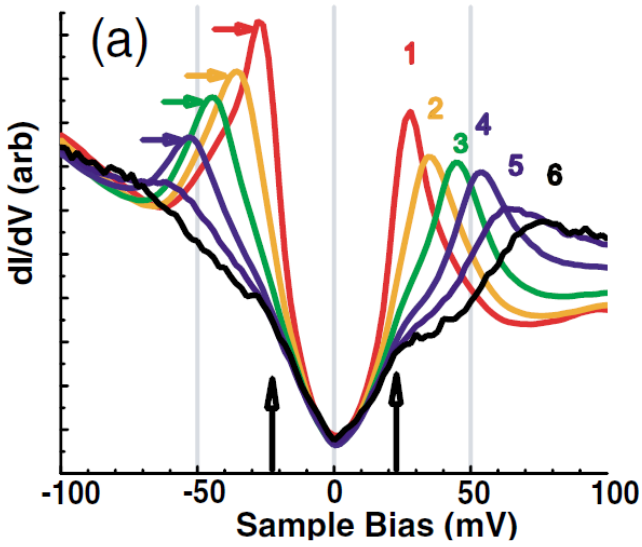

Fig. 4.1: Figure taken from Reference [50] showing STM results with Bi2212 samples taken at 20K (so the sample is in the superconducting state). Both the SG and PG are evident, the SG indicated by the black vertical arrows, the PG by the horizontal arrows. Each colour indicates tunnelling spectra taken at a different doping concentration. The SG is unaffected by the doping unlike the PG. Reproduced with permission from J. C. Davis. (K. McElroy, K. M. Lang, J. Lee, E. W. Hudson, H. Eisaki, S. Uchida and J. C. Davis, Phys. Rev. Lett. **94** 197005 (2005). © American Physical Society.)

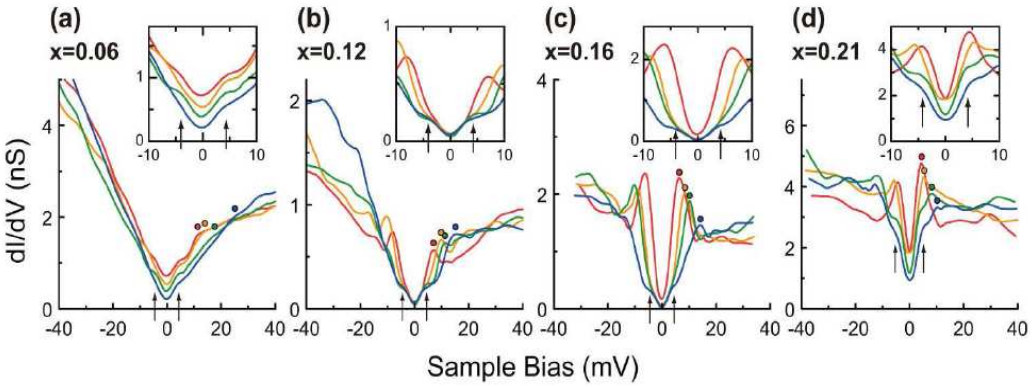

Fig. 4.2: Figure taken from Reference [54] showing STM results with LSCO. These results are more difficult to obtain than STM with Bi2212 since it cannot be cleaved so easily. Asymmetry is present in each spectrum as is the SG and PG. From left to right the doping level is increased from $x = 0.06$, which is strongly underdoped, to $x = 0.21$, which is overdoped. At each doping level the spectra is taken at different spatial positions on the LSCO sample. Here, the SG is almost position and doping independent, the PG is dependent on both position and doping. Notice the similarity of these results with those of Bi2212, Fig. 4.1. Reproduced with permission from T. Kato and JPSJ. (T. Kato, T. Maruyama, S. Okitsu and H. Sakata, J. Phys. Soc. Jpn. **77** 054710 (2008). © JPSJ.)

SG [60, 61] in underdoped Bi2212 samples, the coexistence of the SG and the PG is seen in Bi2201 [62] and Bi2212 [63] and quasiparticle energy gaps are found in Bi2212 tunnelling spectra [64, 65].

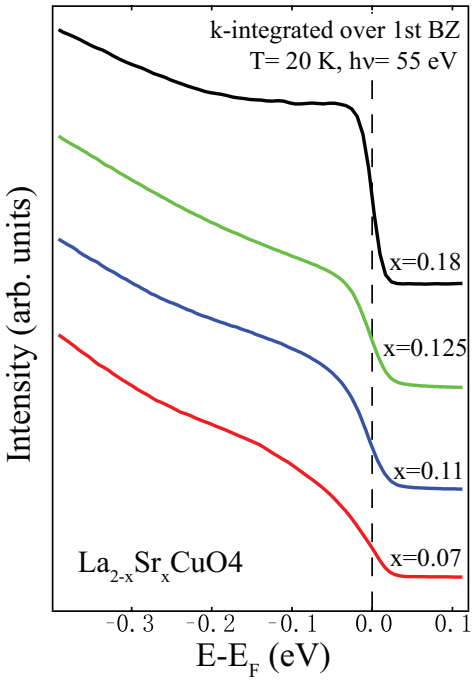

Fig. 4.3: Momentum integrated photoemission over the first Brillouin zone of $La_{2-x}Sr_xCuO_4$ [67], showing no sign of the van Hove singularity. Reproduced with permission from R. H. He.

4.3 Asymmetry in NS Tunnelling

Another intriguing characteristic feature of cuprates seen in NS tunnelling experiments is the asymmetry between the positive and negative bias in the tunnelling spectra. This asymmetry reveals that the direction of the tunnelling carriers affects the tunnelling conductance. One possible explanation of the asymmetry was offered by the van Hove singularity of the DOS. The presence of this would lead to a breakdown of the particle-hole symmetry, as a consequence an asymmetry with respect to zero bias would be expected [66]. Also the group velocity is zero. If this was the case there would be a hump visible in ARPES data, however this is not present in the momentum integrated photoemission (see Fig. 4.3 and Reference [67]) and therefore does not seem possible.

The spectra of metal-semiconductor tunnelling and metal-Mott insulator tunnelling are

expected to demonstrate asymmetry because there is an imbalance between the number of holes and electrons in the metal and the sample. The magnitude of the asymmetry can be found by considering a simple one dimensional formulation neglecting electron kinetic energy.

Consider a semiconductor: each ion can accommodate a spin up and spin down electron, so the number of electrons, N_e, is twice the number of ions, N_{ion}; $N_e = 2N_{ion}$. If X electrons are removed from the sample, for example by doping, then the number of electrons is $2N_{ion} - X$. The application of a positive bias means electrons tunnel from the tip to the sample, negative bias means the electrons tunnel in the opposite direction. Thus for negative bias, the probability of tunnelling is proportional to the number of electrons available in the semiconductor sample, this is $2N_{ion} - X$, for positive bias the probability is proportional to the number of holes available for the tip electrons to tunnel to, this is X. The ratio of the integrated negative and positive conductance is given by $R_{semi} = (2 - x)/x$ where $x = X/N$, the hole concentration. Similarly, we can consider the tunnelling between a metal and Mott-insulator. This time, the Coulomb repulsion is so strong the electrons cannot share the same ion, instead the number of electrons is now equal to the number of ions, $N_e = N_{ion}$. Following the same procedure, removing X electrons from the sample gives the result $R_{Mott} = (1 - x)/2x$ [68]. This is shown in Fig. 4.4. The magnitude of asymmetry can be found in the cuprates by finding the area under the tunnelling spectra (since the area is the same as finding the integral and the conductance is given by the differential of the current with respect to the voltage) for the negative and positive voltage and finding the ratio between the two. Obviously, in conventional metal-metal tunnelling this ratio would be equal to one because there is particle-hole symmetry and we have Ohm's Law. Fig. 4.4 illustrates the results from extrinsic tunnelling experiments for $R = I(-\infty)/I(+\infty)$. For this to work, a large field of view is required (i.e. $|V_{max}|$ to be as large as possible) to ensure all filled states are accounted for. However, in many experiments the hole concentration was not necessarily known and had to be found by use of the transition temperature and the following equation taken from Reference [69]:

$$\frac{T_c}{T_{c_{max}}} = 1 - 82.6(x - 0.16)^2. \tag{4.2}$$

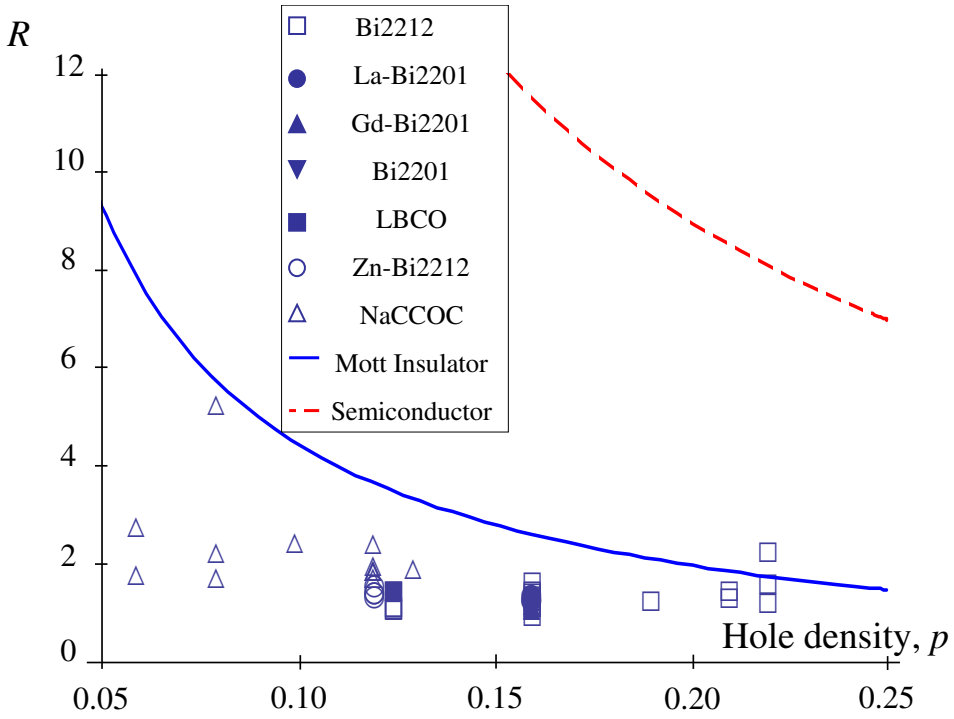

Fig. 4.4: Ratio of the negative bias NS tunnelling conductance to the positive bias $R = I_{NS}(-100)/I_{NS}(+100)$, integrated from 0 to $\mp$100meV respectively, carried out for some cuprate superconductors over a wide range of atomic hole density. The two curves express the asymmetry you would expected to see from a Mott insulator (solid blue) and conventional semiconductor (dashed red) without electron hopping. Figure taken from Reference [15].

Fig. 4.4 shows that although Mott-insulator and semiconductor tunnelling demonstrate asymmetry, neither can account for the magnitude of the asymmetry exhibited in cuprates.

4.4 Key Pairing Interaction in Cuprate Superconductors

Despite intensive research, a detailed microscopic theory capable of describing unusual ARPES and tunnelling data has remained elusive and so the relationship between the SG and PG has remained unknown. A detailed and consistent interpretation of SG and PG could shed light on the key pairing interaction in cuprate superconductors.

High values of T_c and the small change in transition temperature due to the isotope effect in optimally doped $YBa_2Cu_3O_{6.9}$ led some authors to believe that the pairing interaction between electrons could not be mediated by phonons. However experiments [70, 71] showed that a partial substitution of Yttrium by Praseodymium, or of Barium by Lanthanum lead to the isotope effect simultaneously with the decrease of T_c. This implies that either these substituted compounds have a different mechanism of superconductivity, or the mechanism is always phonons and the absence of the isotope effect in YBCO is due to something else. Preferring the latter option is the evidence from the tunnelling spectra at higher voltages of NCCO [72] and BSCCO [73, 74]. Support from the doping dependent oxygen effect (OIE) on T_c and the substantial OIE on the carrier mass suggests a strong EPI in cuprate superconductors, where lattice vibrations play a major but unconventional role in high-temperature superconductivity, see Reference [75] and references therein.

There are numerous publications indicating towards the pairing interaction in cuprates being through a bosonic mode (phonons) and this being responsible for high- temperature superconductivity beyond the BCS theory with Cooper (momentum) pairs. For example, the resistive transitions both in [76] and out [77] of plane remain sharp in overdoped, optimally doped and underdoped high quality samples. The possibility of any residual superconducting order about T_c is slim due to the sharpness of transition and little magnetoresistance [78, 79, 80]. The full suppression of superconductivity requires fields as high as 150 Tesla in cuprates, such a field correspond to a very short zero-temperature coherence length, $\xi = \sqrt{\phi_0/2\pi H_{c2}} \leq 1.5$nm, which is less than (or about) the distance between carriers. This extremely small coherence length rules out the preformed Cooper pair scenario which requires $\xi >> d$. In Cooper pairs the pairs

overlap, however in cuprates they do not [75].

Also, there are clear dip and hump features in superconducting YBCO and Bi2212 that can be seen in the second derivative of the tunnelling current. This is due to strong coupling to the bosonic modes which mediate the pairing of electrons. In this spectrum, the position of the energy peaks match precisely with those in the phonon DOS obtained by inelastic neutron scattering. This result points towards phonons being the bosonic modes mediating the electron pairing and indicates that high-temperature superconductivity arises primarily from strong coupling to multiple phonon modes, [81].

Reference [82] indicates that for the electron doped cuprate PrLaCeCuO, the spectral fine structure below 35meV is consistent with strong coupling to a bosonic mode at about 16meV. This is in good quantitative agreement with early tunnelling spectra of NdCeCuO. Since the energy of the bosonic mode is significantly higher than that of the magnetic resonance mode (observed by inelastic neutron scattering), the coupling feature at about 16meV cannot arise from strong coupling to the magnetic mode. It is found in Reference [82] that the magnetic resonance like mode cannot be the origin of high temperature superconductivity in electron-doped cuprates.

4.5 Bosonic Superconductivity

There has been a huge theoretical effort to try and understand the mechanism behind this "new" superconductivity. Extending the BCS theory in the Fermi liquid framework towards electron-electron interactions gives kinetic, plasmonic, excitonic and magnetic theories of interactions that cause superconductivity, in the non-Fermi liquid regime there are spin polaron and RVB ideas [11]. However, if instead we increase the coupling strength between electrons and phonons we have the bipolaron theory.

The BCS theory [7] is capable of giving a successful description of the superconducting properties of elemental superconductors with a small EPI strength. If the coupling constant is increased above $\lambda \approx 0.5$ [11], the kinetic energy of electrons becomes small compared to the potential they feel from the local lattice deformation, so all the electrons lying in the Bloch band become dressed with phonons (for a recent review see Reference [83]). This means the electron becomes a quasiparticle, a small polaron which can propagate through the lattice in a narrow polaronic band. The idea of a quasiparticle first came from Landau who produced the Fermi liquid theory, similar to the Fermi gas. A moving electron causes an inertial reaction in the surrounding electron liquid and in the ionic lattice, increasing the effective mass of the electron. The quasiparticle may be thought of as a single particle accompanied by a distortion cloud in an electron gas. The quasiparticles have a one-to-one correspondence with the single particle excitations of the free gas [6].

Expanding the BCS theory further towards a stronger interaction between electrons and ion vibrations, where $\lambda > 0.5$, it was predicted that rather than momentum-spacing pairing of electrons (Cooper pairs), the electrons would instead be paired in real-space and form tightly bound small bipolarons that create a charged Bose-gas [84] with a polaronic BCS-like high-T_c superconductivity in the crossover region [85].

The ground state of such a strongly coupled system is the condensation of all single polarons into bosonic bipolarons which can be described as a charged Bose-liquid on a lattice, as long as the carrier density is small enough to avoid their overlap [86]. At finite

temperature but below the transition temperature there will be some thermally excited single polarons and these will interact with the condensate through the same potential that binds them together [15]. The exact single-particle Hamiltonian is described by

$$H_{\text{exact}} = \sum_{\nu} \xi_{\nu} p_{\nu}^{\dagger} p_{\nu} + \sum_{\nu,\nu'} V_{\nu_1\nu_2}^{\nu_1'\nu_2'} p_{\nu_1'}^{\dagger} p_{\nu_2'}^{\dagger} p_{\nu_2} p_{\nu_1}, \tag{4.3}$$

where ξ_{ν} is the energy of a particle in quantum state ν relative to the chemical potential. The operators p and $p^{\dagger}$ are annihilation and creation operators of electrons respectively, they annihilate/create an electron in the state given by the subscript, $V_{\nu_1\nu_2}^{\nu_1'\nu_2'}$ describes the potential between the electrons. In a homogeneous sample, translational symmetry is obeyed and the quantum number is the wavevector, or momentum, with spin. So more generally $\xi_{\nu} = E(\nu) - \mu$ where $E(\nu)$ is an eigenvalue of the Hamiltonian:

$$\left[-\frac{\hbar^2 \nabla^2}{2m_e} + V(\boldsymbol{r}) + V_{\text{imp}}(\boldsymbol{r}) \right] \Psi = E\Psi, \tag{4.4}$$

H_{exact} is not diagonalisable, so the Bogoliubov approximation is needed where the anomalous "average" of two operators is taken as a number, i.e. the averaged $\left\langle p^{\dagger} p^{\dagger} \right\rangle = \Delta \approx \sqrt{n_c(T)}$. Here $n_c(T)$ is the BEC density. This is a good approximation that works and has been used many times, e.g. BCS theory. Doing this puts the Hamiltonian in a diagonalisable form:

$$H_{\text{diag}} = \sum_{\nu} \epsilon_{\nu} \left(\alpha_{\nu}^{\dagger} \alpha_{\nu} + \beta_{\nu}^{\dagger} \beta_{\nu} + \gamma_{\nu}^{\dagger} \gamma_{\nu} + \cdots \right), \tag{4.5}$$

where $\alpha_{\nu},\ \beta_{\nu},\ \gamma_{\nu}$ are operators for new quasiparticles that do not interact (unlike p_{ν}).

Now, we have our Hamiltonian:

$$H_0 = \sum_{\nu} \left[\xi_{\nu} p_{\nu}^{\dagger} p_{\nu} + \frac{\Delta_{c\nu}}{2} \left(p_{\bar{\nu}}^{\dagger} p_{\nu}^{\dagger} + h.c. \right) \right], \tag{4.6}$$

where $\xi_{\nu} = E_{\nu} - \mu$, E_{ν} is the normal-state single polaron energy spectrum, μ is the chemical potential and $\Delta_{c\nu}$ is the coherent potential which is proportional to the square-root of the condensate density. $\Delta_{c\nu} = -\Delta_{c\bar{\nu}}$ where $\bar{\nu}$ is the time reversed state ν.

4.5.1 Bogoliubov Transformation of H_0

Equation (4.6) can be diagonalised using the Bogoliubov transformation, where linear expressions are used as a substitution

$$p_\nu = u_\nu \alpha_\nu + v_\nu \beta_\nu^\dagger \tag{4.7}$$

$$p_{\bar{\nu}} = u_\nu \beta_\nu - v_\nu \alpha_\nu^\dagger, \tag{4.8}$$

(both $\alpha,\ \beta$ used as a "guess" to find the diagonalisable form).

These new quasiparticles described by α and β operators must obey the same anticommutation relations as $p_\nu,\ p_{\bar{\nu}}$ otherwise they will not obey Fermi-Dirac statistics and the Pauli exclusion principle. If this was the case the thermodynamics of the system would be unobtainable, so if they violate these relations there is little point in using them! So:

$$\left\{p_\nu^\dagger, p_\nu\right\} = 1;\ \left\{\alpha_\nu^\dagger, \alpha_\nu\right\} = 1, \tag{4.9}$$

and we have

$$\left\{p_\nu^\dagger, p_\nu\right\} = \left(u_\nu \alpha_\nu^\dagger + v_\nu \beta_\nu\right)\left(u_\nu \alpha_\nu + v_\nu \beta_\nu^\dagger\right) + \left(u_\nu \alpha_\nu + v_\nu \beta_\nu^\dagger\right)\left(u_\nu \alpha_\nu^\dagger + v_\nu \beta_\nu\right) = 1, \tag{4.10}$$

which means we are left with

$$u_\nu^2 + v_\nu^2 = 1. \tag{4.11}$$

Now, substitute the linear expressions for $p_\nu,\ p_{\bar{\nu}}$ into H_0 (Equation (4.6)) where $\xi_\nu = \xi_{\bar{\nu}}$ due to time reversal symmetry, $E_\uparrow(\boldsymbol{k}) = E_\downarrow(-\boldsymbol{k})$ (in a translationally invariant system, for example),

$$\begin{aligned} H_0 = \sum_\nu \big[& \alpha_\nu^\dagger \alpha_\nu \left(\xi_\nu (u_\nu^2 - v_\nu^2) + 2\Delta_{c\nu} u_\nu v_\nu\right) \\ & + \beta_\nu^\dagger \beta_\nu \left(\xi_\nu (u_\nu^2 - v_\nu^2) + 2\Delta_{c\nu} u_\nu v_\nu\right) \\ & + \alpha_\nu^\dagger \beta_\nu^\dagger \left(2\xi_\nu u_\nu v_\nu + 2\xi_\nu (v_\nu^2 - u_\nu^2)\right) \\ & + \alpha_\nu \beta_\nu \left(-2\xi_\nu u_\nu v_\nu - 2\xi_\nu (v_\nu^2 - u_\nu^2)\right) \\ & + \text{constants that give the ground state} \big]. \end{aligned} \tag{4.12}$$

Since we are trying to diagonalise the Hamiltonian, the non-diagonal parts must be zero

$$\Rightarrow 2\xi_\nu u_\nu v_\nu = \Delta_{c\nu}(u_\nu^2 - v_\nu^2), \tag{4.13}$$

we also know, $u_\nu^2 + v_\nu^2 = 1$ and $\epsilon_\nu^2 = \Delta_{c\nu}^2 + \xi_\nu^2$, removing $\Delta_{c\nu}$ from above:

$$2\xi_\nu u_\nu v_\nu = \sqrt{\epsilon_\nu^2 - \xi_\nu^2}(u_\nu^2 - v_\nu^2). \tag{4.14}$$

Remove v_ν^2

$$2\xi_\nu u_\nu \sqrt{1-u_\nu^2} = \sqrt{\epsilon_\nu^2 - \xi_\nu^2}(u_\nu^2 - (1-u_\nu^2)), \tag{4.15}$$

$$\Rightarrow u_\nu^4(-4\xi_\nu^2 + 4\xi_\nu^2 - 4\epsilon_\nu^2) + u_\nu^2(4\xi_\nu^2 + 4\epsilon_\nu^2 - 4\xi_\nu^2) + (4\xi_\nu^2 + 4\epsilon_\nu^2) = 0. \tag{4.16}$$

Using the quadratic formula, we have:

$$\begin{aligned} u_\nu^2 &= \frac{-4\epsilon_\nu^2 \pm \sqrt{16\epsilon_\nu^4 + 16\epsilon_\nu^2(\xi_\nu^2 - \epsilon_\nu^2)}}{-8\epsilon_\nu^2} \\ &= \frac{1}{2} \pm \sqrt{\frac{\xi_\nu^2}{4\epsilon_\nu^2}}. \end{aligned} \tag{4.17}$$

Therefore we have:

$$u_\nu^2 = \frac{1}{2}\left(1 + \frac{\xi_\nu}{\epsilon_\nu}\right);\ v_\nu^2 = \frac{1}{2}\left(1 - \frac{\xi_\nu}{\epsilon_\nu}\right). \tag{4.18}$$

The Hamiltonian is thus written:

$$H_0 = \sum_\nu \epsilon_\nu \left(\alpha_\nu^\dagger \alpha_\nu + \beta_\nu^\dagger \beta_\nu\right), \tag{4.19}$$

where $p_\nu = u_\nu \alpha_\nu + v_\nu \beta_\nu^\dagger$, $p_{\bar{\nu}} = u_\nu \beta_\nu - v_\nu \alpha_\nu^\dagger$, $\epsilon_\nu = \sqrt{\xi_\nu^2 + \Delta_{c\nu}^2}$ with $u_\nu^2,\ v_\nu^2 = \frac{1}{2}\left(1 \pm \frac{\xi_\nu}{\epsilon_\nu}\right)$. This is different to the quasiparticle spectrum in the BCS theory because here the chemical potential is negative with respect to the bottom of the single-particle band, $\mu = -\Delta_p$, see Fig. 4.5.

The PG is a temperature-independent incoherent gap that is half of the binding energy of the bipolaron pairs and it lies within the charge-transfer gap. Without disorder in the sample and considering a point-like pairing potential the temperature-dependent coherent gap can be written $\Delta_{c\boldsymbol{k}} \approx \Delta_c$. Combining the two gaps into one global temperature-dependent gap [86] we have

$$\Delta(T) = \sqrt{\Delta_p^2 + \Delta_c^2(T)}. \tag{4.20}$$

This means that at zero temperature the full gap is given by $\Delta(0) = \sqrt{\Delta_p^2 + \Delta_c^2(0)}$, and in the normal state the SG, Δ_c, vanishes leaving $\Delta = \Delta_p$, so the full gap becomes

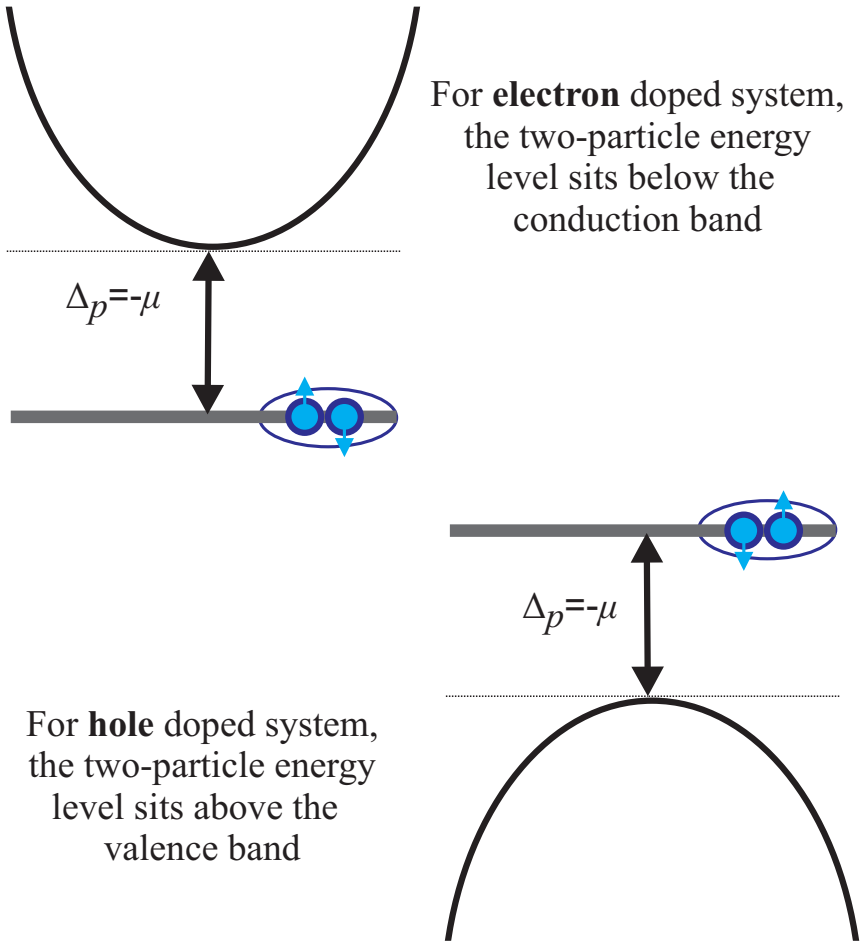

Fig. 4.5: When the system is electron doped, the two particle energy level sits Δ_p below the bottom of the conduction band. This means that taking the energy relative to the conduction band, the chemical potential is negative with respect when the pairs are real-space bipolarons rather than momentum-space Cooper pairs. The bottom figure shows a similar situation for hole-doped systems.

temperature independent. Equation (4.20) describes well the experimental observation of the anomalous gap in $YBa_2Cu_3O_{7-\delta}$ in the electron loss spectra by Demuth et al [87]. It quantitatively describes some earlier and more recent observations [59], including Andreev reflection in cuprates [11]. In the absence of a barrier (for example the interface between a normal metal and superconductor) an incoming electron from the normal side of the normal/superconducting contact is reflected as a hole along the same trajectory [88, 89]. This is "Andreev reflection" and it causes an increase in the tunnelling conductance in the voltage range $|eV| \lesssim \Delta$, which is in sharp contrast to what happens if there is a barrier [11]. Reference [86] indicates the existence of two gaps, the first (presumably the PG) being temperature independent below T_c and persist to exist above T_c, whilst a second gap (presumably the SG) become evident by the study of Andreev reflection. An incoming electron from the normal side of the normal/superconducting contact is reflected as a hole along the same trajectory revealing a much smaller gap edge than the bias at the tunnelling conductance maxima in some cuprates [86].

The PG is considered to be half the bipolaron binding energy, where real-space pairs are formed if the condition $E_F < 2\Delta_p$ (where E_F is the polaron Fermi energy) is satisfied [86], in this case the ground state of the system is a BEC [86]. The chemical potential is pinned below the band edge by about Δ_p both in the normal and superconducting state [90], so the normal-state single-particle gap is Δ_p. To emphasise: this spectrum is different to the BCS quasiparticle spectrum as the chemical potential is negative with respect to the single-particle band, $\mu = -\Delta_p$ (the single-particle gap is given by Equation (4.20)).

4.5.2 Energy Band Structure of Cuprates

The parent band structure is in the form of a Mott insulator and semiconductor insulator. Since cuprates are discussed, we have copper oxygen planes which are quasi-2D layers held together by the parent lattice. The copper band is split into two; an upper and lower band which makes the Mott insulator. The electrons (or holes) sit in

the d-orbital (see Appendix D) and their wavefunction has a small radius, therefore they feel a larger Coulomb repulsion (or Hubbard U, since they are on the same site), this results in the gap between the two bands being approximately 5-8eV. Therefore they exhibit Mott-Hubbard physics. The electrons (or holes) in the oxygen lie in the p-orbital. This has a wavefunction of larger radius and so they experience a smaller Coulomb repulsion, therefore the charge transfer gap here is approximately 1-2eV and they obey semiconductor physics. Therefore, our parent structure is half semiconductor, half Mott insulator. We have assumed the local density approximation and generalised tight-binding ("LDA+GTB") band structure [91] for undoped cuprates. See Fig. 4.6 and for an explanation of LDA and GTB see Appendix C.

In spite of the success of the LDA and its extensions for conventional metallic systems, it appears to be inadequate for strongly correlated electron systems. It predicts La_2CuO_4 to be a metal, whereas in reality it is an insulator. Several approaches to include strong correlations in the LDA method are known, for example LDA+U [92] and LDA-SIC [93] (SIC refers to self interaction correction). Both of these result in the correct antiferromagnetic insulator ground state for La_2CuO_4. A generalised tight-binding method [94] has been proposed to study the electronic structure of strongly correlated electron systems as a generalisation of Hubbard ideas for the realistic multiband Hubbard-like models. The GTB method allows the calculation of the electronic structure within the multiband Hubbard model, which combines the exact diagonalisation of the model Hamiltonian for a small cluster (unit cell) with perturbation treatment of the intercluster hopping and interactions. For undoped La_2CuO_4 and Nd_2CuO_4 this scheme results in charge-transfer insulators with correct values of gaps and dispersions of bands in agreement with ARPES data [91].

Reference [95] points out that the "LDA+GTB" approach predicts the charge transfer gap at any doping, with the chemical potential pinned near the top of the valence band (in hole-doped cuprates) or near the bottom of the conduction band (in electron doped cuprates), similar to doping a semiconductor, explained earlier in Section 3.1.

When impurities are added to the parent insulator through the process of doping, each

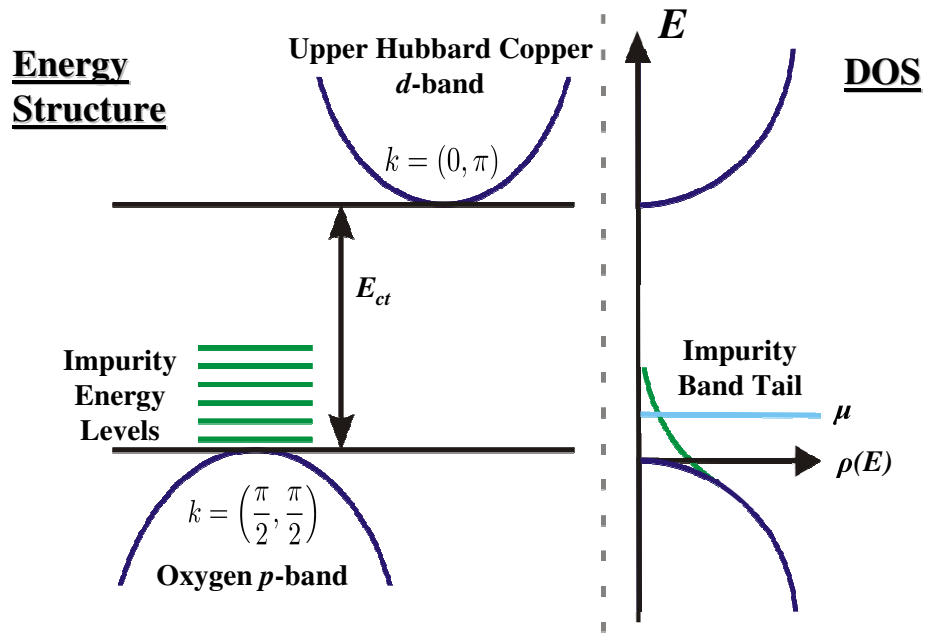

Fig. 4.6: The local density approximation and generalised tight binding model is adopted to give this band structure. The doping of the parent lattice inserts impurity energy levels in the energy gap, these levels form an impurity bandtail similar to a heavily doped semiconductor. Figure taken from Reference [15].

impurity ion locally introduces a discrete energy level inside the charge transfer gap. The random spatial distribution of the impurities causes a bandtail of the DOS as seen in Reference [95]. This is similar to heavily doping a semiconductor [96].

This band structure explains the charge transfer gap seen in photo-absorption and photo-conduction experiments [97], when light is shone on to the sample it is absorbed but does not provide extra conductivity, this is evidence of localised states within the charge transfer gap.

Reference [95] introduces the idea of the impurity bandtail in the DOS, they identify the sharp quasiparticle peaks near $(\pi/2, \pi/2)$ of the Brillouin zone, see Fig. 4.7, they propose the peaks are due to hydrogen-like impurity states that are localised near the surface of doped charge-transfer Mott insulators. Their model accounts for the rapid loss of intensity in some directions of the Brillouin zone [95], giving "Fermi arcs". The inclusion of the impurity bandtail also accounts for a high energy waterfall observed by ARPES in underdoped cuprate superconductors [95].

It has however been suggested that the Fermi arcs seen by ARPES could form part of a larger Fermi surface, thus implying a metallic parent structure. This idea does not take into account strong correlations and the existence of the charge-transfer gap over a wide range of dopings.

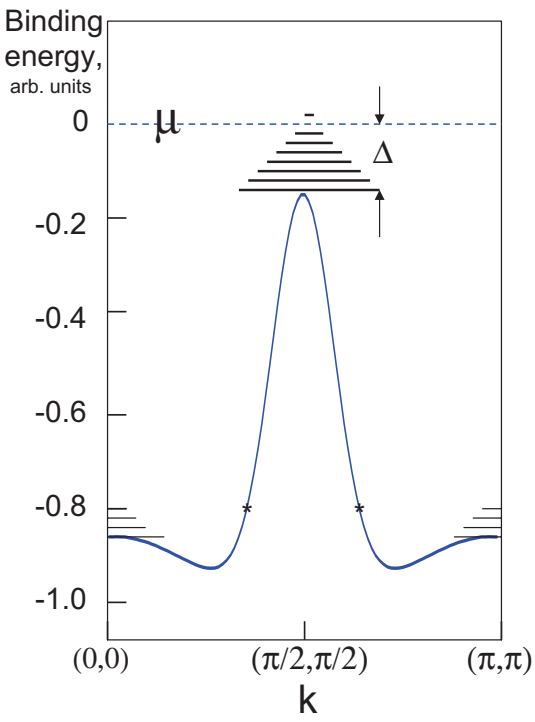

Fig. 4.7: LDA+GTB band structure gives the valence band dispersion [91] with the impurity bandtails [95] which are the ladder lines near Γ, $(\pi/2, \pi/2)$ and (π, π) ($\boldsymbol{k}$ measured in units of a). Figure taken from Reference [95].

4.6 Modelling the DOS

To be able to find the tunnelling spectra with Mott insulators and/or semiconductors with real-space pairs, an approximation of the DOS is needed for the superconductor in its normal-state. As mentioned, we have the bandtail in the DOS due to the impurities introduced to the parent lattice. A DOS is required that gives the correct bandtail shape, this is given by

$$\rho_N(\xi) = \frac{\rho_b}{2}\left[1 + \tanh\left(\frac{\xi - \Delta_p}{\Gamma}\right)\right], \tag{4.21}$$

where ρ_b is the band DOS which is approximately a constant near a two dimensional band edge, Δ_p is the PG and Γ is the characteristic width of the band tail.

The definition of the DOS is

$$\rho(E) \equiv \sum_\nu \delta(E - \epsilon_\nu). \tag{4.22}$$

The DOS in the superconducting state can be found.

We consider *s*- and *d*- wave superconductivity, for more information about this please see Appendix D.

4.6.1 *s*-wave DOS

For *s*-wave superconductivity, the coherent gap does not depend on the quantum number ν and by definition $\epsilon_\nu = \sqrt{\xi_\nu^2 + \Delta_c^2}$, if we substitute this in, we have

$$\begin{aligned}\sum_\nu \delta(\sqrt{\xi_\nu^2 + \Delta_c^2} - E) &= \int_{-\infty}^{\infty} d\xi \rho_N(\xi)\delta(\sqrt{\xi^2 + \Delta_c^2} - E) \\ &= \int_0^{\infty} d\xi \left[\rho_N(\xi) + \rho_N(-\xi)\right]\delta(E - \sqrt{\xi^2 + \Delta_c^2}).\end{aligned} \tag{4.23}$$

We integrate over only positive values of ξ since we include the term $\rho(-\xi)$ and in the delta function ξ^2 is an even function and therefore will not be affected. From

$\epsilon = \sqrt{\xi^2 + \Delta_c^2}$, $\xi = \pm\sqrt{\epsilon^2 - \Delta_c^2}$. Upon substitution

$$\int_{\Delta_c}^{\infty} \left[\rho_N(\sqrt{\epsilon^2 - \Delta_c^2}) + \rho_N(-\sqrt{\epsilon^2 - \Delta_c^2})\right] \delta(E - \epsilon) \frac{\epsilon}{\sqrt{\epsilon^2 - \Delta_c^2}} d\epsilon$$
$$= \left[\rho_N(\sqrt{E^2 - \Delta_c^2}) + \rho_N(-\sqrt{E^2 - \Delta_c^2})\right] \frac{E}{\sqrt{E^2 - \Delta_c^2}}. \quad (4.24)$$

If the coherent gap is small compared with the bandtail width, $\Delta_c << \Gamma$, it can be ignored in ρ_N in Equation (4.24). For a continuous function, Δ_c can be ignored, giving:

$$\rho(E) = [\rho_N(E) + \rho_N(-E)]\, \rho_s(E), \quad (4.25)$$

where $\rho_s(E)$ is the superconducting DOS, given by

$$\rho_s(E) = \frac{E}{\sqrt{E^2 - \Delta_c^2}}. \quad (4.26)$$

4.6.2 *d*-wave DOS

For *d*-wave symmetry, the coherent potential is dependent on the quantum number as it is not constant around the constant energy contour and changes with angle ϕ and $\Delta_{c\nu} = \Delta_0 \cos 2\phi$. Strictly speaking, when finding the DOS with impurities there is disorder and so the sample is not homogeneous, therefore $\boldsymbol{k}$ is not a good quantum number and instead we could use

$$\sum_{\nu} = \int d\xi \rho_N(\xi) \int d\phi, \quad (4.27)$$

so that

$$\sum_{\nu} F(\xi_\nu, \phi) = \int d\xi \rho_N(\xi) \int d\phi F(\xi, \phi), \quad (4.28)$$

where $F(\xi_\nu, \phi)$ is any function. Here $F(\xi_\nu, \phi) = \delta(E - \sqrt{\xi_\nu^2 + \Delta_{c\nu}^2})$, and so

$$\sum_{\nu} \delta(E - \sqrt{\xi_\nu^2 + \Delta_{c\nu}^2 \cos^2 2\phi}) = \int_{-\infty}^{\infty} d\xi \rho_N(\xi) \int_0^{2\pi} d\phi \delta(E - \sqrt{\xi^2 + \Delta_0^2 \cos^2 2\phi}). \quad (4.29)$$

We consider the impurity bandtail width to be much larger than the SG, and so $\rho_N(\xi) \approx \rho_N(E)$. Since this can be factorised out I look now for only the superconducting DOS,

$\rho_s(E)$. Letting $Y = \frac{\xi}{\Delta_0},\ X = \frac{E}{\Delta_0}$, gives

$$\begin{aligned}\rho_s(E) &= \int_{-\infty}^{\infty} dY \int_0^{2\pi} d\phi \delta(X - \sqrt{Y^2 + \cos^2 2\phi}) \\ &= \int_{-\infty}^{\infty} dY \int_0^{\frac{\pi}{2}} d\psi \delta(X - \sqrt{Y^2 + \sin^2 \psi}),\end{aligned} \tag{4.30}$$

where $\phi = \pi - 2\psi$. Now making a change of variables, let $t = \sin\psi \Rightarrow \frac{dt}{d\psi} = \cos\psi \Rightarrow d\psi = \frac{dt}{\sqrt{1-t^2}}$, which means the DOS is

$$\rho_s(E) = \int_{-\infty}^{\infty} dY \int_0^1 dt \frac{1}{\sqrt{1-t^2}} \delta(X - \sqrt{Y^2 + t^2}). \tag{4.31}$$

Now, let $\epsilon = \sqrt{Y^2 + t^2} \Rightarrow\ dY = \frac{\epsilon}{\sqrt{\epsilon^2 - t^2}} d\epsilon$ and the DOS becomes

$$\rho_s(E) = \int_0^1 dt \frac{1}{\sqrt{1-t^2}} \int_t^{\infty} d\epsilon \frac{\epsilon}{\sqrt{\epsilon^2 - t^2}} \delta(X - \epsilon). \tag{4.32}$$

The lower limit of integration over ϵ must be capped because a negative denominator gives zero when integrated. There are two different situations to consider, either $X \geq 1$ or $X < 1$, first consider $X \geq 1$:

$$\rho_s(E) = \int_0^X dt \frac{X}{\sqrt{1-t^2}\sqrt{X^2 - t^2}} = K\left(\frac{1}{X}\right) = K\left(\frac{\Delta_0}{E}\right), \tag{4.33}$$

where K is the complete elliptic integral. Now consider $X < 1$:

$$\rho_s(E) = \int_0^1 d\tau \frac{X}{X\sqrt{1 - X^2\tau}\sqrt{1-\tau^2}} = XK(X) = \frac{E}{\Delta_0} K\left(\frac{E}{\Delta_0}\right). \tag{4.34}$$

Therefore, we have the d-wave DOS in the superconducting state as

$$\rho_s(E) = \Theta\left(\frac{E}{\Delta_0} - 1\right) K\left(\frac{\Delta_0}{E}\right) + \Theta\left(1 - \frac{E}{\Delta_0}\right) \frac{E}{\Delta_0} K\left(\frac{E}{\Delta_0}\right). \tag{4.35}$$

5. TUNNELLING IN CUPRATES

We consider single-particle tunnelling only despite having bound pairs of electrons. This is because we compare our results to STM and intrinsic tunnelling experiments which only utilises single-particle tunnelling.

5.1 Extrinsic (NS) Tunnelling

Extrinsic tunnelling is the tunnelling of a charge carrier between a metallic tip and superconducting sample. To find the tunnelling Hamiltonian each different tunnelling scenario needs to be considered. Suppose the metallic tip is on the left and the superconductor on the right. The metallic tip will have undressed carriers whereas the superconductor will have polarons and bipolarons interacting with one another as already mentioned. Tunnelling left to right means the annihilation of a free carrier in the metal accompanied by the creation of a polaron in the superconductor. Alternatively, we might have the annihilation of a carrier on the left and a polaron on the right and the combination of the two to create a bipolaron in the superconductor, see Fig. 5.1. This can be expressed using the tunnelling Hamiltonian [98]

$$H_{NS} = P\sum_{\nu\nu'} p^\dagger_{\nu'} c_\nu + \frac{B}{\sqrt{N}} \sum_{\nu\nu'\eta'} b^\dagger_{\eta'} p_{\bar{\nu}'} c_\nu + h.c. \tag{5.1}$$

Here c_ν and $b^\dagger_{\eta'}$ are the annihilation of a carrier in the metallic tip in state ν and the creation of a composed boson in the superconductor in state η' respectively, N is the number of lattice cells. P and B are tunnelling matrix elements with and without the involvement of a bipolaron respectively. Generally $B \gtrsim P$, because the presence of an

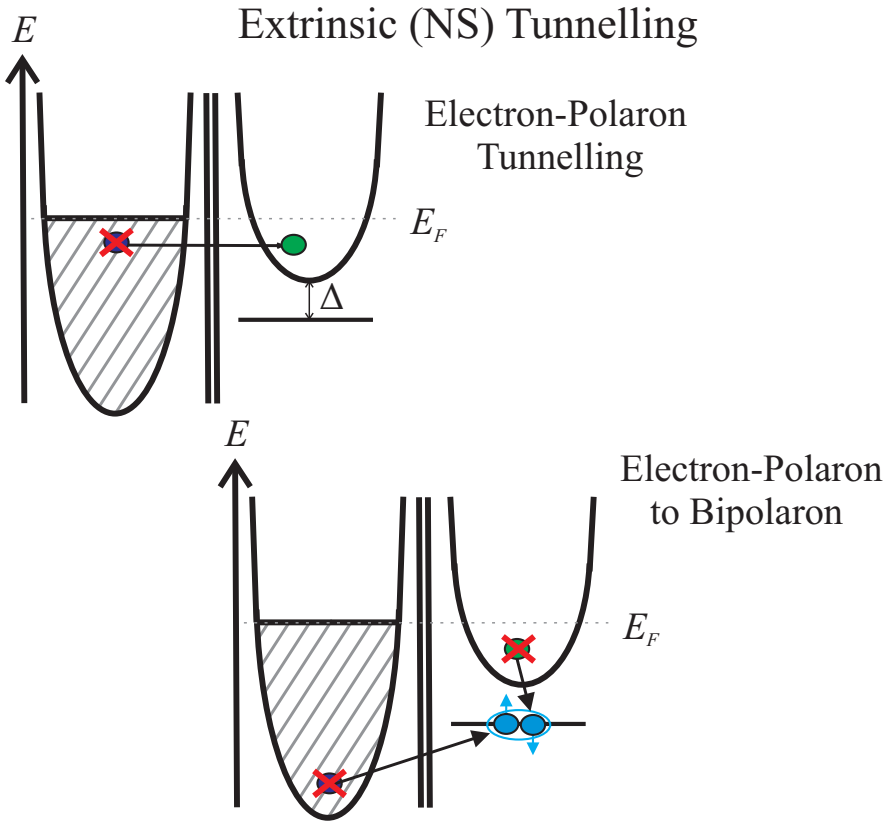

Fig. 5.1: Cartoon demonstrating the two possible single-particle tunnelling scenarios. The first is the annihilation of an electron in the normal-metal on the left and the creation of a polaron on the right, as described in the first part of the tunnelling Hamiltonian. The second illustrates the tunnelling process with the involvement of a bipolaron. For normal-metal to superconductor tunnelling, this is the annihilation of an electron in the metal and the annihilation of a polaron in the superconductor with the creation of a composed boson, this is described in the second term of Equation (5.1). Energy is conserved in the tunnelling process [15].

additional hole lowers the tunnelling barrier for an injection of the electron [98]. The matrix elements determine the probability of a tunnelling charge carrier being involved with either the first or second term. Using the Bogoliubov coefficients found earlier, Equation (4.18), the polaron operators can be replaced with linear combinations of the quasiparticle operators to give:

$$\begin{aligned} H_{NS} &= P\sum_{\nu\nu'}\left(u_{\nu'}\alpha^{\dagger}_{\nu'}+v_{\nu'}\beta_{\nu'}\right)c_{\nu} \\ &\quad +\frac{B}{\sqrt{N}}\sum_{\nu\nu'\eta'}b^{\dagger}_{\eta'}\left(u_{\nu'}\beta_{\nu'}-v_{\nu'}\alpha^{\dagger}_{\nu'}\right)c_{\nu}+h.c. \end{aligned} \tag{5.2}$$

To find the current, the FDGR (Equation (2.5)) is applied which gives

$$\begin{aligned} W^{\mathrm{met}\to\mathrm{super}}_{NS} &= \frac{2\pi P^2}{\hbar}\sum_{\nu\nu'}\left[u^2_{\nu'}(1-f_{\nu'})F_{\nu}\delta(\xi_{\nu}+eV-\epsilon_{\nu'})\right. \\ &\qquad \left.+v^2_{\nu'}f_{\nu'}F_{\nu}\delta(\xi_{\nu}+eV+\epsilon_{\nu'})\right] \\ &\quad +\frac{2\pi B^2}{\hbar N}\sum_{\nu\nu'\eta'}(1+n_{\eta'})\left[u^2_{\nu'}f_{\nu'}F_{\nu}\delta(E_{\eta'}-\xi_{\nu}-eV-\epsilon_{\nu'})\right. \\ &\qquad \left.+v^2_{\nu'}(1-f_{\nu'})F_{\nu}\delta(E_{\eta'}-\xi_{\nu}-eV+\epsilon_{\nu'})\right], \end{aligned} \tag{5.3}$$

and

$$\begin{aligned} W^{\mathrm{super}\to\mathrm{met}}_{NS} &= \frac{2\pi P^2}{\hbar}\sum_{\nu\nu'}\left[u^2_{\nu'}f_{\nu'}(1-F_{\nu})\delta(\xi_{\nu}+eV-\epsilon_{\nu'})\right. \\ &\qquad \left.+v^2_{\nu'}(1-f_{\nu'})(1-F_{\nu})\delta(\xi_{\nu}+eV+\epsilon_{\nu'})\right] \\ &\quad +\frac{2\pi B^2}{\hbar N}\sum_{\nu\nu'\eta'}n_{\eta'}\left[u^2_{\nu'}(1-f_{\nu'})(1-F_{\nu})\delta(E_{\eta'}-\xi_{\nu}-eV-\epsilon_{\nu'})\right. \\ &\qquad \left.+v^2_{\nu'}f_{\nu'}(1-F_{\nu})\delta(E_{\eta'}-\xi_{\nu}-eV+\epsilon_{\nu'})\right]. \end{aligned} \tag{5.4}$$

Here $W^{\mathrm{met}\to\mathrm{super}}$ and $W^{\mathrm{met}\to\mathrm{super}}$ are transition rates in and out of the superconductor respectively, $f_{\nu'}=1/(e^{\epsilon_{\nu'}/k_BT}+1)$ is the single quasiparticle distribution function, $n_{\eta'}$ is the bipolaron (Bose) distribution function, $F_{\nu}=1/(e^{\xi_{\nu}/k_BT}+1)$ describes the distribution of carriers in the normal metal, V is the voltage drop across the junction and the bipolaron chemical potential in the superconductor differs from the normal-metal by $2eV$. Using Equation (2.18) gives the current as

$$I_{NS}= \frac{2\pi eP^2}{\hbar}\sum_{\nu\nu'}\left[u^2_{\nu'}(F_{\nu}-f_{\nu'})\delta(\xi_{\nu}+eV-\epsilon_{\nu'})\right.$$

$$+v_{\nu'}^2(F_\nu + f_{\nu'} - 1)\delta(\xi_\nu + eV + \epsilon_{\nu'})\big]$$
$$+\frac{2\pi eB^2}{\hbar N}\sum_{\nu\nu'\eta'}\left\{u_{\nu'}^2\left[f_{\nu'}F_\nu - n_{\eta'}(1-F_\nu - f_{\nu'})\right]\delta(E_{\eta'} - \xi_\nu - eV - \epsilon_{\nu'})\right.$$
$$\left.+v_{\nu'}^2\left[F_\nu(1-f_{\nu'}) + n_{\eta'}(F_\nu - f_{\nu'})\right]\delta(E_{\eta'} - \xi_\nu - eV + \epsilon_{\nu'})\right\}. \quad (5.5)$$

Taking

$$\frac{1}{N}\sum_{\eta'} n_{\eta'}\delta(E_{\eta'} - \xi_\nu - eV - \epsilon_{\nu'}) \;\rightarrow\; \frac{x}{2}\delta(\xi_\nu + eV + \epsilon_{\nu'})$$
$$\frac{1}{N}\sum_{\eta'} n_{\eta'}\delta(E_{\eta'} - \xi_\nu - eV + \epsilon_{\nu'}) \;\rightarrow\; \frac{x}{2}\delta(\xi_\nu + eV - \epsilon_{\nu'}), \quad (5.6)$$

since $x/2$ is the density of composed bosons in the superconductor. We approximate that the bipolaron distribution is relatively narrow and therefore we neglect it which is a reasonable estimate if it is assumed that the Coulomb bipolaron-bipolaron repulsion is relatively weak [98]. This gives

$$I_{NS} = \frac{2\pi eP^2}{\hbar}\sum_{\nu\nu'}\left[u_{\nu'}^2(F_\nu - f_{\nu'})\delta(\xi_\nu + eV - \epsilon_{\nu'})\right.$$
$$\left.+v_{\nu'}^2(F_\nu + f_{\nu'} - 1)\delta(\xi_\nu + eV + \epsilon_{\nu'})\right]$$
$$+\frac{2\pi eB^2}{\hbar}\sum_{\nu\nu'}\left\{u_{\nu'}^2\left[f_{\nu'}F_\nu - \frac{x}{2}(1-F_\nu - f_{\nu'})\right]\delta(\xi_\nu + eV + \epsilon_{\nu'})\right.$$
$$\left.+\,v_{\nu'}^2\left[F_\nu(1-f_{\nu'}) + \frac{x}{2}(F_\nu - f_{\nu'})\right]\delta(\xi_\nu + eV - \epsilon_{\nu'})\right\}. \quad (5.7)$$

Using Equations (2.9) and (2.10) we have:

$$\sum_\nu \rightarrow \int_{-\infty}^{\infty} d\xi\rho_M(\xi); \qquad \sum_{\nu'} \rightarrow \int_{-\infty}^{\infty} d\xi'\rho_N(\xi'), \quad (5.8)$$

and can substitute this into the equation for the current above. Where $\rho_M(\xi)$ is DOS of metal, its energy dependence can be ignored since we are considering it near the Fermi-energy as discussed previously in Section 2, and so it is a constant. $\rho_N(\xi')$ is the normal-state single-particle DOS in the doped charge-transfer insulator.

$$I_{NS} = \frac{2\pi eP^2\rho_M}{\hbar}\int_{-\infty}^{\infty} d\xi\int_{-\infty}^{\infty} d\xi'\rho_N(\xi')\left[u^2(\xi')(F(\xi - eV) - f(\epsilon'))\delta(\xi - \epsilon')\right.$$
$$\left.+v^2(\xi')(F(\xi - eV) + f(\epsilon') - 1)\delta(\xi + \epsilon')\right]$$

$$+\frac{2\pi eB^2\rho_M}{\hbar}\int_{-\infty}^{\infty}d\xi\int_{-\infty}^{\infty}d\xi'\rho_N(\xi')\Big\{u^2(\xi')\Big[f(\epsilon')F(\xi-eV) -\frac{x}{2}\Big(1-F(\xi-eV)-f(\epsilon')\Big)\Big]\delta(\xi+\epsilon') + v^2(\xi')\Big[F(\xi-eV)(1-f(\epsilon')) +\frac{x}{2}\Big(F(\xi-eV)-f(\epsilon')\Big)\Big]\delta(\xi-\epsilon')\Big\}. \quad (5.9)$$

At zero temperature, the Fermi-Dirac distribution of the electrons in the metal becomes a step function

$$\begin{aligned} F(\xi-eV)\rightarrow &\quad \Theta(eV-\xi)\\ \frac{\partial\Theta(eV-\xi)}{\partial(eV)}= &\quad \delta(eV-\xi), \end{aligned} \quad (5.10)$$

and all the polarons have condensed into the bipolaronic condensate and so $f(\epsilon')=0$. So, using Equation (2.20) the conductance is given by

$$\begin{aligned}\sigma_{NS} &= \frac{2\pi eP^2}{\hbar}\rho_M\int_{-\infty}^{\infty}d\xi\int_{-\infty}^{\infty}d\xi'\rho_N(\xi')\delta(eV-\xi)\Big[u^2(\xi')\delta(\xi-\epsilon')+v^2(\xi')\delta(\xi+\epsilon')\\ &+\frac{B^2}{P^2}\frac{x}{2}u^2(\xi')\delta(\xi+\epsilon')+v^2(\xi')\frac{B^2}{P^2}\left(\frac{x}{2}+1\right)\delta(\xi-\epsilon')\Big]. \end{aligned} \quad (5.11)$$

Considering positive bias only ($eV>0$), means we can disregard terms containing $\delta(\xi+\epsilon')$.

$$\begin{aligned}\sigma_{NS}(eV>0)= &\quad \frac{2\pi eP^2\rho_M}{\hbar}\int_{-\infty}^{\infty}d\xi\int_{-\infty}^{\infty}d\xi'\delta(eV-\xi)\delta(\xi-\epsilon')\rho_N(\xi')\\ &\times\left[u^2(\xi')+v^2(\xi')\frac{B^2}{P^2}\left(1+\frac{x}{2}\right)\right]. \end{aligned} \quad (5.12)$$

Taking the integral with respect to ξ

$$\begin{aligned}\sigma_{NS}(eV>0) &= \frac{2\pi eP^2\rho_M}{\hbar}\int_{-\infty}^{\infty}d\xi'\delta(eV-\epsilon')\rho_N(\xi')\\ &\quad\times\left[u^2(\xi')+v^2(\xi')\frac{B^2}{P^2}\left(1+\frac{x}{2}\right)\right]\\ &= \frac{2\pi eP^2\rho_M}{\hbar}\int_{0}^{\infty}d\xi'\delta(eV-\epsilon')\rho_N(\xi')\\ &\quad\times\left[u^2(\xi')+v^2(\xi')\frac{B^2}{P^2}\left(1+\frac{x}{2}\right)\right] \end{aligned}$$

$$+\frac{2\pi eP^2\rho_M}{\hbar}\int_0^\infty d\xi'\delta(eV-\epsilon')\rho_N(-\xi') \times\left[u^2(-\xi')+v^2(-\xi')\frac{B^2}{P^2}\left(1+\frac{x}{2}\right)\right]. \quad (5.13)$$

Using $\xi'=\sqrt{\epsilon'^2-\Delta_c^2}$ means $d\xi'=\frac{\epsilon' d\epsilon'}{\sqrt{\epsilon'^2-\Delta_c^2}}$ and

$$\begin{aligned}\sigma_{NS}(eV>0) &= \frac{2\pi eP^2\rho_M}{\hbar}\int_{\Delta_c}^\infty\frac{\epsilon' d\epsilon'}{\sqrt{\epsilon'^2-\Delta_c^2}}\delta(eV-\epsilon')\rho_N(\sqrt{\epsilon'^2-\Delta_c^2}) \\ &\times\left[u^2(\sqrt{\epsilon'^2-\Delta_c^2})+v^2(\sqrt{\epsilon'^2-\Delta_c^2})\frac{B^2}{P^2}\left(1+\frac{x}{2}\right)\right] \\ &+\frac{2\pi eP^2\rho_M}{\hbar}\int_{\Delta_c}^\infty\frac{\epsilon' d\epsilon'}{\sqrt{\epsilon'^2-\Delta_c^2}}\delta(eV-\epsilon')\rho_N(-\sqrt{\epsilon'^2-\Delta_c^2}) \\ &\times\left[u^2(-\sqrt{\epsilon'^2-\Delta_c^2})+v^2(-\sqrt{\epsilon'^2-\Delta_c^2})\frac{B^2}{P^2}\left(1+\frac{x}{2}\right)\right]. \quad (5.14)\end{aligned}$$

The DOS of a superconductor with an s-wave coherent gap is given by $\rho_S(\epsilon')=\frac{\epsilon'}{\sqrt{\epsilon'^2-\Delta_c^2}}$ and the conductance over positive bias is given by:

$$\begin{aligned}\sigma_{NS}(eV>0) &= \frac{2\pi eP^2\rho_M}{\hbar}\Theta(eV-\Delta_c)\rho_S(eV) \\ &\times\left\{\rho_N(\sqrt{(eV)^2-\Delta_c^2})\left[\frac{1}{2}\left(1+\frac{\sqrt{(eV)^2-\Delta_c^2}}{eV}\right)\right.\right. \\ &\left.+\frac{1}{2}\left(1-\frac{\sqrt{(eV)^2-\Delta_c^2}}{eV}\right)\frac{B^2}{P^2}\left(1+\frac{x}{2}\right)\right] \\ &+\rho_N(-\sqrt{(eV)^2-\Delta_c^2})\left[\frac{1}{2}\left(1-\frac{\sqrt{(eV)^2-\Delta_c^2}}{eV}\right)\right. \\ &\left.\left.+\frac{1}{2}\left(1+\frac{\sqrt{(eV)^2-\Delta_c^2}}{eV}\right)\frac{B^2}{P^2}\left(1+\frac{x}{2}\right)\right]\right\}. \quad (5.15)\end{aligned}$$

For negative bias ($eV<0$) all terms containing $\delta(\xi-\epsilon')$ can be neglected.

$$\begin{aligned}\sigma_{NS}(eV<0) &= \frac{2\pi eP^2\rho_M}{\hbar}\int_{-\infty}^\infty d\xi\int_{-\infty}^\infty d\xi'\rho_N(\xi')\delta(eV-\xi)\delta(\xi+\epsilon') \\ &\times\left[v^2(\xi')+u^2(\xi')\frac{B^2}{P^2}\frac{x}{2}\right] \\ &= \frac{2\pi eP^2\rho_M}{\hbar}\int_{-\infty}^\infty d\xi'\rho_N(\xi')\delta(eV+\epsilon')\end{aligned}$$

$$
\begin{aligned}
& \times \left[v^2(\xi') + u^2(\xi') \frac{B^2}{P^2} \frac{x}{2} \right] \\
= \; & \frac{2\pi e P^2 \rho_M}{\hbar} \int_0^\infty d\xi' \rho_N(\xi') \delta(eV + \epsilon') \\
& \times \left[v^2(\xi') + u^2(\xi') \frac{B^2}{P^2} \frac{x}{2} \right] \\
& + \frac{2\pi e P^2 \rho_M}{\hbar} \int_0^\infty d\xi' \rho_N(-\xi') \delta(eV + \epsilon') \\
& \times \left[v^2(-\xi') + u^2(-\xi') \frac{B^2}{P^2} \frac{x}{2} \right] \\
= \; & \frac{2\pi e P^2 \rho_M}{\hbar} \Theta(-eV - \Delta_c) \rho_S(-eV) \\
& \times \left\{ \rho_N(\sqrt{(eV)^2 - \Delta_c^2}) \left[\frac{1}{2} \left(1 + \frac{\sqrt{(eV)^2 - \Delta_c^2}}{eV} \right) \right. \right. \\
& \left. + \frac{1}{2} \left(1 - \frac{\sqrt{(eV)^2 - \Delta_c^2}}{eV} \right) \frac{B^2}{P^2} \frac{x}{2} \right] \\
& + \rho_N(-\sqrt{(eV)^2 - \Delta_c^2}) \left[\frac{1}{2} \left(1 - \frac{\sqrt{(eV)^2 - \Delta_c^2}}{eV} \right) \right. \\
& \left. \left. + \frac{1}{2} \left(1 + \frac{\sqrt{(eV)^2 - \Delta_c^2}}{eV} \right) \frac{B^2}{P^2} \frac{x}{2} \right] \right\}. \qquad (5.16)
\end{aligned}
$$

So, for s-wave symmetry, where the coherence gap does not depend on the quantum number ν, we have:

$$
\begin{aligned}
\sigma_{NS} \; = \; & \frac{2\pi e P^2 \rho_M}{\hbar} \Theta(eV - \Delta_c) \rho_S(eV) \\
& \times \left\{ \rho_N(\sqrt{(eV)^2 - \Delta_c^2}) \left[\frac{1}{2} \left(1 + \frac{\sqrt{(eV)^2 - \Delta_c^2}}{eV} \right) \right. \right. \\
& \left. + \frac{1}{2} \left(1 - \frac{\sqrt{(eV)^2 - \Delta_c^2}}{eV} \right) \frac{B^2}{P^2} \left(1 + \frac{x}{2} \right) \right] \\
& + \rho_N(-\sqrt{(eV)^2 - \Delta_c^2}) \left[\frac{1}{2} \left(1 - \frac{\sqrt{(eV)^2 - \Delta_c^2}}{eV} \right) \right. \\
& \left. \left. + \frac{1}{2} \left(1 + \frac{\sqrt{(eV)^2 - \Delta_c^2}}{eV} \right) \frac{B^2}{P^2} \left(1 + \frac{x}{2} \right) \right] \right\} \\
+ \; & \frac{2\pi P^2 \rho_M}{\hbar} \Theta(-eV - \Delta_c) \rho_S(-eV)
\end{aligned}
$$

$$\times\left\{\rho_N(\sqrt{(eV)^2-\Delta_c^2})\left[\frac{1}{2}\left(1+\frac{\sqrt{(eV)^2-\Delta_c^2}}{eV}\right)\right.\right.$$
$$\left.+\frac{1}{2}\left(1-\frac{\sqrt{(eV)^2-\Delta_c^2}}{eV}\right)\frac{B^2}{P^2}\frac{x}{2}\right]$$
$$+\rho_N(\sqrt{-(eV)^2-\Delta_c^2})\left[\frac{1}{2}\left(1-\frac{\sqrt{(eV)^2-\Delta_c^2}}{eV}\right)\right.$$
$$\left.\left.+\frac{1}{2}\left(1+\frac{\sqrt{(eV)^2-\Delta_c^2}}{eV}\right)\frac{B^2}{P^2}\frac{x}{2}\right]\right\}. \tag{5.17}$$

See Fig. 5.2. In the normal state, the asymmetry and the PG are evident. Below the transition temperature these features are still clearly apparent, however we now have the SG at lower magnitudes of the bias. This is evidence that our theory provides the characteristics expected with extrinsic tunnelling in cuprates.

When tunnelling occurs, if there is no favourable tunnelling scenario, i.e. if tunnelling involving an electron and a polaron only was equally as likely as tunnelling involving a bipolaron, then the matrix elements P and B are equal. The extrinsic tunnelling spectra for this case is shown in Fig. 5.3. In this case, the same features are seen in the superconducting state, we have asymmetry, which is as expected from Equation 5.17 since as well as the matrix elements, doping contributes to the asymmetry.

NS Tunnelling with d-wave Symmetry of the Coherent Gap

Different to s-wave, the coherent gap now depends on the energy contour, ϕ, where $\Delta_{c\nu}=\Delta_0\cos 2\phi$, this needs to be considered when finding the conductance.

Referring back to Equation (5.7) consider the system at zero temperature, which means Equations (5.10) and $f_{\nu'}=0$ can be utilised (as we now have no free polarons, they have all condensed into the bipolaronic condensate) giving

$$\sigma_{NS} = \frac{2\pi eP^2}{\hbar}\sum_{\nu\nu'}\left[u_{\nu'}^2\delta(eV-\xi_\nu)\delta(\xi_\nu-\epsilon_{\nu'})+v_{\nu'}^2\delta(eV-\xi_\nu)\delta(\xi_\nu+\epsilon_{\nu'})\right]$$
$$+\frac{2\pi eP^2}{\hbar}\sum_{\nu\nu'}\left[u_{\nu'}^2\frac{x}{2}\delta(eV-\xi_\nu)\delta(\xi_\nu+\epsilon_{\nu'})\right.$$

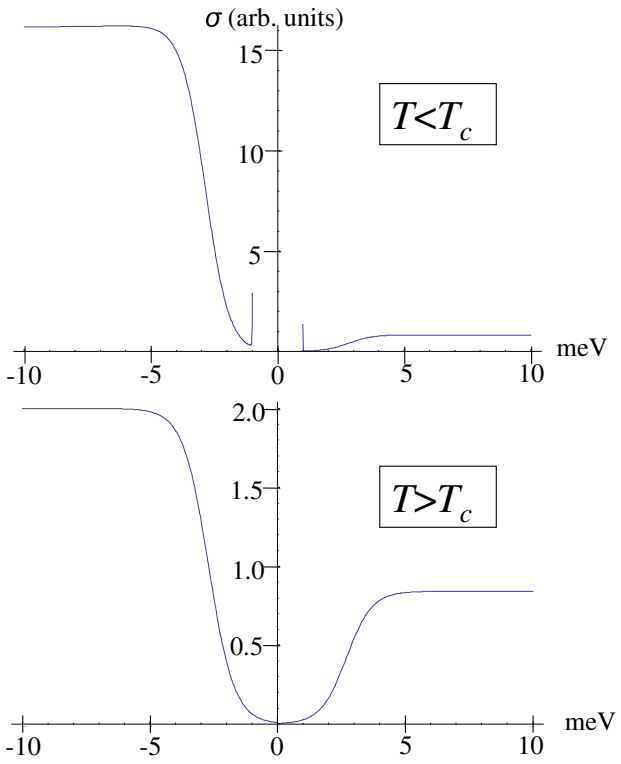

Fig. 5.2: The extrinsic tunnelling spectra with s-wave symmetry, the top figure depicts the conductance in the superconducting state, here the SG, PG and asymmetry are evident. The bottom figure is in the normal state and shows the persistence of the PG above the transition temperature. Note: our theory has been produced for charge carriers being electrons whereas in cuprates it is believed that they are holes, so here I have multiplied the "eV" terms by minus one. Here $x = 0.12$, $B^2/P^2 = 2.7$, $\Gamma = 1\text{meV}$ and $\Delta_p = 2.7\text{meV}$.

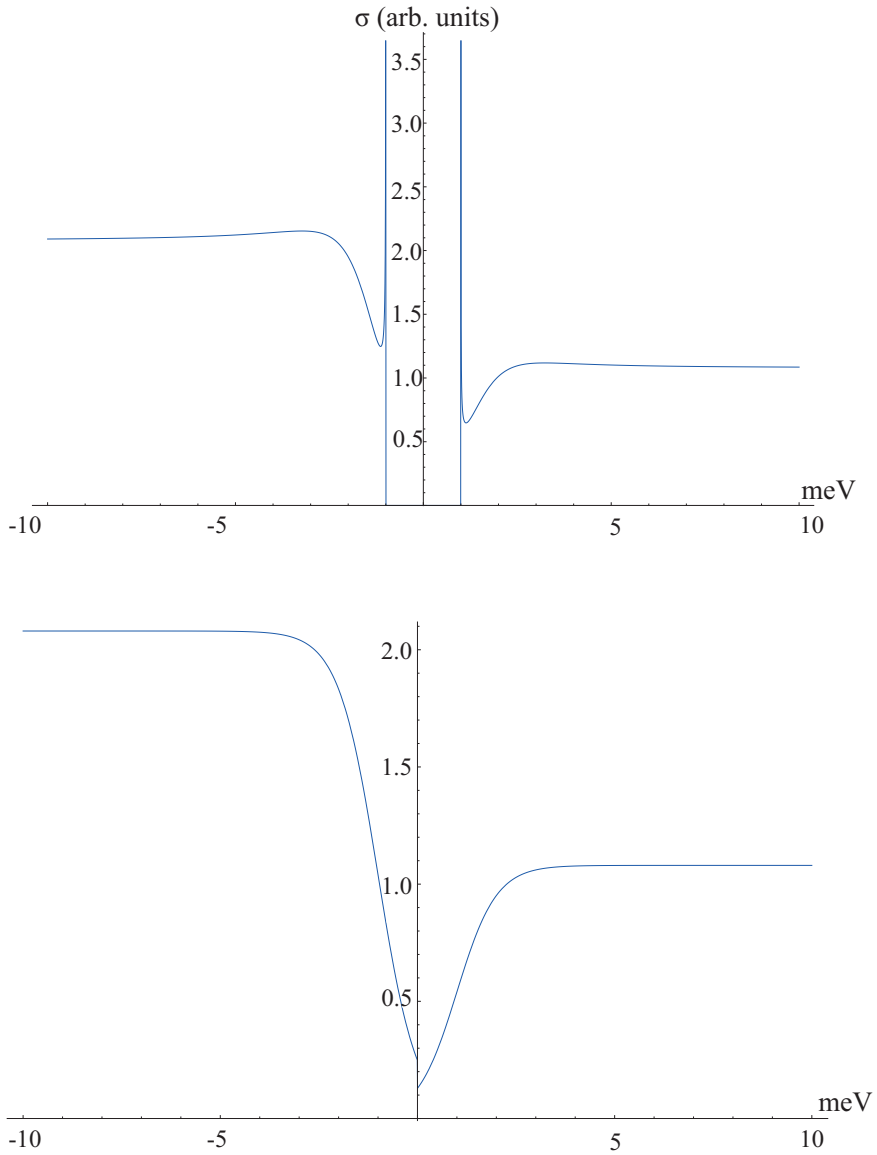

Fig. 5.3: The extrinsic tunnelling spectra with s-wave symmetry, when the matrix elements P and B are equal. The top figure depicts the conductance in the superconducting state, the bottom figure is in the normal state. Note: our theory has been produced for charge carriers being electrons whereas in cuprates it is believed that they are holes, so here I have multiplied the "eV" terms by minus one. This is at optimum doping level ($x = 0.16$) and $\Delta_p = 1\text{meV}$, $\Gamma = 1\text{meV}$.

$$+v_{\nu'}^2\left(1+\frac{x}{2}\right)\delta(eV-\xi_\nu)\delta(\xi_\nu-\epsilon_{\nu'})\Big]. \tag{5.18}$$

For positive bias, $eV>0$ we have

$$\sigma_{NS}(eV>0)=\frac{2\pi eP^2}{\hbar}\sum_{\nu'}\left[u_{\nu'}^2\delta(eV-\epsilon_{\nu'})+\frac{B^2}{P^2}v_{\nu'}^2\left(1+\frac{x}{2}\right)\delta(eV-\epsilon_{\nu'})\right]. \tag{5.19}$$

Substituting in the Bogoliubov coefficients Equation (4.18) gives

$$\sigma_{NS}\propto\sum_{\nu'}\delta(eV-\epsilon_{\nu'})\left(1+\frac{\xi_{\nu'}}{\epsilon_{\nu'}}\right)+\frac{B^2}{P^2}\sum_{\nu'}\delta(eV-\epsilon_{\nu'})\left(1-\frac{\xi_{\nu'}}{\epsilon_{\nu'}}\right)\left(1+\frac{x}{2}\right). \tag{5.20}$$

Which gives us two equations to work with:

$$\begin{aligned} I_1 &= \sum_{\nu'}\delta(eV-\epsilon_{\nu'}) \\ I_2 &= \sum_{\nu'}\frac{\xi_{\nu'}}{\epsilon_{\nu'}}\delta(eV-\epsilon_{\nu'}). \end{aligned} \tag{5.21}$$

Here we can calculate these integrals using the normal DOS, defined as:

$$\sum_{\nu'}F(\xi_{\nu'},\phi)=\frac{1}{2\pi}\int_{-\infty}^{\infty}d\xi\rho_N(\xi)\int_0^{2\pi}d\phi F(\xi,\phi), \tag{5.22}$$

where $F(\xi,\phi)$ is an arbitrary function of the normal-state energy ξ and the angle ϕ on the constant energy "contour". Note that $\epsilon_{\nu'}=\sqrt{\xi_{\nu'}^2+\Delta_0^2\cos^2 2\phi}$, then we get

$$\begin{aligned} I_1 &= \frac{1}{2\pi}\int_{-\infty}^{\infty}d\xi\rho_N(\xi)\int_0^{2\pi}d\phi\delta(eV-\sqrt{\xi^2+\Delta_0^2\cos^2 2\phi}) \\ &= \frac{1}{2\pi}\int_0^{\infty}d\xi\int_0^{2\pi}d\phi\left[\rho_N(\sqrt{(eV)^2-\Delta_0^2\cos^2 2\phi})+\rho_N(-\sqrt{(eV)^2-\Delta_0^2\cos^2 2\phi})\right] \\ &\quad\times\delta(eV-\sqrt{\xi^2+\Delta_0^2\cos^2 2\phi}) \\ &\approx [\rho_N(eV)+\rho_N(-eV)]\int_0^{\infty}d\xi\int_0^{2\pi}d\phi\delta(eV-\sqrt{\xi^2+\Delta_0^2\cos^2 2\phi}) \\ &\propto [\rho_N(eV)+\rho_N(-eV)]\,\rho_S(eV), \end{aligned} \tag{5.23}$$

where we approximate $\rho_N(\sqrt{(eV)^2-\Delta_0^2\cos^2 2\phi})\approx\rho_N(eV)$ since we consider the characteristic bandwidth to be much bigger than the superconducting gap, $\Gamma>>\Delta_{c\nu}$.

using the DOS from Section 4.6. Similarly, we can calculate I_2:

$$\begin{aligned} I_2 &\approx [\rho_N(eV)+\rho_N(-eV)]\int_0^\infty d\xi\int_0^{2\pi} d\phi \frac{\xi}{\sqrt{\xi^2+\Delta_0^2\cos^2 2\phi}}\delta(eV-\sqrt{\xi^2+\Delta_0^2\cos^2 2\phi}) \\ &= [\rho_N(eV)+\rho_N(-eV)] \\ &\quad \times\Big[4\Theta(eV-\Delta_0)\int_0^{\frac{\pi}{2}} d\psi + 4\Theta(eV-\Delta_0)\int_{\arccos(eV/\Delta_0)}^{\frac{\pi}{2}} d\psi\Big]. \end{aligned} \tag{5.24}$$

Which gives

$$\begin{aligned} \sigma_{NS} \propto\ & A^+\rho_S(|eV|)\left[\rho_N(eV)+\rho_N(-eV)\right] \\ & +A^-\Big[1-\frac{2}{\pi}\arccos\left(\frac{|eV|}{\Delta_0}\right)\Theta\left(1-\frac{|eV|}{\Delta_0}\right)\Big]\Big[\rho_N(-eV)-\rho_N(eV)\Big], \end{aligned} \tag{5.25}$$

where

$$A^\pm = 1 \pm \frac{B^2}{P^2}\left(\Theta(-eV)+\frac{x}{2}\right). \tag{5.26}$$

This equation has been plotted in Fig. 5.4, it can clearly be seen that the theory is capable of producing the asymmetry (which is a result of x, B and P), superconducting gap (Δ_c) and pseudogap (results from $\mu < 0$). The asymmetry is due to the broken electron-hole symmetry in the impurity band and the charge transfer gap in cuprates, as a result the single particle DOS is strongly energy dependent near the Fermi level in cuprates.

A plot of the NS theoretical and experimental conductance on the same graph cannot be produced, as with spatially dependent scanning tunnelling spectroscopy the DOS is highly spatially dependent, $\rho(E) \to \rho(E, \boldsymbol{r})$. This is due to the random distribution of impurities within the sample. This would mean having a different equation for the DOS for each STM scan.

A one-to-one correlation with disorder in the sample and oxygen distribution has been found experimentally by McElroy et al. [99].

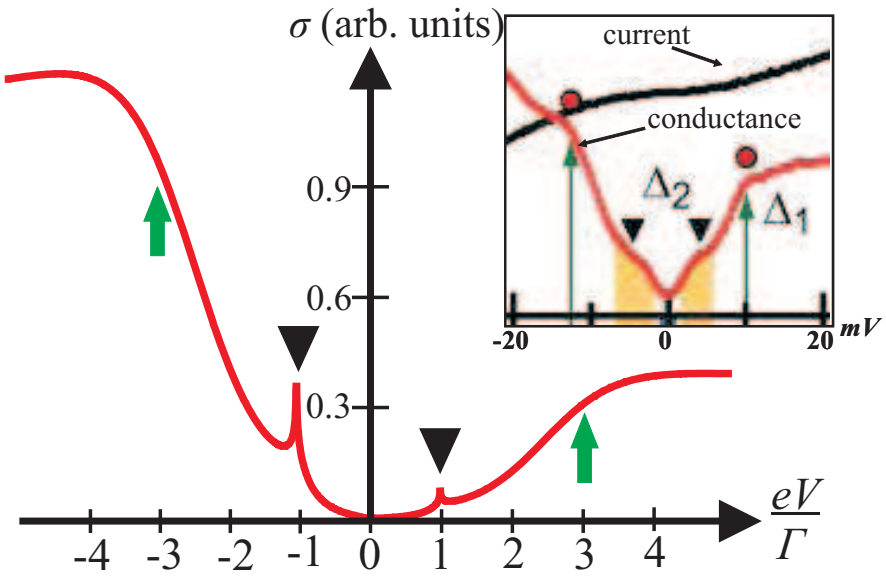

Fig. 5.4: Theoretical NS conductance for a d-wave superconductor, Equation (5.25), for $\Delta_0 = \Gamma$, $\Delta_p = 2.7\Gamma$ and $B = 2.65P$. The superconducting gap and the pseudogap are indicated by the black triangles and green arrows respectively, the asymmetry between the positive and negative bias is clearly present. Our theoretical result is compared to the inset, which is taken from Reference [54] which shows a representative STS spectrum of $La_{2-x}Sr_xCuO_4$ with $x = 0.12$ at $T = 4.2K$. As is evident, our features match those of the inset nicely. Figure taken from Reference [100].

5.2 Intrinsic (SS) Tunnelling

Intrinsic tunnelling is considered where single particles tunnel between two identical superconductors. Intrinsic tunnelling experiments [55, 56, 57, 58, 59] on mesas have indicated a nonzero conductance at zero voltage near and above the transition temperature. The PG and SG are also present.

Only polaron tunnelling is measurable in the intrinsic measurements but bipolarons can be involved. If there is enough voltage to overcome the binding energy of the bipolaron then it can break into its constituent parts and one of these polarons then has a probability of tunnelling while the other goes into the polaron band, energy is conserved in this process.

The effective Hamiltonian is

$$H = H_0 + H_{SS}, \tag{5.27}$$

where H_0 is described by Equation (4.6) and the tunnelling Hamiltonian, H_{SS}, is given by

$$H_{SS} = P\sum_{\nu\nu'} p^\dagger_{\nu'} p_\nu + \frac{B}{\sqrt{N}}\sum_{\nu\nu'}\left(\sum_{\eta} p^\dagger_{\nu'} p^\dagger_{\bar{\nu}} b_\eta + \sum_{\eta'} b^\dagger_{\eta'} p_\nu p_{\bar{\nu}'}\right) + h.c. \tag{5.28}$$

The first term here describes tunnelling without the involvement of a bipolaron; it describes the annihilation of a charge carrier on one of the superconductors, say the left one, and the creation of a charge carrier on the other superconductor. The second term describes tunnelling where there is a bipolaronic involvement. The bipolaron must first be annihilated with one of the constituent polarons being created in the other superconductor and the other being created in the polaronic band, as aforementioned. This bipolaronic term also involves the annihilation of two polarons, one in each superconductor and the creation of a bipolaron on the superconductor, say on the right. The different tunnelling possibilities can be seen in Fig. 5.5.

Applying the Bogoliubov transformation, where $p_\nu = u_\nu\alpha_\nu + v_\nu\beta^\dagger_\nu$ and $p_{\bar{\nu}} = u_\nu\beta_\nu - v_\nu\alpha^\dagger_\nu$ then upon application of the FDGR, Equation (2.5), the first term of Equation (5.28)

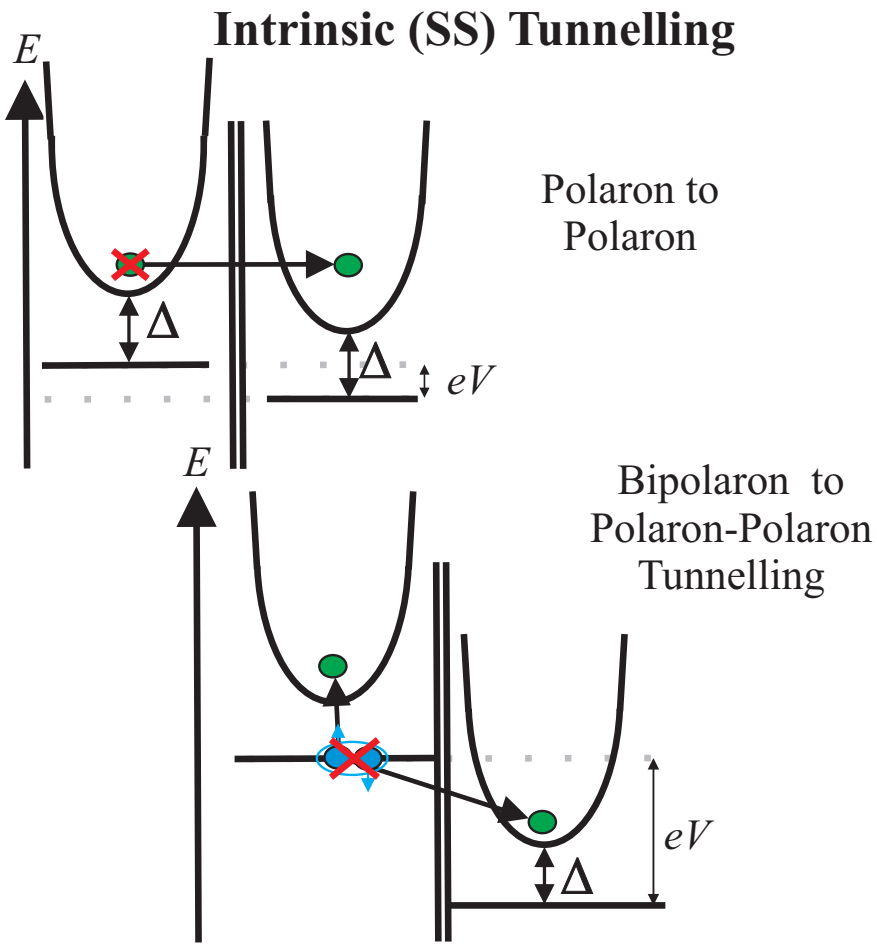

Fig. 5.5: Cartoon demonstrating different single-particle tunnelling processes in SS tunnelling. The first is the annihilation of a polaron in the superconductor on the left and the creation of a polaron on the right, the same as for NS tunnelling. This is described in the first part of the tunnelling Hamiltonian, Equation (5.28). The second illustrates a tunnelling process involving a bipolaron, where on the left a bipolaron is annihilated into two polarons, one of these moves into the polaron band on the left, the other tunnels to the superconductor on the right, as described by the second term of Equation (5.28). Figure taken from Reference [15].

becomes

$$\begin{aligned}
W^{(i)}_{l\to r} &= \frac{2\pi P^2}{\hbar}\sum_{\nu\nu'}\big\{u_\nu^2u_{\nu'}^2f_\nu(1-f_{\nu'})\delta(\epsilon_\nu+eV-\epsilon_{\nu'})+u_\nu^2v_{\nu'}^2f_\nu f_{\nu'}\delta(\epsilon_\nu+eV-\epsilon_{\nu'})\\
&\quad +u_{\nu'}^2v_\nu^2(1-f_\nu)(1-f_{\nu'})\delta(\epsilon_\nu-eV+\epsilon_{\nu'})+v_\nu^2v_{\nu'}^2(1-f_\nu)f_{\nu'}\delta(\epsilon_\nu-eV-\epsilon_{\nu'})\big\}\\
W^{(i)}_{r\to l} &= \frac{2\pi P^2}{\hbar}\sum_{\nu\nu'}\big\{u_\nu^2u_{\nu'}^2(1-f_\nu)f_{\nu'}\delta(\epsilon_\nu+eV-\epsilon_{\nu'})\\
&\quad +u_\nu^2v_{\nu'}^2(1-f_\nu)(1-f_{\nu'})\delta(\epsilon_\nu+eV-\epsilon_{\nu'})\\
&\quad +u_{\nu'}^2v_\nu^2f_\nu f_{\nu'}\delta(\epsilon_\nu-eV+\epsilon_{\nu'})+v_\nu^2v_{\nu'}^2f_\nu(1-f_{\nu'})\delta(\epsilon_\nu-eV-\epsilon_{\nu'})\big\}\,. \qquad (5.29)
\end{aligned}$$

Using Equation (2.18), the current is

$$\begin{aligned}
I^{(i)} &= \frac{2\pi eP^2}{\hbar}\sum_{\nu\nu'}\big\{u_\nu^2u_{\nu'}^2(f_\nu-f_{\nu'})\delta(\epsilon_\nu+eV-\epsilon_{\nu'})\\
&\quad +u_\nu^2v_{\nu'}^2(f_\nu+f_{\nu'}-1)\delta(\epsilon_\nu+eV-\epsilon_{\nu'})\\
&\quad +u_{\nu'}^2v_\nu^2(1-f_\nu-f_{\nu'})\delta(\epsilon_\nu-eV+\epsilon_{\nu'})\\
&\quad +v_\nu^2v_{\nu'}^2(f_{\nu'}-f_\nu)\delta(\epsilon_\nu-eV-\epsilon_{\nu'})\big\}\,. \qquad (5.30)
\end{aligned}$$

Following the same procedure for the second and third terms of Equation (5.28)

$$\begin{aligned}
W^{(ii)}_{l\to r} &= \frac{2\pi B^2}{\hbar N}\sum_{\nu\nu'\eta}n_\eta\big\{u_\nu^2u_{\nu'}^2(1-f_\nu)(1-f_{\nu'})\delta(E_\eta-\epsilon_\nu-\epsilon_{\nu'}-eV)\\
&\quad +u_{\nu'}^2v_\nu^2f_\nu(1-f_{\nu'})\delta(E_\eta+\epsilon_\nu-\epsilon_{\nu'}-eV)\\
&\quad +u_\nu^2v_{\nu'}^2(1-f_\nu)f_{\nu'}\delta(E_\eta-\epsilon_\nu+\epsilon_{\nu'}-eV)\\
&\quad +v_\nu^2v_{\nu'}^2f_\nu f_{\nu'}\delta(E_\eta+\epsilon_\nu+\epsilon_{\nu'}-eV)\big\}\,,\\
W^{(ii)}_{r\to l} &= \frac{2\pi B^2}{\hbar N}\sum_{\nu\nu'\eta}(1+n_\eta)\big\{u_\nu^2u_{\nu'}^2f_\nu f_{\nu'}\delta(E_\eta-\epsilon_\nu-\epsilon_{\nu'}-eV)\\
&\quad +u_{\nu'}^2v_\nu^2(1-f_\nu)f_{\nu'}\delta(E_\eta+\epsilon_\nu-\epsilon_{\nu'}-eV)\\
&\quad +u_\nu^2v_{\nu'}^2f_\nu(1-f_{\nu'})\delta(E_\eta-\epsilon_\nu+\epsilon_{\nu'}-eV)\\
&\quad +v_\nu^2v_{\nu'}^2(1-f_\nu)(1-f_{\nu'})\delta(E_\eta+\epsilon_\nu+\epsilon_{\nu'}-eV)\big\}\,,\\
I^{(ii)} &= \frac{2\pi eB^2}{\hbar N}\sum_{\nu\nu'\eta}\big\{u_\nu^2u_{\nu'}^2\left[n_\eta(1-f_\nu-f_{\nu'})-f_\nu f_{\nu'}\right]\delta(E_\eta-\epsilon_\nu-\epsilon_{\nu'}-eV)\\
&\quad +u_{\nu'}^2v_\nu^2\left[n_\eta(f_\nu-f_{\nu'})-(1-f_\nu)f_{\nu'}\right]\delta(E_\eta+\epsilon_\nu-\epsilon_{\nu'}-eV)\\
&\quad +u_\nu^2v_{\nu'}^2\left[n_\eta(f_{\nu'}-f_\nu)-f_\nu(1-f_{\nu'})\right]\delta(E_\eta-\epsilon_\nu+\epsilon_{\nu'}-eV)\\
&\quad +v_\nu^2v_{\nu'}^2\left[n_\eta(f_\nu+f_{\nu'}-1)-(1-f_\nu)(1-f_{\nu'})\right]\\
&\quad \times\delta(E_\eta+\epsilon_\nu+\epsilon_{\nu'}-eV)\big\}\,, \qquad (5.31)
\end{aligned}$$

and

$$
\begin{aligned}
W^{(iii)}_{l\to r} &= \frac{2\pi B^2}{\hbar N}\sum_{\nu\nu'\eta'}(1+n_{\eta'})\left\{u^2_\nu u^2_{\nu'} f_\nu f_{\nu'}\delta(E_{\eta'}-\epsilon_\nu-\epsilon_{\nu'}-eV)\right.\\
&\quad +u^2_\nu v^2_{\nu'} f_\nu(1-f_{\nu'})\delta(E_{\eta'}-\epsilon_\nu+\epsilon_{\nu'}-eV)\\
&\quad +u^2_{\nu'} v^2_\nu (1-f_\nu) f_{\nu'}\delta(E_{\eta'}+\epsilon_\nu-\epsilon_{\nu'}-eV)\\
&\quad \left.+v^2_\nu v^2_{\nu'}(1-f_\nu)(1-f_{\nu'})\delta(E_{\eta'}+\epsilon_\nu+\epsilon_{\nu'}-eV)\right\},\\
W^{(iii)}_{r\to l} &= \frac{2\pi B^2}{\hbar N}\sum_{\nu\nu'\eta'} n_{\eta'}\left\{u^2_\nu u^2_{\nu'}(1-f_\nu)(1-f_{\nu'})\delta(E_{\eta'}-\epsilon_\nu-\epsilon_{\nu'}-eV)\right.\\
&\quad +u^2_\nu v^2_{\nu'}(1-f_\nu) f_{\nu'}\delta(E_{\eta'}-\epsilon_\nu+\epsilon_{\nu'}-eV)\\
&\quad +u^2_{\nu'} v^2_\nu f_\nu(1-f_{\nu'})\delta(E_{\eta'}+\epsilon_\nu-\epsilon_{\nu'}-eV)\\
&\quad \left.+v^2_\nu v^2_{\nu'} f_\nu f_{\nu'}\delta(E_{\eta'}+\epsilon_\nu+\epsilon_{\nu'}-eV)\right\},\\
I^{(iii)} &= \frac{2\pi B^2}{\hbar N}\sum_{\nu\nu'\eta'}\left\{u^2_\nu u^2_{\nu'}\left[n_{\eta'}(f_\nu+f_{\nu'}-1)+f_\nu f_{\nu'}\right]\delta(E_{\eta'}-\epsilon_\nu-\epsilon_{\nu'}-eV)\right.\\
&\quad +u^2_\nu v^2_{\nu'}\left[n_{\eta'}(f_\nu-f_{\nu'})+f_\nu(1-f_{\nu'})\right]\delta(E_{\eta'}-\epsilon_\nu+\epsilon_{\nu'}-eV)\\
&\quad +u^2_{\nu'} v^2_\nu\left[n_{\eta'}(f_{\nu'}-f_\nu)+f_{\nu'}(1-f_\nu)\right]\delta(E_{\eta'}+\epsilon_\nu-\epsilon_{\nu'}-eV)\\
&\quad +v^2_\nu v^2_{\nu'}\left[n_{\eta'}(1-f_\nu-f_{\nu'})+(1-f_\nu)(1-f_{\nu'})\right]\\
&\quad \left.\times\delta(E_{\eta'}+\epsilon_\nu+\epsilon_{\nu'}-eV)\right\}. \qquad (5.32)
\end{aligned}
$$

As before we can neglect the bipolaron dispersion, setting $E_{\eta'}=0$ and $E_\eta=2eV$, where eV is the difference in energy across the junction due to the applied potential.

5.2.1 Tunnelling Above T_c

In the normal state, where the temperature is above the transition temperature, $T>T_c$, there is no superconducting gap since its onset is at the transition temperature, therefore $\Delta_{c\nu}=0$, this means that from $\xi=\sqrt{\epsilon^2+\Delta^2_{c\nu}}$, $\xi=\epsilon$ and so the Bogoliubov coefficients (Equation (4.18)) become $u^2=1,\ v^2=0$ and we have

$$
\begin{aligned}
I_{SS}(T>T_c) &= \frac{2\pi eP^2}{\hbar}\sum_{\nu\nu'}(f_\nu-f_{\nu'})\delta(\xi_\nu+eV-\xi_{\nu'})\\
&\quad +\frac{2\pi eB^2}{\hbar}\sum_{\nu\nu'}\left[\frac{x}{2}(1-f_\nu-f_{\nu'})-f_\nu f_{\nu'}\right]\\
&\quad \times\left[\delta(\xi_\nu-eV+\xi_{\nu'})-\delta(\xi_\nu+eV+\xi_{\nu'})\right]. \qquad (5.33)
\end{aligned}
$$

This is using $\sum_\eta \frac{n_\eta}{N} = \sum_{\eta'} \frac{n_{\eta'}}{N} = \frac{x}{2}$. Here $f(\xi)$ is the polaron distribution, not the Bogoliubov quasiparticle $f(\epsilon)$ as before, so, at zero temperature it is not equal to zero. For higher voltages, $eV > k_B T$, the Fermi-Dirac distribution, Equation (2.1), can be approximated as a step function.

$$f(\xi_\nu) = \Theta(-\xi_\nu),\ f(\xi_{\nu'}) = \Theta(-\xi_{\nu'}). \tag{5.34}$$

So

$$\begin{aligned}
I &= \frac{2\pi e P^2}{\hbar} \sum_{\nu\nu'} \left[\Theta(-\xi_\nu) - \Theta(-\xi_{\nu'})\right] \delta(\xi_\nu + eV - \xi_{\nu'}) \\
&\quad + \frac{2\pi e B^2}{\hbar} \sum_{\nu\nu'} \left\{ \frac{x}{2} \left[1 - \Theta(-\xi_\nu) - \Theta(-\xi_{\nu'})\right] - \Theta(-\xi_\nu)\Theta(-\xi_{\nu'}) \right\} \\
&\quad \times \left[\delta(\xi_\nu - eV + \xi_{\nu'}) - \delta(\xi_\nu + eV + \xi_{\nu'})\right] \\
&= \frac{2\pi e P^2}{\hbar} \int_{-\infty}^{\infty} d\xi \int_{-\infty}^{\infty} d\xi' \rho(\xi)\rho(\xi') \left[\Theta(-\xi) - \Theta(-\xi')\right] \delta(\xi + eV - \xi') \\
&\quad + \frac{2\pi e B^2}{\hbar} \int_{-\infty}^{\infty} d\xi \int_{-\infty}^{\infty} d\xi' \rho(\xi)\rho(\xi') \left\{ \frac{x}{2} \left[1 - \Theta(-\xi) - \Theta(-\xi')\right] - \Theta(-\xi)\Theta(-\xi') \right\} \\
&\quad \times \left[\delta(\xi - eV + \xi') - \delta(\xi + eV + \xi')\right] \\
&= \frac{2\pi e P^2}{\hbar} \int_{-\infty}^{0} d\xi \rho(\xi)\rho(\xi + eV) - \frac{2\pi e P^2}{\hbar} \int_{-\infty}^{-eV} d\xi \rho(\xi)\rho(\xi + eV) \\
&\quad + \frac{\pi e B^2 x}{\hbar} \int_{-\infty}^{\infty} d\xi \rho(\xi)\rho(\xi - eV) - \frac{\pi e B^2 x}{\hbar} \int_{-\infty}^{0} d\xi \rho(\xi)\rho(\xi - eV) \\
&\quad - \frac{\pi e B^2 x}{\hbar} \int_{eV}^{\infty} d\xi \rho(\xi)\rho(\xi - eV) - \frac{\pi e B^2 x}{\hbar} \int_{-\infty}^{\infty} d\xi \rho(\xi)\rho(-\xi - eV) \\
&\quad + \frac{\pi e B^2 x}{\hbar} \int_{-\infty}^{0} d\xi \rho(\xi)\rho(-\xi - eV) + \frac{\pi e B^2 x}{\hbar} \int_{-eV}^{\infty} d\xi \rho(\xi)\rho(-\xi - eV) \\
&\quad + \frac{\pi e B^2 x}{\hbar} \int_{-eV}^{0} d\xi \rho(\xi)\rho(-\xi - eV).
\end{aligned} \tag{5.35}$$

For $eV > 0$:

$$\begin{aligned}
I_{SS}(T > T_c; V > 0) &= \frac{2\pi e P^2}{\hbar} \int_0^{eV} d\xi \rho(-\xi)\rho(eV - \xi) \\
&\quad + \frac{\pi e B^2 x}{\hbar} \int_0^{eV} d\xi \rho(\xi)\rho(eV - \xi) \\
&\quad + \frac{\pi e B^2 (x+2)}{\hbar} \int_0^{eV} d\xi \rho(-\xi)\rho(\xi - eV),
\end{aligned} \tag{5.36}$$

Following the procedure in Appendix E we find the I_{SS} current to be:

$$I_{SS} \propto \frac{a^2}{2(a^2-1)}\left[\ln\frac{a^2(b^2+1)}{a^2b^2+1} - \frac{1}{a^2}\ln\frac{a^2+b^2}{1+b^2}\right] + \frac{B^2x}{2P^2}\frac{a^2}{a^2-b^4}\ln\frac{a^2+b^2}{a(1+b^2)} + \frac{B^2(2+x)}{2P^2}\frac{1}{a^2b^4-1}\ln\frac{1+a^2b^2}{a(1+b^2)}, \quad (5.37)$$

where

$$\begin{aligned} y &= e^{\xi/k_BT} \\ b &= e^{\Delta_p/k_BT} \\ a &= e^{eV/k_BT}. \end{aligned} \quad (5.38)$$

See Fig. 5.6 for the intrinsic tunnelling conductance (which is the derivative of Equation (5.37), with respect to the voltage) with the Fermi-Dirac distribution approximated as a step function. Here there is no asymmetry as the two materials the carriers are tunnelling from/to are exactly the same. It can be seen that for higher voltages we have a good agreement with the experimental data from Reference [58], however for lower bias experiments indicate a gapped conductance which is not apparent in our theory. Note that as we are dealing with temperature near and above the transition temperature we have only the PG and there is no sign of the SG in these spectra. At this stage of the research it was thought that finite temperature effects were the cause of the gapped conductance, and so for lower voltages making the approximation of the Fermi-Dirac distribution a step function was not sufficient.

5.2.2 Finite Temperature Effects on the Normal-State Intrinsic Conductance

To test the hypothesis that the gapped conductance seen in experiments [58] may be due to finite temperature effects, the approximation of the Fermi-Dirac distribution being a step function is now dropped. Now, for nonzero temperature, $T \neq 0$, we must include the effect of temperature on $f(\xi)$ as this is the distribution of charge carriers which is not zero for finite temperature (unlike $f(\epsilon)$). Referring back to Equation (5.33) we have

$$I_{SS} = \frac{2\pi eP^2}{\hbar}\sum_{\nu\nu'}(f_\nu - f_{\nu'})\delta(\xi_\nu + eV - \xi_{\nu'})$$

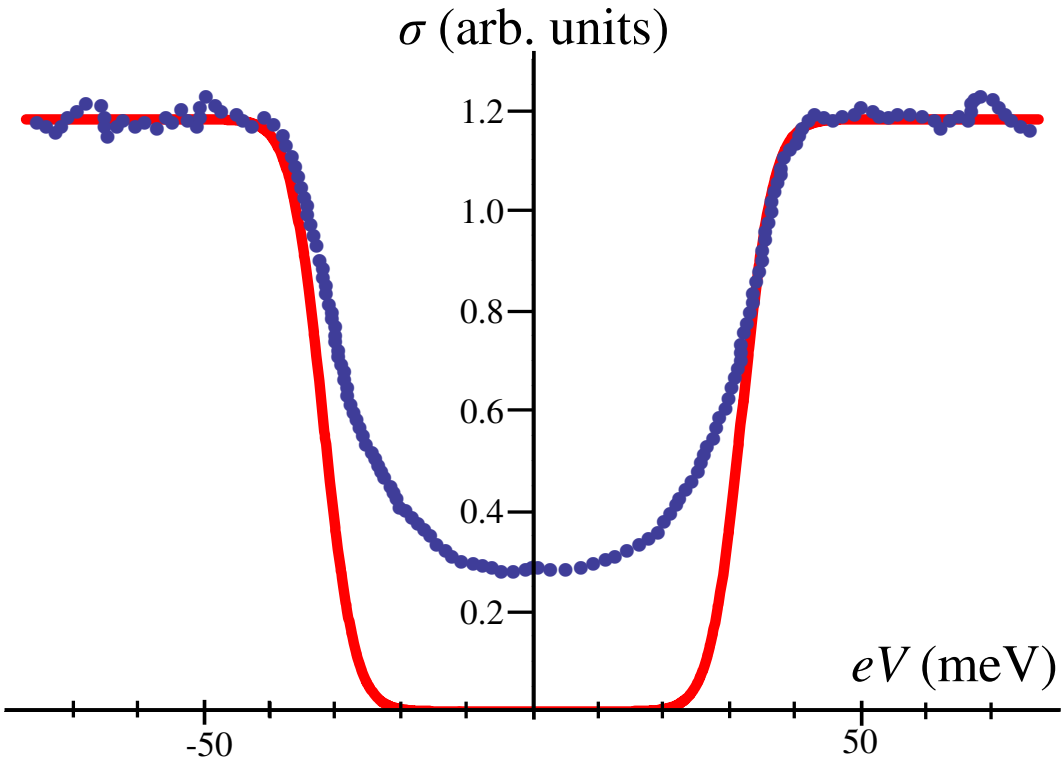

Fig. 5.6: The experimental results from Reference [58] are shown in blue and compared to the theory (in red). Here it can be seen that making the approximation of the Fermi-Dirac distribution being a step function, Equation (5.34), means the conductance can be well described for higher voltages. However for smaller bias there is a gapped conductance evident experimentally that is unaccounted for. The experimental mesa is of underdoped Bi2212 and the spectra is taken at 90K which is approximately the transition temperature, so the SG is not visible. Here $\Gamma = 3.2$meV and $\Delta_p = 16$meV. Figure taken from Reference [100].

$$
\begin{aligned}
&+\frac{2\pi eB^2}{\hbar}\sum_{\nu\nu'}\left[\frac{x}{2}\left(1-f_\nu-f_{\nu'}\right)-f_\nu f_{\nu'}\right]\delta(\xi_\nu-eV+\xi_{\nu'})\\
&-\frac{2\pi eB^2}{\hbar}\sum_{\nu\nu'}\left[\frac{x}{2}\left(1-f_\nu-f_{\nu'}\right)-f_\nu f_{\nu'}\right]\delta(\xi_\nu+eV+\xi_{\nu'})\\
=\;&\frac{2\pi eP^2}{\hbar}\int_{-\infty}^{\infty}d\xi\rho_N(\xi)\rho_N(\xi+eV)\left[f(\xi)-f(\xi+eV)\right]\\
&+\frac{2\pi eB^2}{\hbar}\int_{-\infty}^{\infty}d\xi\rho_N(\xi)\rho_N(eV-\xi)\left[\frac{x}{2}\left(1-f(\xi)-f(eV-\xi)\right)-f(\xi)f(eV-\xi)\right]\\
&-\frac{2\pi eB^2}{\hbar}\int_{-\infty}^{\infty}d\xi\rho_N(\xi)\rho_N(-eV-\xi)\\
&\qquad\times\left[\frac{x}{2}\left(1-f(\xi)-f(-eV-\xi)\right)-f(\xi)f(-eV-\xi)\right].
\end{aligned}
\tag{5.39}
$$

Making the substitution $F(\xi)=\rho_N(\xi)f(\xi)$ means we have a convergent integral. So, the first term becomes

$$
\begin{aligned}
&\frac{2\pi eP^2}{\hbar}\int_{-\infty}^{\infty}d\xi\left[F(\xi)\rho_N(\xi+eV)-F(\xi+eV)\rho_N(\xi)\right]\\
&=\frac{2\pi eP^2}{\hbar}\int_{-\infty}^{\infty}d\xi F(\xi)\left[\rho_N(\xi+eV)-\rho_N(\xi-eV)\right].
\end{aligned}
\tag{5.40}
$$

Using the normal-state DOS:

$$
\begin{aligned}
&\rho_N(\xi+eV)=\frac{1}{2}\left[1+\tanh\left(\frac{\xi+eV-\Delta_p}{\Gamma}\right)\right];\\
&\frac{\mathrm{d}}{\mathrm{d}(eV)}\rho_N(\xi+eV)=\frac{1}{2\Gamma}\mathrm{sech}^2\left(\frac{\xi+eV-\Delta_p}{\Gamma}\right)\\
\text{Similarly}\quad&\frac{\mathrm{d}}{\mathrm{d}(eV)}\rho_N(\xi-eV)=-\frac{1}{2\Gamma}\mathrm{sech}^2\left(\frac{\xi-eV-\Delta_p}{\Gamma}\right).
\end{aligned}
\tag{5.41}
$$

So the conductance is

$$
\sigma_{SS}^{(i)}=\frac{\pi eP^2}{\hbar\Gamma}\int_{-\infty}^{\infty}d\xi F(\xi)\left[\mathrm{sech}^2\left(\frac{\xi+eV-\Delta_p}{\Gamma}\right)-\mathrm{sech}^2\left(\frac{\xi-eV-\Delta_p}{\Gamma}\right)\right].
\tag{5.42}
$$

The second term becomes

$$
\begin{aligned}
&\frac{\pi eB^2}{\hbar}x\int_{-\infty}^{\infty}d\xi\rho_N(\xi)\rho_N(eV-\xi)\left(1-f(\xi)-f(eV-\xi)\right)\\
&-\frac{\pi eB^2}{\hbar}x\int_{-\infty}^{\infty}d\xi\rho_N(\xi)\rho_N(-eV-\xi)\left(1-f(\xi)-f(-eV-\xi)\right)\\
=\;&\frac{\pi eB^2}{\hbar}x\int_{-\infty}^{\infty}d\xi\rho_N(\xi)\left\{\rho_N(eV-\xi)\left[f(\xi-eV)-f(\xi)\right]\right.
\end{aligned}
$$

$$
\begin{aligned}
& -\rho_N(-eV-\xi)\left[f(\xi+eV)-f(\xi)\right]\} \\
= \quad & \frac{\pi e B^2}{\hbar} x \int_{-\infty}^{\infty} d\xi \rho_N(\xi)\left[\rho_N(eV-\xi)f(\xi-eV)-\rho_N(eV-\xi)f(\xi)\right. \\
& \left.-\rho_N(-eV-\xi)f(\xi+eV)+\rho_N(-eV-\xi)f(\xi)\right]. \qquad (5.43)
\end{aligned}
$$

With a change of variables we have

$$
\begin{aligned}
& \frac{\pi e B^2}{\hbar} x \int_{-\infty}^{\infty} d\xi \rho_N(-\xi)\left\{\rho_N(\xi+eV)\left[f(\xi)-f(-\xi)\right]-\rho_N(\xi-eV)\left[f(\xi)-f(-\xi)\right]\right\} \\
= \quad & \frac{\pi e B^2}{2\hbar} x \int_{-\infty}^{\infty} d\xi \rho_N(-\xi)\left[f(\xi)-f(-\xi)\right] \\
& \times\left[\operatorname{sech}^2\left(\frac{\xi+eV-\Delta_p}{\Gamma}\right)+\operatorname{sech}^2\left(\frac{\xi-eV-\Delta_p}{\Gamma}\right)\right]. \qquad (5.44)
\end{aligned}
$$

For small values of eV the first term is dominant, for larger eV the second term takes over. The third term is the bipolaron term, this is negligible compared to the other two terms. Therefore, the conductance is given by

$$
\begin{aligned}
\sigma_{SS} \quad \approx \quad & \frac{\pi e}{\hbar\Gamma}\int_{-\infty}^{\infty} d\xi\left[\operatorname{sech}^2\left(\frac{\xi+eV-\Delta_p}{\Gamma}\right)-\operatorname{sech}^2\left(\frac{\xi-eV-\Delta_p}{\Gamma}\right)\right] \\
& \times\left[P^2F(\xi)+\frac{B^2x}{2}\rho_N(-\xi)[f(\xi)-f(-\xi)]\right]. \qquad (5.45)
\end{aligned}
$$

5.2.3 Experimental Techniques in Mesas and Theory

Comparing Equation (5.45) for intrinsic tunnelling to experimental results on underdoped Bi2212 mesas, we can see in Fig. 5.7 that our theoretical results closely resemble those found by Krasnov [58]. To produce this theoretical spectra Equation (5.45) is used, where Γ is fixed at 10meV for each temperature, the ratio between the tunnelling coefficients squared and the doping is kept fixed $B^2x/P^2 = 1.96$. However, to give the best fit, Δ_p must change with temperature. It can be seen in Fig. 5.7 that we can now account for the gapped conductance at the lower voltages for different temperatures by making the approximation that the DOS follows the simple bandtail shape described by Equation (4.21).

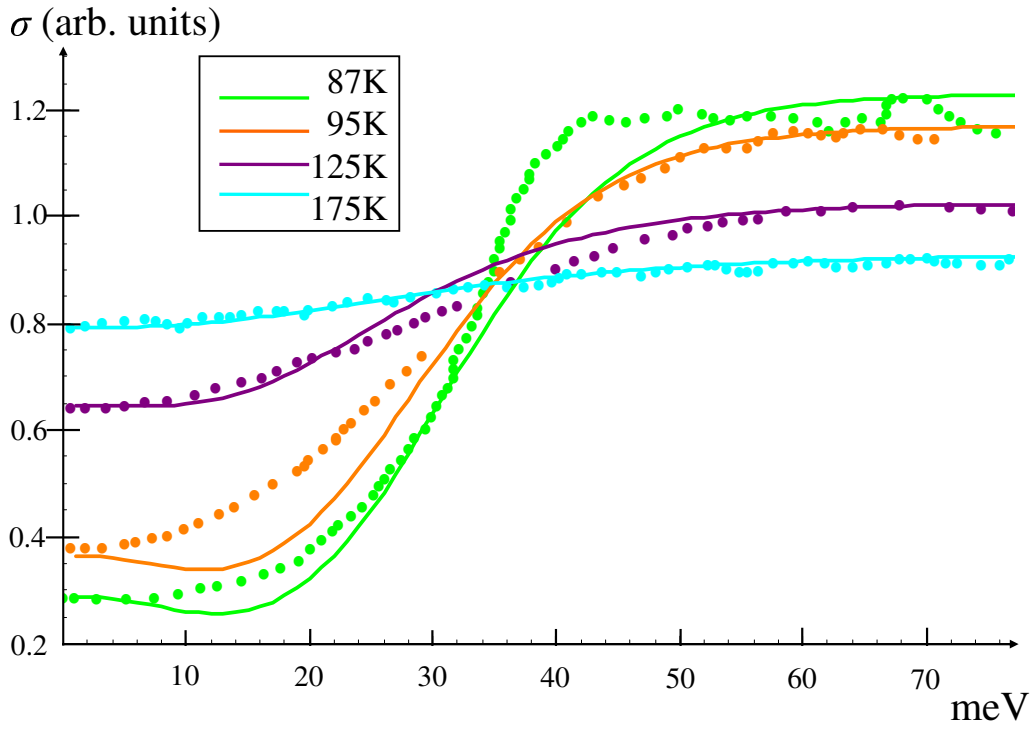

Fig. 5.7: It is shown that for a range of temperatures the conductance is well described, particularly the zero bias conductance is well produced for each temperature. The theoretical results are compared against experimental results from Krasnov [58]. To get this fit Equation (5.45) is used and for each temperature the characteristic width of the bandtail is fixed, $\Gamma = 10$meV, the matrix element squared ratio with the doping is kept fixed $B^2x/P^2 = 1.96$ but the PG value is temperature dependent. Fig. 5.8 shows the behaviour of Δ_p with temperature. It is remarkable that the model bandtail DOS for the normal-state of the superconductor can give such results. Figure taken from Reference [15].

The temperature dependence of the PG is displayed in Fig. 5.8 where it is compared to that found experimentally by Krasnov [58]. Both the experimental and theoretical results exhibit a decrease in the gap as temperature is increased, a phenomenon that could be due to many-particle effects. The doping is kept fixed and temperature is increased, this means more polarons become thermally excited from their bipolaronic state and they screen the electron-phonon interaction, this causes a decrease in the bipolaron binding energy. This effect is similar to that expected when temperature is kept fixed but doping is increased [101].

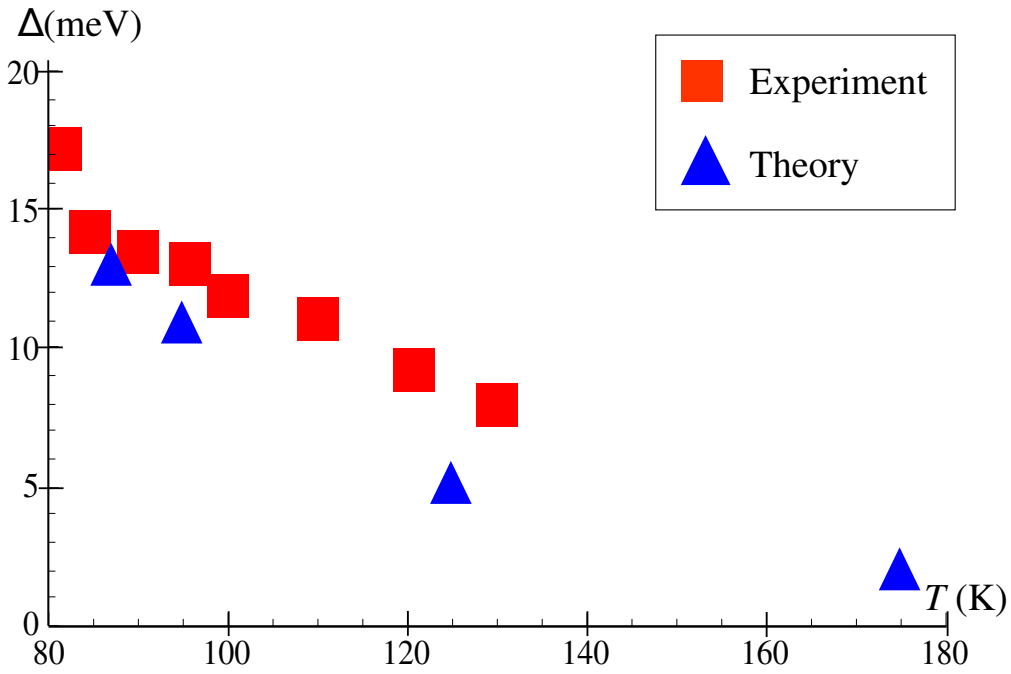

Fig. 5.8: The theory points here are taken from the fit of the theoretical model to the data from Reference [58] (see Fig. 5.7), rather than a microscopic theory. The fitted PG decreases with increasing temperature. Krasnov found a similar dependence [58] as shown by the experiment points.

6. CONCLUSIONS

The use of the Fermi-Dirac golden rule has enabled the calculation of the conductance in different materials.

For metal-metal tunnelling at different temperatures it has allowed the construction of Ohm's law, where the current has a linear dependence on the voltage and the conductance is independent of the voltage. Tunnelling of electrons from a metal to a semiconductor and vice versa has given Ohm's law but with a gap in the conductance (and current) that coincides with the voltage range where there lies an energy gap, therefore it is the result expected.

Now moving onto superconductors, I have discussed a theory of intrinsic and extrinsic tunnelling in cuprate superconductors and compared this to experimental evidence.

Tunnelling experiments provide invaluable data that gives a huge insight into the low-energy excitations and thus the way high-temperature superconductors work. NS tunnelling in cuprates has indicated two energy scales, the first is the SG that vanishes above T_c. The second gap is the PG which depends on the doping concentration and it persists above the transition temperature, so exists in both the normal and superconducting states. The PG does however remain a mystery, we are without a general consensus as to what it is and why it even exists.

STM with cuprates has indicated that the tunnelling conductance of charge carriers in one direction (say tip to sample) is different to the tunnelling conduction in the opposite direction. This presents asymmetry in the tunnelling spectra. Again, there is no general consensus as to why this is the case. Remarkably, the position of the tip on the cuprate sample gives different tunnelling results.

A two gap structure has been revealed by intrinsic tunnelling and break junction experiments. Recent experiments have provided evidence that the PG is dependent on the temperature and decreases as the temperature increases above T_c. To provide a successful theory for tunnelling with cuprates, each of these puzzling features should be accounted for in both NS and SS tunnelling.

I have presented a theory that is capable of accounting for these features. The theory is based in the *ab initio* "LDA+GTB" band structure which gives a charge transfer gap, where the minimum of the conductance band is at $(0, \pi)$ of the Brillouin zone and the maximum of the valence band is at $(\pi/2, \pi/2)$. This results in a charge-transfer Mott insulator. The doping of impurities gives localised hydrogen-like states within the charge transfer gap, the random spatial distribution of the impurities causes a bandtail in the normal-state DOS.

An extension of the BCS theory has been made in the strong coupling regime, which gives bosonic (bipolaronic) carriers which are the real-space pairs of polarons. the size of a pair is comparable to the distance between the two polarons and a true Bose-Einstein condensate can form. Different to the BCS theory the pairs do not overlap and here they survive above the transition temperature.

Using the Fermi Dirac golden rule I have calculated the tunnelling of charge carriers between a metal and a cuprate superconductor initially for zero temperature, then for finite temperature, including above T_c. I have also found the tunnelling spectra of carriers tunnelling between two identical cuprates and/or between CuO_2 planes in mesas above the transition temperature which has demonstrated the temperature dependence of the pseudogap.

Comparing the results of the theory to data from experiments shows qualitative agreement.

APPENDIX

A. IDENTITY OF PARTICLES

Reference [102] tells us about the identity of particles.

For the quantum theory of systems of identical particles, the principle of indistinguishability plays a fundamental role. If we first consider a system of two identical particles then because of their identity, the states of the system must not be changed when the particles are interchanged. This means the wavefunction can change only by an unimportant phase factor. If $\psi(\xi_1, \xi_2)$ is the wavefunction of the system, (where ξ_1 and ξ_2 denote the three spatial coordinates and spin projection for each particle) then following Reference [102] we have

$$\psi(\xi_1, \xi_2) = e^{i\alpha}\psi(\xi_2, \xi_1), \tag{A.1}$$

(where α is a real constant). If the particles are interchanged again, they return to their initial state while the wavefunction is multiplied by $e^{2i\alpha}$, so $e^{i\alpha} = \pm 1$ thus

$$\psi(\xi_1, \xi_2) = \pm\psi(\xi_2, \xi_1). \tag{A.2}$$

Therefore there are two possibilities: either the wavefunction is symmetrical (and unchanged when the particles are interchanged) or antisymmetrical (and the sign is changed when the interchange is made). These results can be generalised to systems consisting of any number of identical particles.

Particles described by antisymmetrical wavefunctions are fermions, described by Fermi-Dirac statistics. Those described by symmetrical wavefunctions are bosons, obeying Bose-Einstein statistics.

From the laws of relativistic quantum mechanics it can be shown that the statistics

obeyed by particles is uniquely related to their spin: particles with integer spin are bosons, those with half integral spin are fermions.

Considering a system of N identical particles and neglecting their mutual interactions, we can let $\psi_1,\ \psi_2,\ \cdots$ be the wavefunctions of the various stationary states which each of the particles separately may occupy. The state of the system as a whole can be defined by giving the numbers of the states which the individual particles occupy.

Letting $p_1,\ p_2,\ \cdots,\ p_N$ be the numbers of the states occupied by the individual particles, then for a system of bosons, the wavefunction $\psi(\xi_1,\ \cdots,\ \xi_N)$ is given by a sum of products:

$$\psi_{\nu_1}(\xi_1)\psi_{\nu_2}(\xi_2)\cdots\psi_{\nu_3}(\xi_3), \tag{A.3}$$

with all possible permutations of the different suffixes $p_1,\ p_2,\ \cdots$; this sum clearly possesses the required symmetry property. For example, for a system of two particles in different states ($p_1 \neq p_2$),

$$\psi(\xi_1,\xi_2) = \left[\psi_{\nu_1}(\xi_1)\psi_{\nu_2}(\xi_2) + \psi_{\nu_2}(\xi_2)\psi_{\nu_1}(\xi_1)\right]/\sqrt{2}, \tag{A.4}$$

where the factor $1/\sqrt{2}$ is introduced for normalisation purposes. All the functions $\psi_1,\ \psi_2,\ \cdots$ are orthogonal and normalised.

For a more general case, consider a system of N identical particles, the normalised wavefunction is then

$$\psi_{N_1N_2\cdots} = \left(\frac{N_1!N_2!\cdots}{N!}\right)^{\frac{1}{2}} \sum \psi_{p_1}(\xi_1)\psi_{p_2}(\xi_2)\cdots\psi_{p_N}(\xi_N), \tag{A.5}$$

here the sum is taken over all permutations of the different suffixes $p_1,\ p_2,\ \cdots,\ p_N$ and the numbers N_i show how many of these suffixes have the same value i (with $\sum N_i = N$). For the integration of $|\psi|^2$ over $\xi_1,\ \xi_2,\ \cdots,\ \xi_N$, all the terms vanish except the squared modulus of each term of the sum; since the total number of terms in the sum A.5 is evidently $N!/N_1!N_2!\cdots$, we obtain the normalisation factor.

If we now consider a system of fermions, we describe the wavefunction ψ as an antisymmetrical combination of the products A.3. First, for a system of two particles

$$\psi(\xi_1,\xi_2) = \left[\psi_{p_1}(\xi_1)\psi_{p_2}(\xi_2) - \psi_{p_2}(\xi_2)\psi_{p_1}(\xi_1)\right]/\sqrt{2}. \tag{A.6}$$

Making this more general consider the case of N particles, the wavefunction can be written in the form of a determinant:

$$\psi_{N_1 N_2 \cdots} = \frac{1}{\sqrt{N!}} \begin{vmatrix} \psi_{\nu_1}(\xi_1) & \psi_{\nu_1}(\xi_2) & \cdots & \psi_{\nu_1}(\xi_N) \\ \psi_{\nu_2}(\xi_1) & \psi_{\nu_2}(\xi_2) & \cdots & \psi_{\nu_2}(\xi_N) \\ \cdots & \cdots & \cdots & \cdots \\ \psi_{\nu_N}(\xi_1) & \psi_{\nu_N}(\xi_2) & \cdots & \psi_{\nu_N}(\xi_N) \end{vmatrix}. \tag{A.7}$$

Here an interchange of two particles corresponds to an interchange of two columns of the determinant, as a result the determinant changes sign.

The following is an important consequence of this expression. If two of the numbers $p_1,\ p_2,\ \cdots$ are the same, it means that two rows of the determinant are the same, therefore it vanishes identically. It will be different from zero only when all the numbers $p_1,\ p_2,\ \cdots$ are different. Thus, in a system of identical fermions, no two (or more) particles can be in the same quantum state. This is the Pauli exclusion principle.

B. BLOCH AND WANNIER FUNCTIONS

B.1 Bloch Functions

Reference [11] tells us about Bloch functions.

If we neglect interactions between carriers and impurities and phonons and take the Coulomb interaction between carriers in the Mean-Field approximation, then we have a one-electron Hamiltonian where the motion of an electron through an infinite periodic lattice is governed by the Schrödinger equation

$$\underbrace{\left[-\frac{\hbar^2}{2m}\nabla^2 + V(\boldsymbol{r})\right]}_{\text{This is the Hamiltonian, } H} \psi(\boldsymbol{r}) = E\psi(\boldsymbol{r}), \tag{B.1}$$

where $V(\boldsymbol{r})$ is the periodic potential from the lattice which is assumed to be symmetric, $V(\boldsymbol{r}) = V(-\boldsymbol{r})$.

The Bloch theorem states that the eigenvalues of Equation (B.1) are classified by the wavevector $\boldsymbol{k}$ and band index n and are given by a Bloch function

$$\psi_{n\boldsymbol{k}}(\boldsymbol{r}) = u_{n\boldsymbol{k}}(\boldsymbol{r})e^{\mathrm{i}\boldsymbol{k}\cdot\boldsymbol{r}}, \tag{B.2}$$

where $u_{n\boldsymbol{k}}(\boldsymbol{r})$ has the same periodicity as the lattice potential $V(\boldsymbol{r})$ and $\boldsymbol{k}$ is real. This can be proven by following the procedure from Reference [11] using the translation operator $T_{\boldsymbol{l}}$ [11] which shifts the argument by lattice vector $\boldsymbol{l}$ while acting upon any function $F(\boldsymbol{r})$, so that

$$T_{\boldsymbol{l}}F(\boldsymbol{r}) = F(\boldsymbol{r} + \boldsymbol{l}). \tag{B.3}$$

Since the Hamiltonian has translational symmetry, it commutes with the translation operator and so the eigenstates of H can be chosen to also be eigenstates of $T_{\boldsymbol{l}}$ such that

$$T_{\boldsymbol{l}}\psi(\boldsymbol{r}) = c(\boldsymbol{l})\psi(\boldsymbol{r}), \tag{B.4}$$

where $c(\boldsymbol{l})$ is a number depending on $\boldsymbol{l}$. The eigenvalues of the translation operators are related as follows:

$$c(\boldsymbol{l}+\boldsymbol{l}') = c(\boldsymbol{l})c(\boldsymbol{l}'), \tag{B.5}$$

since shifting the argument by $\boldsymbol{l}+\boldsymbol{l}'$ is the same as making two successive translations, $T_{\boldsymbol{l}+\boldsymbol{l}'} = T_{\boldsymbol{l}}T_{\boldsymbol{l}'}$. This is satisfied if

$$c(\boldsymbol{l}) = e^{\mathrm{i}\boldsymbol{k}\cdot\boldsymbol{l}}, \tag{B.6}$$

for any $\boldsymbol{k}$. If an appropriate boundary condition is imposed on the wavefunction, then the wavevectors $\boldsymbol{k}$ can be kept real and within the first Brillouin zone. For convenience the Born-von Karman condition is enforced:

$$\psi(\boldsymbol{r}+N_j\boldsymbol{a}_j) = \psi(\boldsymbol{r}), \qquad j = 1,2,3. \tag{B.7}$$

$\boldsymbol{a}_j$ are three primitive lattice vectors of the crystal lattice and N_j are large integers such that $N = N_1N_2N_3$ is the total number of primitive cells in the crystal (of the order $10^{23}\mathrm{cm}^{-3}$). This requires that

$$e^{\mathrm{i}N_j\boldsymbol{k}\cdot\boldsymbol{a}_j} = 1. \tag{B.8}$$

So the electron wavefunction can be expressed in the form

$$\boldsymbol{k} = \frac{n_1}{N_1}\boldsymbol{b}_1 + \frac{n_2}{N_2}\boldsymbol{b}_2 + \frac{n_3}{N_3}\boldsymbol{b}_3, \tag{B.9}$$

where n_i are integers and $\boldsymbol{b}_1$, $\boldsymbol{b}_2$ and $\boldsymbol{b}_3$ are basis vectors of the reciprocal lattice such that

$$\begin{aligned} \boldsymbol{b}_1 &= \frac{2\pi\boldsymbol{a}_2\times\boldsymbol{a}_3}{\Omega_0} \\ \boldsymbol{b}_2 &= \frac{2\pi\boldsymbol{a}_3\times\boldsymbol{a}_1}{\Omega_0} \\ \boldsymbol{b}_3 &= \frac{2\pi\boldsymbol{a}_1\times\boldsymbol{a}_2}{\Omega_0}, \end{aligned} \tag{B.10}$$

here Ω_0 is the volume of the unit cell, $\Omega_0 = \boldsymbol{a}_1 \cdot (\boldsymbol{a}_2 \times \boldsymbol{a}_3)$, and $\boldsymbol{b}_i \boldsymbol{a}_j = 2\pi\delta_{ij}$. Distinct values of $\boldsymbol{k}$ lie within the interval

$$-\pi < \boldsymbol{k} \cdot \boldsymbol{a}_j \leq \pi, \qquad (j = 1, 2, 3), \tag{B.11}$$

which is in the first Brillouin zone. If $\boldsymbol{k}' = \boldsymbol{k} + \boldsymbol{m}$, where $\boldsymbol{m} = \sum_{i=1}^{3} m_i \boldsymbol{b}_i$ is an arbitrary lattice vector of the reciprocal lattice, is substituted in for $\boldsymbol{k}$, then

$$\begin{aligned} e^{\mathrm{i}\boldsymbol{k}'\cdot\boldsymbol{a}_j} &= e^{\mathrm{i}\boldsymbol{k}\cdot\boldsymbol{a}_j} e^{\mathrm{i}\boldsymbol{b}_m\cdot\boldsymbol{a}_j} \\ &= e^{\mathrm{i}\boldsymbol{k}\cdot\boldsymbol{a}_j} e^{2\pi\mathrm{i}\times\text{integer}} \\ &= e^{\mathrm{i}\boldsymbol{k}\cdot\boldsymbol{a}_j}. \end{aligned} \tag{B.12}$$

Here $\boldsymbol{k}$ and $\boldsymbol{k}'$ correspond to the same representation, they are equivalent. So only the values of $\boldsymbol{k}$ for which $\boldsymbol{k} \cdot \boldsymbol{a}_j$ lie in the interval given by Equation (B.11) need to be considered.

B.2 Wannier Functions

Bloch wavefunctions describe electrons free to move through the crystal lattice with a periodic potential from the lattice. Conduction electrons in semiconductors frequently experience an additional field which for example can be from an impurity ion, a lattice defect, a free surface on the crystal. This can create a localised electron state in the lattice. In some cases it is convenient to use Wannier functions since they play the part of "site representation" [103]. Both Bloch electrons and localised electrons can be described using Wannier functions, since Bloch electrons are periodic in momentum space with the period of the reciprocal lattice $\boldsymbol{b}_i$ $(i = 1, 2, 3)$. This means that $\psi_{n\boldsymbol{k}}(\boldsymbol{r})$ can be expanded in $\boldsymbol{k}$-space in a Fourier series [103]:

$$\psi_{n\boldsymbol{k}}(\boldsymbol{r}) = \frac{1}{\sqrt{N}} \sum_{\boldsymbol{m}} \phi_n(\boldsymbol{r} - \boldsymbol{m}) e^{\mathrm{i}\boldsymbol{k}\cdot\boldsymbol{m}}, \tag{B.13}$$

where $\phi_n(\boldsymbol{r} - \boldsymbol{m})$ is the Wannier function which can be approximated by the atomic orbital of a single ion on site $\boldsymbol{m}$, where $\boldsymbol{m} = \{m_x.m_y, m_z\}$ and each $m_x.m_y, m_z$ is

an integer multiple of a, the lattice spacing. The periodic potential of the lattice is included explicitly in the Wannier functions:

$$\psi_{n\boldsymbol{k}}(\boldsymbol{r}+\boldsymbol{l}) = \frac{1}{\sqrt{N}} \sum_{\boldsymbol{m}} \phi_n(\boldsymbol{r}-\boldsymbol{m}+\boldsymbol{l}) e^{\mathrm{i}\boldsymbol{k}\cdot\boldsymbol{m}}, \tag{B.14}$$

Substituting $\boldsymbol{m}-\boldsymbol{l}=\boldsymbol{m}'$:

$$\begin{aligned} \psi_{n\boldsymbol{k}}(\boldsymbol{r}+\boldsymbol{l}) &= \frac{1}{\sqrt{N}} \sum_{\boldsymbol{m}'} e^{\mathrm{i}\boldsymbol{k}\cdot(\boldsymbol{m}'+\boldsymbol{l})} \phi(\boldsymbol{r}-\boldsymbol{m}) \\ &= \frac{1}{\sqrt{N}} \sum_{\boldsymbol{m}'} e^{\mathrm{i}\boldsymbol{k}\cdot\boldsymbol{l}} e^{\mathrm{i}\boldsymbol{k}\cdot\boldsymbol{m}'} \phi(\boldsymbol{r}-\boldsymbol{m}) \\ &= \psi_{n\boldsymbol{k}}(\boldsymbol{r}+\boldsymbol{l}) e^{\mathrm{i}\boldsymbol{k}\cdot\boldsymbol{l}}. \end{aligned} \tag{B.15}$$

For Wannier functions to be orthogonal and normalised, they must obey:

$$\begin{aligned} \int \phi^*(\boldsymbol{r}-\boldsymbol{m}')\phi^*(\boldsymbol{r}-\boldsymbol{m})d\boldsymbol{r} &= \delta_{\boldsymbol{m}\boldsymbol{m}'}, \\ \text{where } \delta_{\boldsymbol{m}\boldsymbol{m}'} &= \begin{cases} 1 \text{ if } \boldsymbol{m}'=\boldsymbol{m} \\ 0 \text{ if } \boldsymbol{m}'\neq\boldsymbol{m}. \end{cases} \end{aligned} \tag{B.16}$$

By making use of the property of a normalised Bloch function, Equation (B.2), inside the crystals principle region ($\int_V \psi^*_{\boldsymbol{k}}(\boldsymbol{r})\psi_{\boldsymbol{k}}(\boldsymbol{r})d^3r = 1$) we can see the Wannier functions are mutually orthogonal with respect to both the band number n and site number $\boldsymbol{m}$ [103].

$$\begin{aligned} \int_V \psi^*_n(\boldsymbol{r}-\boldsymbol{m})\psi_{n'}(\boldsymbol{r}-\boldsymbol{m}')d\boldsymbol{r} &= \frac{1}{\sqrt{N}} \sum_{\boldsymbol{k}\boldsymbol{k}'} e^{\mathrm{i}(\boldsymbol{k}\cdot\boldsymbol{m}-\boldsymbol{k}'\cdot\boldsymbol{m}')} \int \psi^*_{n\boldsymbol{k}}(\boldsymbol{r})\psi_{n'\boldsymbol{k}'}(\boldsymbol{r})d^3r \\ &= \frac{1}{\sqrt{N}} \sum_{\boldsymbol{k}\boldsymbol{k}'} e^{\mathrm{i}\boldsymbol{k}\cdot(\boldsymbol{m}-\boldsymbol{m}')} e^{\mathrm{i}(\boldsymbol{k}-\boldsymbol{k}')\cdot\boldsymbol{m}'} \delta_{nn'}\delta_{\boldsymbol{k}\boldsymbol{k}'} \\ &= \frac{\delta_{nn'}}{\sqrt{N}} \sum_{\boldsymbol{k}} e^{\mathrm{i}\boldsymbol{k}\cdot(\boldsymbol{m}-\boldsymbol{m}')} \\ &= \delta_{nn'}\delta_{\boldsymbol{k}\boldsymbol{k}'}. \end{aligned} \tag{B.17}$$

It has been stated that Wannier functions are localised and this can be proven. To simplify the proof a simple cubic lattice is considered and the Bloch function is approximated to be a plane wave [103], $\psi_{\boldsymbol{k}}(\boldsymbol{r}) = V^{-\frac{1}{2}} e^{\mathrm{i}\boldsymbol{k}\cdot\boldsymbol{r}}$, so the Wannier function can

be written

$$\phi_n(\boldsymbol{r}-\boldsymbol{m}) = C\sum_{k_x} e^{\mathrm{i}k_x\xi}\sum_{k_y} e^{\mathrm{i}k_y\eta}\sum_{k_z} e^{\mathrm{i}k_z\zeta}, \tag{B.18}$$

where C is a normalising coefficient of the wavefunction, ϕ_n. ξ,η,ζ are rectangular components of the position vector $\boldsymbol{m}' = \boldsymbol{r}-\boldsymbol{m}$ and the wavevector is given by $k_i = 2\pi g_i/Ga$ where $-\frac{1}{2}G \leq g_i \leq \frac{1}{2}G$ with a being the edge of the simple cubic lattice. Adding up the sum over k_x (over g as a geometrical progression), we obtain

$$\begin{aligned}\sum_{k_x} e^{\mathrm{i}k_x\xi} &= 1+\sum_{g=1}^{\frac{1}{2}G} e^{\frac{2\pi\mathrm{i}\xi}{Ga}g} + \sum_{g=-1}^{-\frac{1}{2}G} e^{\frac{2\pi\mathrm{i}\xi}{Ga}g} \\ &= \frac{e^{\frac{\pi\mathrm{i}\xi}{a}}e^{\frac{2\pi\mathrm{i}\xi}{Ga}} - e^{-\frac{\pi\mathrm{i}\xi}{a}}}{e^{\frac{2\pi\mathrm{i}\xi}{Ga}}-1}.\end{aligned} \tag{B.19}$$

If it is assumed that the principal region of the crystal is sufficiently large then we have $\frac{\xi}{Ga} << 1$, which means $e^{\frac{2\pi\mathrm{i}\xi}{Ga}} \approx 1$. So the above can be written:

$$\sum_{k_x} e^{\mathrm{i}k_x\xi} \approx \frac{\sin\frac{\pi\xi}{a}}{\frac{\pi\xi}{a}}. \tag{B.20}$$

This equation has a maximum at 1 when $\xi = 0$, as ξ increases, Equation (B.20) decreases, rapidly oscillating in the process. Hence, the Wannier function $\phi(\boldsymbol{r}-\boldsymbol{m})$ has its maximum when $\boldsymbol{r} = \boldsymbol{m}$ which rapidly decreases as $\boldsymbol{r}-\boldsymbol{m}$ is increased. This shows that the Wannier functions are localised around point $\boldsymbol{m}$ [103].

C. THE LOCAL DENSITY APPROXIMATION, TIGHT BINDING MODEL AND COMBINING THEM

The wavefunctions of electrons in semiconductors are different from plane waves because they are affected by the periodic potential from the lattice. Generally, the band structure should be calculated numerically. However we can calculate analytically by making some approximations and using models. For example the Local Density Approximation (LDA) and the Generalised Tight Binding model (GTB).

C.1 Local Density Approximation

The local density approximation (LDA) states that for a region where the charge density varies slowly, the exchange energy per particle at each spatial point can be considered the same as that for a locally uniform electron gas of the same density. By Reference [104] we have the exchange correlation energy as:

$$E_{xc} = \int n(\boldsymbol{r})\epsilon_{xc}(n(\boldsymbol{r}))d\boldsymbol{r}, \tag{C.1}$$

where $n(\boldsymbol{r})$ is the density, $\epsilon_{xc}(n(\boldsymbol{r}))$ is the exchange and correlation energy per electron of a uniform electron gas of density n.

Despite the simplicity of the approximation, for many systems it is surprisingly accurate. However it tends to under predict atomic ground state energies and ionisation energies, while over predicting binding energies.

C.2 Tight Binding Model

In many solids the electrons are localised on atomic sites and only occasionally hop to neighbouring sites. This is the tight-binding model.

Following the procedure given by Reference [6], if we start with neutral atoms that are separated and then allow the charge distributions of two adjacent atoms to overlap as the atoms are brought together to form a crystal, we can look at what happens to the atomic energy levels.

Consider two hydrogen atoms each with electron in the 1s ground state. When they are brought together, their wave functions overlap. Consider the two contributions $\psi_A \pm \psi_B$. Each combination shares an electron with the two protons, but an electron in the state $\psi_A + \psi_B$ will have a lower energy than one in state $\psi_A - \psi_B$.

For $\psi_A + \psi_B$ the electron spends part of the time in the region midway between the two protons, here it is in the attractive region of two protons at the same time, thus increasing the binding energy. In $\psi_A - \psi_B$ the probability density vanishes midway between the nuclei and so there is no extra binding energy.

As the two separate atoms are brought closer together, two separate energy levels are formed for each level of the isolated atom. For N atoms, N orbitals are formed for each orbital of the isolated atom. As free atoms are brought together, the Coulomb interaction between the atom cores and the electron splits the energy levels, spreading them into bands. Each state (of given quantum number) of the free atom is spread in the crystal into a band of energies. The width of the band is proportional to the strength of the overlap interaction between neighbouring atoms. There will also be bands formed from $p,\ d \cdots$ states ($l = 1, 2, \cdots$) of the free atoms. Each will have a different energy from any other band over any substantial range of the wavevector. Bands may coincide in energy at certain values of k in the Brillouin zone. The approximation that starts out from the wavefunctions of the free atoms is known as the "tight-binding approximation" or LCAO (linear combination of atomic orbitals).

C.3 Combining the Two

Reference [91]. The LDA makes good approximations for conventional metallic systems but it appears to be inadequate for strongly correlated systems. For example, it predicts La_2CuO_4 to be a metal whereas in reality it is an insulator. Several approaches have been made to include strong correlations in the LDA method, for example "LDA+U" [92] where U is the Hubbard Coulomb parameter, "LDA-SIC" [93] and "LDA+DMFT" [105] (where DMFT is the Dynamical Mean Field Theory and SIC refers to self interaction correction).

Reference [91] proposed a GTB method to study the electronic structure of strongly correlated electron systems as a generalisation of Hubbard ideas for realistic multiband Hubbard-like models. The GTB method combines the exact diagonalisation of the intracell part of the Hamiltonian, construction of the Hubbard operators on the basis of the exact intracell multielectron eigenstates, and the perturbation treatment of the intercell hoppings and interactions. The practical realisation of the GTB method for cuprates requires an explicit construction of Wannier functions to overcome the nonorthogonality of the oxygen molecular orbitals at the neighbouring CuO_6 cells. The GTB calculations for undoped and underdoped cuprates are in good agreement with ARPES data both in the dispersion of the valence band and in the spectral intensity. A strong redistribution of spectral weight with hole doping and the formation of the in-gap states have been obtained. Reference [91] supplied a hybrid LDA+GTB scheme that allows the calculation of GTB parameters by the *ab initio* LDA approach (usually these parameters are found experimentally).

D. SYMMETRY OF THE ORDER PARAMETER

The Schrödinger equation describes the electron in terms of a standing wave around the nucleus, it gives different densities corresponding to the probability of finding the electron. The standing wave is called an orbital. The equation can be solved exactly for hydrogen but in heavier atoms the electrons interact with eachother in complex ways so the equation cannot be solved exactly but they can be approximated to higher energy levels of hydrogen.

Fig. D.1 shows some of the possible orbitals for an excited electron in the hydrogen atom. The lowest energy level is the spherical orbital and it is called the s-orbital. On the next energy level electrons have more freedom and the wave equation means that the wavefunction can give four different possible shapes, one of them is again an s-orbital but this time it has a larger radius.

The superconducting gap is believed to obey some sort of symmetry, it is mainly believed that in cuprates the SG obeys d-wave symmetry, however, some believe cuprates obey s-wave symmetry.

Fig. D.1 shows that for s-wave symmetry ($l = 0$), the order parameter does not depend on the angle around the constant energy contour, i.e. it is spherically symmetrical. However, for d-wave symmetry the charge density of the wavefunction changes with the angle. Therefore, we have equations:

$$\begin{aligned} \Delta_{c\nu} &= \Delta_c \text{ for } s\text{-wave symmetry} \\ \Delta_{c\nu} &= \Delta_0 \cos 2\phi \text{ for } d\text{-wave symmetry, the quantum number } \nu \text{ depends} \\ &\qquad \text{on the angle } \phi \text{ around the constant energy contour.} \end{aligned} \tag{D.1}$$

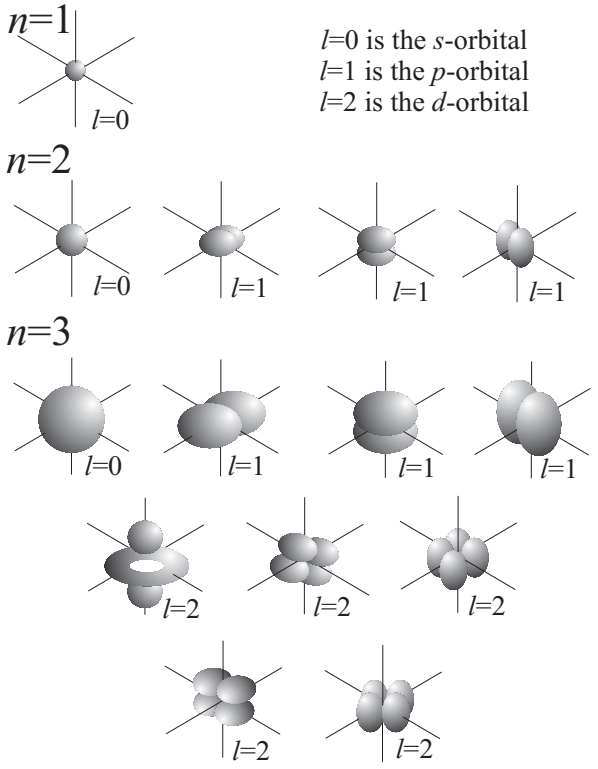

Fig. D.1: Some of the possible orbitals for an excited electron in a hydrogen atom. This depicts the density distribution (which is the modulus of the wavefunction squared, $|\psi^2|$) where the density corresponds to the probability density of the electrons.

E. FINDING THE EXTRINSIC TUNNELLING CURRENT

From Equation (5.36) we consider $eV > 0$ only, since $I(V) = I(-V)$ when the two materials are the same. We can substitute in the normal-state DOS given by Equation (4.21) and we can make the change of variables:

$$\begin{aligned} y &= e^{\xi/k_BT} \\ b &= e^{\Delta_p/k_BT} \\ a &= e^{eV/k_BT}, \end{aligned} \tag{E.1}$$

then

$$\begin{aligned} \rho(\xi) &\rightarrow \frac{1}{2}\left(1+\frac{\frac{y}{b}-\frac{b}{y}}{\frac{y}{b}+\frac{b}{y}}\right) = \frac{1}{2}\left(1+\frac{y^2-b^2}{y^2+b^2}\right) \\ \rho(-\xi) &\rightarrow \frac{1}{2}\left(1+\frac{1-y^2b^2}{1+y^2b^2}\right) \\ \rho(\xi-eV) &\rightarrow \frac{1}{2}\left(1+\frac{y^2-a^2b^2}{y^2+a^2b^2}\right) \\ \rho(eV-\xi) &\rightarrow \frac{1}{2}\left(1+\frac{a^2-y^2b^2}{a^2+y^2b^2}\right). \end{aligned} \tag{E.2}$$

First consider

$$\begin{aligned} \int_0^{eV} d\xi\rho(\xi)\rho(eV-\xi) &= \frac{1}{4}\int_1^a \frac{dy}{y}\left(1+\frac{y^2-b^2}{y^2+b^2}\right)\left(1+\frac{a^2-y^2b^2}{a^2+y^2b^2}\right) \\ &= a^2\int_1^a dy\frac{y}{(y^2+b^2)(a^2+y^2b^2)}, \end{aligned} \tag{E.3}$$

upon substitution $z = y^2$

$$\int_0^{eV} d\xi\rho(\xi)\rho(eV-\xi) = \frac{a^2}{2}\int_1^{a^2} dz\frac{1}{(z+b^2)(a^2+zb^2)}$$

$$\begin{aligned} &= \frac{a^2}{2(a^2-b^4)}\int_1^{a^2} dz\left(\frac{1}{z+b^2}-\frac{1}{\frac{a^2}{b^2}+z}\right) \\ &= \frac{a^2}{2(a^2-b^4)}\left[\ln\frac{z+b^2}{\frac{a^2}{b^2}+z}\right]_1^{a^2} \\ &= \frac{a^2}{a^2-b^4}\ln\frac{a^2+b^2}{a(1+b^2)}. \end{aligned} \tag{E.4}$$

Now, consider

$$\begin{aligned} \int_0^{eV} d\xi\rho(-\xi)\rho(\xi-eV) &= \frac{1}{4}\int_1^a \frac{dy}{y}\left(1+\frac{1-y^2b^2}{1+y^2b^2}\right)\left(1+\frac{y^2-a^2b^2}{y^2+a^2b^2}\right) \\ &= \int_1^a dy\frac{y}{(1+y^2b^2)(y^2+a^2b^2)} \\ &= \frac{1}{2(a^2b^4-1)}\int_1^{a^2} dz\left[\frac{1}{(\frac{1}{b^2}+z)-\frac{1}{z+a^2b^2}}\right] \\ &= \frac{1}{a^2b^4-1}\ln\frac{1+a^2b^2}{a(1+b^2)}. \end{aligned} \tag{E.5}$$

Now following the same procedure, consider

$$\int_0^{eV} d\xi\rho(-\xi)\rho(eV-\xi) = \frac{a^2}{b^2(a^2-1)}\int_1^a \frac{dy}{y}\left[\frac{1}{y^2+\frac{1}{b^2}}-\frac{1}{y^2+\frac{a^2}{b^2}}\right] \tag{E.6}$$

The first term here can be rewritten

$$\begin{aligned} \int_1^a \frac{dy}{y}\frac{1}{y^2+\frac{1}{b^2}} &= b^2\int_b^{ab}\frac{dx}{x}\frac{1}{x^2+1} \\ &= b^2\left[\ln\frac{x}{(x^2+1)^{\frac{1}{2}}}\right]_b^{ab} \\ &= \frac{b^2}{2}\ln\frac{a^2(b^2+1)}{a^2b^2+1}, \end{aligned} \tag{E.7}$$

and the second term

$$\begin{aligned} \int_1^a \frac{dy}{y}\frac{1}{y^2+\frac{a^2}{b^2}} &= \frac{b^2}{a^2}\int_{\frac{b}{a}}^b \frac{dx}{x}\frac{1}{x^2+1} \\ &= \frac{b^2}{2a}\ln\frac{a^2+b^2}{1+b^2}. \end{aligned} \tag{E.8}$$

Therefore, the extrinsic current can be described as

$$I_{ss} \propto \frac{a^2}{2(a^2-1)}\left[\ln\frac{a^2(b^2+1)}{a^2b^2+1}-\frac{1}{a^2}\ln\frac{a^2+b^2}{1+b^2}\right]+\frac{B^2x}{2P^2}\frac{a^2}{a^2-b^4}\ln\frac{a^2+b^2}{a(1+b^2)}$$

$$+\frac{B^2(2+x)}{2P^2}\frac{1}{a^2b^4-1}\ln\frac{1+a^2b^2}{a(1+b^2)}. \tag{E.9}$$

BIBLIOGRAPHY

[1] A. Sommerfeld and H. Bethe, *Handbuch der Physik von Geiger und Scheel* (Julius Springer-Verlag, Berlin, 1933), Vol. 24/2, p450

[2] R. Holm, J. Appl. Phys. **22** 569 (1951)

[3] G. D. Mahan, *Many-Particle Physics* (Second Edition, Plenum Press, New York, 1980, 1981), Chapter 9, p788

[4] J. W. Conley, C. B. Duke, G. D. Mahan and J. J. Tiemann, Phys. Rev. **150** 466 (1966)

[5] R. A. Smith, *Semiconductors* (Second Edition, Cambridge University Press, Cambridge, 1978)

[6] C. Kittel, *Introduction to Solid State Physics*, 7th Edition. John Wiley & Sons, Inc., 1996.

[7] J. Bardeen, L. N. Cooper and J. R. Schrieffer, Phys. Rev. **108** 1175 (1957)

[8] L. N. Cooper, Phys. Rev. **104** 1189 (1956)

[9] G. M. Eliashberg, Zh. Eksp. Teor. Fiz. **38** 966 (1960) [Sov. Phys. JETP **11** 696 (1960)]; **39** 1437 (1960) [**12** 1000 (1961)]

[10] H. Fröhlich, Phys. Rev. **79** 845 (1950)

[11] A. S. Alexandrov, *Theory of Superconductivity: From Weak to Strong Coupling*, IOP Publishing, Bristol, 2003.

[12] J. G. Bednorz and K. A. Müller, Z. Phys. B **64** 189 (1986)

[13] T. Imai, T. Shimizu, H. Yasuoka, Y. Ueda and K. Kosuge, J. Phys. Soc. Jpn. **57** 2280 (1988); T. Imai, T. Shimizu, T. Tsuda, H. Yasuoka, T. Takabatake, Y. Nakazawa and M. Ishikawa, J. Phys. Soc. Jpn. **57** 1771 (1988)

[14] J. Geerk, X. X. Xi and G. Linker, Z. Phys. B **73** 329 (1988)

[15] J. Beanland and A. S. Alexandrov, Journal of Physics: Condensed Matter, provisionally scheduled for September 2010.

[16] O. Fischer, M. Kugler, I. Maggio-Aprile, C. Berthod and Ch. Renner, Rev. Mod. Phys. **79** 353 (2007)

[17] P. A. Lee, N. Nagaosa and X. -G. Wen, Rev. Mod. Phys. **78** 17 (2006)

[18] P. W. Anderson, P. A. Lee, M. Randeria, T. M. Rice, N. Trivedi and F. C. Zhang, J. Phys. Condens. Matter **16** R755 (2004)

[19] A. P. Kampf and J. P. Schrieffer, Phys. Rev. B **42** 7967 (1990)

[20] S. V. Varlamov, M. V. Eremin and I. M. Eremin, JETP Lett. **66** 569 (1997)

[21] B. Pradhan, B. K. Raj and G. C. Rout, Physica C **468** 2332 (2008)

[22] E. V. L. de Mello, M. T. D. Orlando, J. L. Gonzalez, E. S. Caixeiro and E. Baggio-Saitovich, Phys. Rev. B **66** 092504 (2002)

[23] V. J. Emery, S. A. Kivelson and H. Q. Lin, Phys. Rev. Lett. **64** 475 (1990)

[24] N. Kristoffel, P. Rubin and T. Örd, Int. J. Mod. Phys B **22** 5299 (2008)

[25] A. S. Alexandrov and D. K. Ray, Phil. Mag. Lett. **63** 295 (1991)

[26] V. J. Emery and S. A. Kivelson, Nature (London) **374** 434 (1995)

[27] Q. Chen, J. Stajic, S. Tan and K. Levin, Phys. Rep. **412** 1 (2005)

[28] J. Ranninger and J. M. Robin, Phys. Rev. Lett **74** 4027 (1995)

[29] J. P. Wallington and J. F. Annett, Phys. Rev. B **61** 1433 (2000)

[30] M. Randeria, N. Trivedi, A. Moreo, and R. T. Scalettar, Phys. Rev. Lett **69** 2001 (1998)

[31] R. Micnas, M. H. Pedersen, S. Schafroth, T. Schneider, J. J. Rodriguez-Nunez and H. Beck, Phys. Rev. B **52** 16223 (1995)

[32] P. E. Lammert and D. S. Rokhsar, arXiv:cond-mat/0108146 (2001)

[33] T. Eckl, D. J. Scalapino, E. Arrigoni and W. Hanke, Phys. Rev. B **66** 140510 (2002)

[34] B. Giovannini and C. Berthod, Phys. Rev. B **63** 144516 (2001)

[35] J. Demsar, K. Biljakovic and D. Mihailovic, Phys. Rev. Lett. **83** 800 (1999)

[36] J. Demsar, R. Hudej, J. Karpinski, V. V. Kabanov and D. Mihailovic, Phys. Rev. B **63** 054519 (2001)

[37] M. Le Tacon, A. Sacuto, A. Georges, G. Kotliar, Y. Gallais, D. Colson and A. Forget, Nature Phys. **2** 537 (2006)

[38] M. R. Norman, H. Ding, J. C. Campuzano, T.Takeuchi, M. Randeria, T. Yokoya, T. Takahashi, T. Mochiku and K. Kadowaki, Phys. Rev. Lett. **79** 3506 (1997)

[39] K. Tanaka, W. S. Lee, D. H. Lu, A. Fujimori, T. Fujii, Risdiana, I. Terasaki, D. J. Scalapino, T. P. Devereaux, Z. Hussain and Z. -X. Shen, Science **314** 1910 (2006)

[40] A. Kanigel, M. R. Norman, M. Randeria, U. Chatterjee, S. Souma, A. Kaminski, H. M. Fretwell, S. Rosenkranz, M. Shi, T. Sato, T. Takahashi, Z. Z. Li, H. Raffy, K. Kadowaki, D. Hinks, L. Ozyuzer and J. C. Campuzano, Nature Phys. **2** 447 (2006).

[41] W. S. Lee, I. M. Vishik, K. Tanaka, D. H. Lu, T. Sasagawa, N. Nagaosa, T. P. Devereaux, Z. Hussain and Z.-X. Shen, Nature **450** 81 (2007)

[42] T. Kondo, T. Takeuchi1, A. Kaminski, S. Tsuda and S. Shin, Phys. Rev. Lett. **98** 267004 (2007)

[43] T. Yoshida, X. J. Zhou, D. H. Lu, S. Komiya, Y. Ando, H. Eisaki, T. Kakeshita, S. Uchida, Z. Hussain, Z.-X. Shen and A. Fujimori, J. Phys.: Condens. Matter **19** 125209 (2007)

[44] T. Valla, A. V. Fedorov, J. Lee, J. C. Davis and G. D. Gu, Science **314** 1914 (2006)

[45] K. M. Shen, F. Ronning, D. H. Lu, F. Baumberger, N. J. C. Ingle, W. S. Lee, W. Meevasana, Y. Kohsaka, M. Azuma, M. Takano, H. Takagi and Z.-X. Shen, Science **307** 901 (2005)

[46] Ch. Renner, B. Revaz, J.-Y. Genoud, K. Kadowaki and O. Fischer, Phys. Rev. Lett. **80** 149 (1998)

[47] K. M. Lang, V. Madhavan, J. E. Hoffman, E. W. Hudson, H. Eisaki, S. Uchida and J. C. Davis, Nature (London) **415** 412 (2002)

[48] C. Howald, P. Fournier and A. Kapitulnik, Phys. Rev. B **64** 100504 (R)

[49] T. Machida, Y. Kamijo, K. Harada, T. Noguchi, R. Saito, T. Kato and H. Sakata, J. Phys. Soc. Jpn. **75** 083708 (2006)

[50] K. McElroy, D. -H. Lee, J. E. Hoffman, K. M. Lang, J. Lee, E. W. Hudson, H. Eisaki, S. Uchida and J. C. Davis, Phys. Rev. Lett. **94** 197005 (2005)

[51] K. K. Gomes, A. N. Pasupathy, A. Pushp, S. Ono, Y. Ando and A. Yazdani, Nature Lett. **447** 569 (2007)

[52] S. H. Pan, J. P. O'Neal, R. L. Badzey, C. Chamon, H. Ding, J. R. Engelbrecht, Z. Wang, H. Eisaki, S. Uchida, A. K. Gupta, K.-W. Ng, E. W. Hudson, K. M. Lang and J. C. Davis, Nature (London) **413** 282 (2001)

[53] T. Kato, S. Okitsu and H. Sakata, Phys. Rev. B **72** 144518 (2005)

[54] T. Kato, T. Maruyama, S. Okitsu and H. Sakata, J. Phys. Soc. Jpn. **77** 054710 (2008)

[55] V. M. Krasnov, A. Yurgens, D. Winkler, P. Delsing and T. Claeson, Phys. Rev. Lett. **84** 5860 (2000)

[56] M. Suzuki and T. Watanabe, Phys. Rev. Lett. **85** 4787 (2000)

[57] X. B. Zhu, S. P. Zhao, Y. F. Wei, H. F. Yang, C. Z. Gu, H. W. Yu and Y. F. Ren, Physica C **460** 963 (2007)

[58] V. M. Krasnov, Phys. Rev. B **79** 214510 (2009)

[59] A. Yurgens, D. Winkler, T. Claeson, S. Ono and Y. Ando, Phys. Rev. Lett. **90** 147005-1 (2003)

[60] N. Miyakawa, P. Guptasarma, J. F. Zasadzinski, D. G. Hinks and K. E. Gray, Phys. Rev. Lett. **80** 157 (1998)

[61] S. I. Vedeneev, A. G. M. Jansen, P. Samuely, V. A. Stepanov, A. A. Tsvetkov, P. N. Lebedev and P. Wyder, Phys Rev. B **49** 9823 (1994)

[62] S. I. Vedeneev, JETP Lett. **68** 230 (1998)

[63] Y. Xuan, H. J. Tao, Z. Z. Li, C. T. Lin, Y. M. Ni, B. R. Zhao and Z. X. Zhao, arXiv:cond-mat/0107540v1 (2001)

[64] N. Miyakawa, J. F. Zasadzinski, L. Ozyuzer, P. Guptasarma, D. G. Hinks, C. Kendziora and K. E. Gray, Phys. Rev. Lett. **83** 1018 (1999)

[65] S. I. Vedeneev and D. K. Maude, arXiv:cond-mat/0510707v1 (2005)

[66] D. Quesada, Physica C **364** 170 (2001)

[67] R. H. He, K. Tanaka, S. K. Mo, T. Sasagawa, M. Fujita, T. Adach, N. Mannella, K. Yamada, Y. Koike, Z. Hussain and Z. X. Shen, Nature Phys. **5** 119 (2009)

[68] W. Rantner and X. G. Wen, Phys. Rev. Lett. **85** 3692 (2000)

[69] M. R. Presland, J. L. Tallon, R. G. Buckley, R. S. liu and N. E. Flower, Physica C **176** 95 (1991)

[70] J. P. Franck, J. Jung, M. A. -K. Mohamed, S. Gygax and G. I. Sproule, Physica B **169** 697 (1991)

[71] H. J. Bournemann and D. E. Morris, Phys. Rev. B **44** 5322 (1991)

[72] N. Tralshawala, J. F. Zasadzinski, L. Coffey, W. Gai, M. Romalis, Q. Huang, R. Vaglio and K. E. Gray, Phys. Rev. B **51** 3812 (1995)

[73] Y. Shiina, D. Shimada, A. Mottate, Y. Ohyagi and N. Tsuda, J. Phys. Soc. Jpn. **64** 2577 (1995)

[74] A. A. Abrikosov, Physica C **341** 97 (2000)

[75] A. S. Alexandrov and G. M. Zhao, Phys. Rev. B **80** 136501 (2009)

[76] A. S. Alexandrov, Phys. Rev. B **53** 2863 (1996)

[77] K. A. Müller, Physica C **341** 11 (2000)

[78] G. M. Zhao and D. E. Morris, Phys. Rev. B **51** 16487 (1995)

[79] G. M. Zhao, M. B. Hunt, H. Keller and K. A. Müller, Nature London **385** 236 (1997)

[80] R. Khasanov, D. G. Eshchenko, H. Luetkens, E. Morenzoni, T. Prokscha, A. Suter, N. Garifianov, M. Mali, J. Roos, K. Conder and H. Keller, Phys. Rev. Lett. **92** 057602 (2004)

[81] G. M. Zhao, Phys. Rev. B **75** 214507 (2007)

[82] G. M. Zhao, Phys. Rev. Lett. **103** 236403 (2009)

[83] A. S. Alexandrov and J. T. Devreese, *Advances in Polaron Physics*, (Springer, New York, 2009)

[84] A. S. Alexandrov and J. Ranninger, Phys. Rev. B **23** 1796 (1981), ibid **24** 1164 (1981)

[85] A. S. Alexandrov, Zh. Fiz. Khim. **57** 273 (1983) [Russ. J. Phys. Chem. **57** 166 (1983)]

[86] A. S. Alexandrov and A. F. Andreev, Europhys. Lett. **54** 373 (2001)

[87] J. E. Demuth, B. N. J. Persson, F. Holtzberg and C. V. Chandrasekhar, Phys. Rev. Lett. **64** 603 (1990)

[88] A. F. Andreev, Zh. Eksp. Teor. Fiz. **46** 1823 (1964)

[89] A. F. Andreev, Sov. Phys.-JETP **19** 1228 (1964)

[90] A. S. Alexandrov and N. F. Mott, Rep. Prog. Phys. **57** 1197 (1994)

[91] M. M. Korshunov, V. A. Gavrichkov, S. G. Ovchinnikov, I. A. Nekrasov, Z. V. Pchelkina and V. I. Anisimov, Phys. Rev. B **72** 165104 (2005)

[92] V. I. Anisimov, J. Zaanen and O. K. Andersen, Phys. Rev. B **44** 943 (1991)

[93] A. Svane and O. Gunnarsson, Phys. Rev. Lett. **65** 1148 (1990)

[94] S. G. Ovchinnikov and I. S. Sandalov, Physica C **161** 607 (1989)

[95] A. S. Alexandrov and K. Reynolds, Phys. Rev. B **76** 132506 (2007)

[96] P. V. Mieghem, Rev. Mod. Phys. **64** 755 (1992)

[97] G. Yu, C. H. Lee, D. Mihailovic, A. J. Heeger, C. Fincher, N. Herron, E. M. McCarron, Phys. Rev. B **48** 7545 (1993)

[98] A. S. Alexandrov, Physica C (Amsterdam) **305** 46 (1998)

[99] J. A. Slezak, J. Lee, M. Wang, K. McElroy, K. Fujita, B. M. Andersen, P. J. Hirschfeld, H. Eisaki, S. Uchida and J. C. Davis, Proceeding of the National Academy of Sciences of the United States of America, **105** 3203 (2008)

[100] A. S. Alexandrov and J. Beanland, Phys. Rev. Lett. **104** 026401 (2010)

[101] A. S. Alexandrov, V. V. Kabanov and N. F. Mott, Phys. Rev. Lett. **77** 4796 (1996)

[102] L. D. Landau and E. M. Lifshitz, *Quantum Mechanics: Non-Relativistic Theory*, Third Edition, Pergamon Press plc, Headington Hill Hall, Oxford, England (1977)

[103] A. Anselm, *Introduction to Semiconductor Theory*, MIR Publishers, Moscow, Prentice-Hall, Inc., Englewood Cliffs, New Jersey 07632. English translation (1981)

[104] W. Kohn and L. J. Sham, Phys. Rev. **140** A1133 (1965)

[105] For example see the reviews (taken from Reference [91]): V. I. Anisimov, A. I. Poteryaev, M. A. Korotin, A. O. Anokhin and G. Kotliar, J. Phys. Condens. Matter **35** 7359 (1997); K. Held, I. A. Nekrasov, N. Blümer, V. I. Anisimov and D. Vollhardt, Int. J. Mod. Phys. B **15** 2611 (2001); K. Held, I. A. Nekrasov, I. A. Nekrasov, G. Keller, N. Blümer, A. K. McMahan, R. T. Scalletar, T. Pruschke, V. I. Anisimov and D. Vollhardt, in *Quantum Simulations of Complex Many-Body Systems: From Theory to Algorithms*, edited by J. Grotendorst, D. Marks and A. Muramatsu, Vol. 10 of *NIC Series* (NIC directors, Forschunszentrum Jülich, Jülich, 2002), p175-209; K. Held, I. A. Nekrasov, G. Keller, V. Eyert, N. Blümer, A. K. McMahan, R. T. Scalettar, Th. Pruschke, V. I. Anisimov and D. Vollhart, psi-k.dl.ac.uk/newsletters/News_56/Highlight_56.pdf; A. I. Lichtenstein and M. I. Katsnelson, Phys. Rev. B **57** 6884 (1998)